

Identification of cytotoxic constituents of selected plants and the synthesis of liposome-stabilized metal oxide nanoparticles for delivery into cancerous cells

Motshewa Justina Mofolo

(217008924)

Dissertation submitted in fulfilment of the requirements for the degree.

MASTER OF HEALTH SCIENCES IN BIOMEDICAL TECHNOLOGY

in the

Department of Health Sciences

Faculty of Health and Environmental Sciences

at the

Central University of Technology, Free State

Supervisor: Prof M.P Sekhoacha, PhD (UCT)

Co-supervisor: Prof S.S. Mashele, PhD (Medunsa)

Co-supervisor: Dr P.H Mfengwana, DHSc (CUT)

BLOEMFONTEIN

2022

STATEMENT REGARDING INDEPENDENT WORK

I, Mofolo Motshewa Justina and _____, do hereby declare that this research project submitted to the Central University of Technology , Free State for the Degree MASTER OF HEALTH SCIENCES IN BIOMEDICAL TECHNOLOGY, is my own independent work ; and complies with the code of Academic Integrity, as well as other relevant policies, procedures, rules and regulations of the Central University of Technology, Free State; and has not been submitted before to any institution by myself or any other person in fulfilment (or partial fulfilment) of the requirements for the attainment of any qualification.

M/MOFOLO

08/12/2022

SIGNATURE OF STUDENT

DATE

Acknowledgements

I would like to thank Professor Mamello Sekhoacha for her guidance, support, and patience and, Professor Mashele for all his support. I would also like to extend my acknowledgments to Dr Mfengwana, your constant support from the start of the project is highly appreciated. Lastly, I would like to thank Dr Chika Ifeanyi Chukwuma for assisting with some practical work. Thank you to the National research foundation for all the financial assistance.

To my dearest mother, thank you for your patience, love, and support. My friends: Ipeleng Kopano Kgosiemang, Tebogo Setlabane Mampa, Vincent Napo, Lerato Khumalo and Relebohile lefojane, thank you for brining joy and love during my studies. I dedicate this book to my late father, Mr Mofolo.

Abstract

Nanotechnology has led to synthesis of small molecules that are used in pharmacology and many other fields. Historically, plants were used to treat a variety of ailments and currently nanotechnology and ethnomedicine is being adjoined to create safer and smaller medicinal molecules for treatment of these ailments. Brain cancer is one of the difficult ailments to treat due to the presence of the blood brain barrier which is very selective of molecules it permits.

In this research, three plants were selected: *Dieffenbachia camilla*, *Adenium multiflorum*, and *Pechuel-loeschea leibnitziae*. Plant-based molecules were extracted from these plants, and the phytochemicals of these plants was analysed. Furthermore, to mimic the brain and the normal human cells, cancerous brain cells and two normal cells were selected to observe the effect of the plant the plant-based molecule and nanoparticles. The inhibitory activity of these molecules was calculated and graphed.

The research found that the plant *P. leibnitziae* exhibited the highest - inhibitory activity against the cancerous cell line. The fractionation of *P. leibnitziae* extract showed the presence of Xerantholide compound. This plant extract was further used to synthesize silver nanoparticles which were further stabilized in liposomes. The inhibitory effect of the plant *P. leibnitziae* (3 µg/mL) extract was shown to have increased when silver nanoparticles were synthesized using this plant, which ranged from 0, 64-0, 71 µg/mL.

Contents

CHAPTER 1	18
BACKGROUND	18
1.1 Introduction.....	19
1.2 Problem Statement.....	20
1.3 Hypothesis.....	21
1.4 Aims and Objective.....	21
1.5 Chapter’s outline.....	22
CHAPTER 2	23
LITERATURE REVIEW	23
2.1 Cancer	24
2.1.1 Diagnosis, treatment, and side effects of brain cancer.....	24
2.2 Brain cancer	25
2.2.1 The type of brain cancer; Gliomas	26
2.2.2 Drugs used to treat gliomas brain cancer	27
2.3 Medicinal Plants in cancer research.....	28
2.4 Use of plants in nanotechnology.....	29
2.4.1 Metal oxide: silver nanoparticles	31

2.4.2	Liposomes nanocarriers.....	32
2.5	Plants of interest.....	33
2.5.1	<i>Dieffenbachia camilla</i>	33
2.5.1.1	Historical uses.....	34
2.5.1.2	Bioactive chemicals of the genus	34
2.5.2	<i>Adenium multiflorum</i>	35
2.5.2.1	Historical use	35
2.5.2.2	Bioactive chemicals	36
2.5.3	<i>Pechuel-Loeschea leibnitziae</i>	36
2.5.3.1	Historical use	37
2.5.3.2	Bioactive chemicals	37
CHAPTER 3	38
MATERIAL AND METHODS	38
3.1	Introduction.....	39
3.2	Plant extraction	39
3.3	Phytochemical analysis	40
3.3.1	Determination of phytosterols	40
3.3.2	Determination of pentose, tannins and saponins	40
3.3.3	Determination of glycosides.....	41
3.3.4	Determination of triterpenoids.....	41

3.3.5	Determination of anthroquines	41
3.3.6	Determination of flavonoids	41
3.3.7	Determination of alkaloids	42
3.4	The MTT assay	42
3.5	Antioxidant activity	43
3.5.1	Total flavonoids.....	43
3.5.2	Total phenolic content.....	43
3.5.3	DPPH radical scavenging assay	44
3.5.4	Ferric reducing antioxidant power	44
3.6	Statistical analysis.....	45
CHAPTER 4		46
<i>Dieffenbachia camilla</i>		46
4.1	Introduction.....	47
4.2	Methodology	47
4.2.1	Extractions, phytochemical analysis and MTT assay	47
4.2.2	GC-MS of HEX and DCM extracts	48
4.3	Results.....	48
4.3.1	The MTT assay results.....	49
4.3.2	Phytochemical analysis.....	52
4.3.3	GC-MS analysis of <i>D. camilla</i>	54

4.3.4 The total phenolic content and total flavonoid content.....	57
4.3.5 The ferric reducing antioxidant power results	58
4.3.6 The DPPH assay	59
4.4 Discussion.....	60
CHAPTER 5	62
<i>Adenium multiflorum</i>	62
5.1 Introduction.....	63
5.2 Results.....	63
5.2.1 Summary of the results.....	63
5.2.2 Phytochemical analysis	64
5.2.3 The total phenolic content and total flavonoid content	65
5.2.4 The ferric reducing antioxidant power (FRAP) results	66
5.2.5 The Free radical scavenging activity of the plant extract activity using the MeOH plant extract of <i>A. multiflorum</i> and antioxidant standard.....	66
5.2.6 The MTT assay results	68
5.3 Discussion.....	71
CHAPTER 6	73
<i>Pechuel-loeschea leibnitziae</i>	73
6.1 Introduction.....	74
6.2 Methodology	75

6.2.1	Phytochemical analysis	75
6.2.2	Silver nanoparticle (AgNP) synthesis	76
6.2.3	Characterization of silver nanoparticles	76
6.2.4	Liposome Synthesis.....	77
6.2.5	Characterization of Liposomes; Transmission electron microscopy	78
6.2.6	Isolation of cytotoxic compounds	78
6.2.7	Thin Layer Chromatography	78
6.3	Results.....	79
6.3.1	Phytochemical analysis	79
6.3.2	Characterization of AgNPs	80
6.3.2.1	UV–vis spectroscopy and XDR analysis.....	80
6.3.2.2	Fourier-transform infrared spectroscopy spectral analysis.....	81
6.3.2.3	Transmission electron microscopy and Scanning electron microscope	82
6.3.2.4	The X-ray photoelectron spectroscopy results	83
6.3.2.5	EDAX analysis of silver oxide nanoparticles.....	85
6.3.3	Characterization of Liposomes.....	86
6.3.4	The MTT assay results	88
6.3.5	Fractionation of the DCM extract and isolation of active compound	91
6.3.5.1	Identification of the chemical structure of the isolated compound	92
6.3.5.2	Cell growth inhibition of CHO cells by <i>P. leibnitziae</i> fractions.	93



6.4	Discussion	95
CHAPTER 7		98
GENERAL DISCUSSION AND CONCLUSION		98
7.1	The relevance of the study	99
7.2	The extent to which objectives have been met	101
7.3	Challenges and limitation	104
7.4	Conclusions.....	104
REFERENCE.....		106
SUPPLEMENTARY PICTURES		124

List of Abbreviations

Ag ₂ O	Silver oxide
AgNPs	Silver nanoparticles
BBB	Blood Brain Barrier
CHO	Chinese hamster ovary cell
CuO	Copper oxide
DCM	Dichloromethane
DMEM	Dulbecco's Modified Eagle Medium
DMSO	Dimethyl sulfoxide
DNA	Deoxyribonucleic acid
EDAX	Energy-dispersive X-ray spectroscopy
FTIR	Fourier-transform infrared spectroscopy
G ₂ /M	Second growth phase in Mitosis
HEX	Hexane
MgO	Magnesium oxide
MTT	3-(4,5-dimethylthiazol-2-yl)-2,5-diphenyltetrazolium bromide
RT	Room temperature
SEM	Scanning electron microscope
Si	Silicon
TEM	Transmission electron microscopy
TiO ₂	Titanium dioxide
U87	Uppsala 87 Malignant Glioma
WHO	World Health Organization



XPS X-ray photoelectron spectroscopy

ZnO Zinc oxide

List of Figures

Figure 1. The location of tumors within the brain. (Source- https://www.webmd.com/cancer/brain-cancer/ss/slideshow-brain-cancer).	26
Figure 2. The endothelial cells which makeup the blood brain barrier (Source; https://images.app.goo.gl/LQo64dghU7fUGRU17)	27
Figure 3. The different nanoparticles according to the nanoscale. Source (http://www.britishsocietynanomedicine.org/what-is-nanomedicine/).....	31
Figure 4. <i>D. camilla</i> leaves (source- https://www.ourhouseplants.com/plants/dieffenbachia ,)	33
Figure 5. The flowers of <i>Adenium multiflorum</i> obtained from safari nursery (source- https://worldofsucculents.com/adenium-multiflorum-impala-lily/)	35
Figure 6. The plant <i>P. leibnitziae</i> (source: https://www.kyffhauser.co.za/Plants3/Pechuel-Loeschea_leibnitziae/Image1.htm)	36
Figure 7. Growth inhibitory effects of <i>D. camilla</i> extracts on CHO cells. Each of the values represents the mean of three independent experiments \pm SD.	51
Figure 8. Inhibitory effects of <i>D. camilla</i> extract on Vero cells. Each of the values represents the mean of three independent experiments \pm SD.	51
Figure 9. The MS spectra of the (a) HEX and (b) DCM extracts.	57
Figure 10. The DPPH results of four samples at a range of concentrations [μ g/mL]. Each of the values represents the mean of three independent experiments \pm SD. The values with different letter are considered significantly different ($P < 0.05$, one-way analysis of variance (ANOVA) followed by Tukey-Kramer test) from each other.	59

Figure 11. Free radical scavenging activity of the MeOH extracts of <i>A. multiflorum</i> , and antioxidant standards.	67
Figure 12. Inhibitory effects of leave extracts [1, 10 and 100 µg/mL] of <i>A. multiflorum</i> on Vero.....	69
Figure 13. Inhibitory effects of roots extracts [1, 10 and 100 µg/mL] of <i>A. multiflorum</i> on Vero cells.	69
Figure 14. Inhibitory effects of leave extracts [1, 10, and 100 µg/mL] of <i>A. Multiflorum</i> on U87 cells.	70
Figure 15. Inhibitory effects of leaves extract [1, 10, and 100 µg/mL] of <i>A. multiflorum</i> on U87.....	70
Figure 16. The UV-vis absorption spectra of silver nanoparticles synthesised using the MeOH extract of <i>P. leibnitziae</i>	80
Figure 17. The XRD pattern of silver oxide nanoparticle synthesized using MeOH extract of <i>P. leibnitziae</i>	81
Figure 18. The FTIR spectra of the silver oxide nanoparticles.....	82
Figure 19. (A), the TEM results of silver oxide nanoparticles observed at 100 nm. (B) SEM results of silver oxide nanoparticles observed at 100 µm.....	83
Figure 20. X-ray photoelectron spectroscopy spectrum of silver oxide nanoparticles. The red line represented before annealing and blue line represents after annealing of the sample.	84
Figure 21. The XPS spectra of components present in the silver oxide nanoparticle sample. Red line represents before annealing and blue line after annealing of sample.....	85
Figure 22. The EDAX spectrum showing peaks of elements present in the sample. Carbon (50%), Oxygen (26%), Nitrogen (18.7%) and Silver (5.3%) were detected. The organic	

elements could be from functional groups of the phytochemical components present in the plant.....86

Figure 23. TEM analysis of stained liposomes. The white circles show empty liposomes, while red circles indicate silver encapsulated liposome. The liposomes were stained with saturated uranyl acetate aqueous solution.87

Figure 24. TEM analysis of unstained liposomes unstained liposomes, white circles indicate empty liposomes and red circles indicated liposomes encapsulating silver nanoparticles (i.e., AgNPs inside of the liposomes).....87

Figure 25. The inhibitory effect of the DCM and MeOH extracts of *P. leubnitziae*; AgNPs, and emetine on Vero cells.....88

Figure 26. The growth pattern of the U87 Glioma over a period of 48 hours; A) The U87 glioma cells on the first day after thawing of the cells, before incubation B) The cells after an hour of incubation, C) The cells after 24 hours of incubation, and D) the cells after 48 hours of incubation.....89

Figure 27. The cell viability count results of the cell culture after 2 hours and 12 hours of incubation with medium containing silver nanoparticles at a concentration of 1 µg/ml.90

Figure 28. The cell growth inhibitory effects of test samples against the U87 cell line, a) batch 1= DCM extracts, batch 2= DCM extract from Namibia. b) Cytotoxic standard drug emetine used as positive control; nanoparticles synthesised using plant material. The synthesis experiment was repeated twice to produce batch 1 and batch 2 of the nanoparticles.91

Figure 29. Fractionation of the DCM extract by column chromatography, A) the TLC plate with the different fractions (F70-F77), and B) the crystalized fractions F70-77 and F78-90 after being combined based on their similar profile on TLC plate.92

- Figure 30.** The structural characterization of a C13 compound with molecular weigh 246.3042 g/mol93
- Figure 31.** Inhibitory effect of DCM fractions of *P. leubnitziae* and Emetine on CHO cells.94
- Figure 32.** Inhibitory effect of DCM fractions of *P. leubnitziae* and Emetine on U87 cells..94
- Figure 33.** Inhibitory effect of DCM fractions of *P. leubnitziae* and Emetine on Vero cells. 95

List of Tables

Table 1. CSIR standard criteria for anticancer and cytotoxicity. (Supplementary table)	49
Table 2. Antioxidant and cytotoxicity activities [$\mu\text{g}/\text{mL}$] exhibited by organic extracts of <i>D. camilla</i>.	50
Table 3. The phytochemical analysis of the roots and leaf plant parts <i>D. camilla</i>.	52
Table 4. The GC-MS analysis of the extracts HEX and DCM of the plant <i>D. camilla</i>.	55
Table 5. A summary of the FRAP results, the total flavonoid and phenolic content results, represented in mean \pm SD.	57
Table 6. The phytochemical analysis <i>A. multiflorum</i> plants	64
Table 7. Total phenolic content, total flavonoid content and antioxidant activity using the MeOH plant extract of <i>A. multiflorum</i>.	65
Table 8. The Summary of Percentage inhibition of DPPH using four different samples.	67
Table 9. The IC_{50} values of the root and leaf extracts against the Vero and U87 cells.	71
Table 10. Summary of Phytochemical analysis for the DCM extract of <i>P. leibnitziae</i>, where (+) means the presence and (-) means the absence of the tested phytochemical.	79
Table 11. The IC_{50} [$\mu\text{g}/\text{mL}$] values of cell growth inhibitory effect of the DCM extracts of <i>P. leibnitziae</i>, the AgNPs and emetine drug	91

CHAPTER 1

BACKGROUND

1.1 Introduction

The normal signal transduction of a cell is an essential factor for proper functioning of human cells. Cancer is a disease that is known to cause defects in the signal transduction of normal cells (Berg et al., 2002), leading to the uncontrollable proliferation of cells. This disease is one of the major causes of mortality in South Africa and the world at large. Amongst many factors that contribute to the formation of cancer, studies have shown that reactive oxygen species contribute by damaging the DNA, which consequently leads to uncontrolled cell proliferation (Borek, 2004). Cancer is classified according to the organ/tissue of origin. The current study focused on glioblastoma multiforme brain cancer. Treatments for cancer range from surgery, radiation, and chemotherapy, depending on the location and type of cancer. Chemotherapy remains the most used form of treatment for cancer. Glioblastoma multiforme, along with other brain tumors, are difficult to treat successfully due to presence of the blood brain barrier, which is known to hinder chemotherapeutic drugs from crossing into the brain by acting as selective barrier between the blood and brain.

Historically, medicinal plants have been used as an affordable alternative treatment for many ailments, including cancer. Medicinal plants have been demonstrated to contain secondary metabolites which are often responsible for the pharmacological properties of the plant. In human nutrients these metabolites can serve as antioxidants capable of reducing reactive oxygen species, thus reducing the increased risks of cancer development. Furthermore, these secondary metabolites have been demonstrated to reduce metal such as silver, gold and many more metals into nanoparticles (Marstin et al., 2018; Leela and Vivekanandan, 2008), in a method known as green synthesis. One of the advantages of these synthesised nanoparticles is

that they minimize side effects when used in treatment. The current study focused on silver nanoparticles due to their demonstrated ability to cross the blood brain barrier (BBB) and induce cell apoptosis (Jinglong Tang et al., 2010; Carlson et al., 2008). The study further develops liposome-silver nanoparticle moiety, which is designed to mimic the cell blood brain barrier in order successfully carry drug through brain compartments while also preventing the silver nanoparticles from damaging healthy brain cells during diffusion across the BBB.

1.2 Problem Statement

The blood brain barrier (BBB), which is made up of endothelial cells, provides a major problem in delivering chemotherapeutic agents across the brain due to its selectivity against drugs based on the particle size and other properties. The endothelial cells of the blood brain barrier are separated by tight junctions that allow only few small polar compounds to diffuse across (Mahringer et al., 2013) and restrict approximately about 98% of small molecule and all large molecular drugs from entering the brain (Jeong et al., 2019), consequently making chemotherapy a more complicated type of treatment. Nanoparticles have demonstrated to have unique size, morphology, and ability to successfully cross the BBB. However, the delivery of metallic nanoparticles including silver nanoparticles to cancerous brain cells is shown to induce epithelial cell damage of the blood brain barrier cells (Xu et al., 2013). Thus, this requires the need to encapsulate the silver nanoparticles in liposomal nano-carriers which are less harmful to cells and mimic the brain environment for easy crossing of the BBB. The study therefore aimed to identify plants with potential anticancer activity, antioxidant activity, and ability to reduce silver to silver nanoparticles, and further stabilize the synthesised nanoparticles in a

nano-carrier that mimics the lipophilic brain environment for easy delivery across the blood brain barrier and brain compartments.

1.3 Hypothesis

The selected plants have the potential to reduce metallic silver to silver nanoparticles. Furthermore, cationic liposomes will successfully encapsulate and stabilize the silver nanoparticles. It is hypothesised that the designed liposome-silver nanoparticles carrier system can deliver silver nanoparticle across the blood brain barrier with minimal toxicity to normal brain cells.

1.4 Aims and Objective

The aim of the study was to discover plant constituents with anti-proliferative activities against brain tumor cells, then design a drug delivery nano-system that mimic the brain environment for efficient delivery of anti-cancer agents into the brain. The objectives were:

1. To extract plants using selected organic solvents and water, and to determine the anti-proliferative activity of the extracts on U87 glioma, and test for selectivity using CHO and Vero mammalian cell lines.
2. To apply chromatographic techniques for fractionation of active extracts and isolation and identification of plant constituents responsible for the observed anti-proliferative activity.
3. To synthesise silver nanoparticles and screen them for increased cytotoxicity effects against the U87 glioma cell line.
4. Synthesise cationic liposomes and encapsulate AgNPs in cationic liposomes.

The scope of the project was limited to in vitro work. Testing of the ability of the encapsulated AgNPs nanoparticle to cross the blood brain barrier in Sprague rats, falls under future work.

1.5 Chapter's outline

The study is presented in seven chapters. Chapter one introduced the study, while chapter two discussed the literature. Chapter 3 summarized the general methods applied on the selected plants, while methods that are specific to a particular plant are covered in chapters of respective plants. The project investigated three families of plants and each family produced an article, which is presented as a chapter.

Chapter 4 focused on the *Dieffenbachia camilla* family, chapter 5 focused on *Adenium multiflorum*, while chapter 6 focused on *Pechuel-loeschea leibnitziae*. The plant *P. leibnitziae* exhibited the highest - inhibitory activity against the U87 glioma cell line, and thus was used to synthesize silver nanoparticles which were further stabilized in liposomes. Finally, chapter 7 summarized and concluded the findings of the research and the extent at which objectives of the study were achieved.

CHAPTER 2

LITERATURE REVIEW

2.1 Cancer

Cancer is a disease which causes defects in signal transduction of normal cells, consequently leading to uncontrolled cellular growth (Berg et al., 2002). The normal functioning of the body requires that strict developmental mechanisms be followed. These include:

- a) **differentiation** - a process where cells become more specialized,
- b) **proliferation** - a process that results when cell increase in number,
- c) **migration** which is the locomotion of cell in response to change in signals and finally,
- d) **apoptosis** known as programmed cell death (Cooper, 2000).

Cancerous cells, however, cease to follow these strict developmental mechanisms, instead they begin excessive proliferation resulting in the formation of either benign or malignant tumor.

Benign tumors are lesions that are characterized by expansive growth, slow rates of proliferation and are non-invasive to surrounding tissues (Baba and Catoi, 2007). Some examples of benign tumors include lipomas, moles, adenomas, and fibroids. When benign tumors metastasize, invade, and colonize new sites in the body, they lead to **malignant tumors** (Nieder et al., 2014), which are life threatening in contrast to benign tumors.

2.1.1 Diagnosis, treatment, and side effects of brain cancer

The causes of brain tumors are difficult to prove, with research showing that only 5% of brain tumors such as neurofibromatosis, tuberous sclerosis is hereditary (cancer.net, 2017, Levin et al., 2001). The diagnosis of brain cancer is limited to; blood test, biopsy, and scanning, which involves brightening up the veins by injecting patients with fluorescent agent and observing the results through the X-ray (Swensen et al., 2002). The diagnosis or detection step is followed

by treatments such as surgery, radiation therapy, and chemotherapy. Surgery aims to remove the tumor cells from healthy cells by excision and is considered suitable for inaccessible tumors (Order et al., 1968). While radiation therapy attempts to destroy cancerous cells using high energy radiation that is focused and delivered towards a target lesion (Fabi et al., 2011). The other treatment that is moderately non-invasive and remains the most used method of treatment to the human body is chemotherapy, which aims to destroy tumor cells using drugs (Doolite et al., 2014).

Although treatment using surgery can assist in decreasing the spread of cancer, some negative side effects have been recorded in patients after and during surgical treatment. These include brain swelling, seizures, muscle weakness, and change in brain function (Charles et al., 2016). Radiation and chemotherapy have been identified to share some similar side effects such as hair loss, low body energy, vomiting and nausea. Furthermore, chemotherapy has been shown to affect normal cells, as well as depress the immune system, resulting in susceptibility to infections (Penn, 1981). The severity of adverse effects depends on the type of cancer, e.g., breast, colon, kidney, lung, and brain cancer (Cooper, 2000), and the specific location of the cancer.

2.2 Brain cancer

Brain cancer is characterized by the low survival rate (Cheng et al., 2014), with approximately 24,000 brain cancer incidences reported annually in adults (Parisot et al., 2016). The presence of brain tumors affects a lot of organs and body functions such as muscle control, sensation, memory to mention, because of the location of the tumors within the brain (figure 1). It has

been shown that 44.4 % of all brain tumors are due to glioma family, 21.6 % are astrocytoma and a large amount, 51.9 %, of recorded brain tumors comprises of glioblastoma (Joshi et al., 2010).

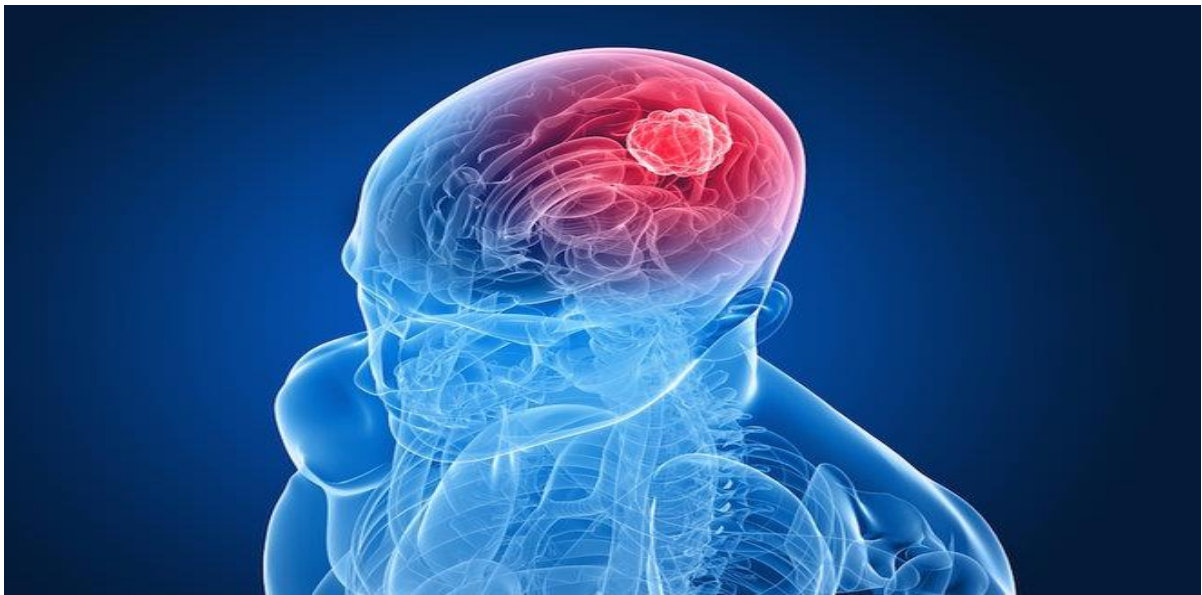


Figure 1. The location of tumors within the brain. (Source-<https://www.webmd.com/cancer/brain-cancer/ss/slideshow-brain-cancer>).

2.2.1 The type of brain cancer; Gliomas

The study focused more on glioma brain cancer. Gliomas are a type of brain tumor that arises from a type of glial cell found in the brain (Béduneau et al., 2007), and are categorized by resistance to apoptosis and diffuse infiltration (Furnari et al., 2007). The actual cause of gliomas brain tumor has not been pinpointed yet, and genetic mutations are the only speculated cause of the disease (Chang et al., 2010). Gliomas include the malignant oligodendrogliomas, ependymomas and astrocytoma which according to WHO, are the most aggressive tumor with treatment just aiming to prolong survival rate in patients (Behin et al., 2003). The treatment of glioma tumors is made even more difficult by the presence of the blood-brain barrier (BBB).

The BBB (depicted in figure 2) is composed of capillary endothelial cells associated with pericytes, which are known to regulate brain capillary blood flow through contraction and relaxation (Davson and Oldendorf, 1967, Peppiatt et al., 2006). The endothelial cells of the blood brain barrier are separated by tight junctions that allow only few small polar compounds to diffuse across (Mahringer et al., 2013) and restricts approximately 98% of small molecule and all large molecular drugs from entering the brain (Jeong et al., 2019), consequently making chemotherapy a more complicated type of treatment.

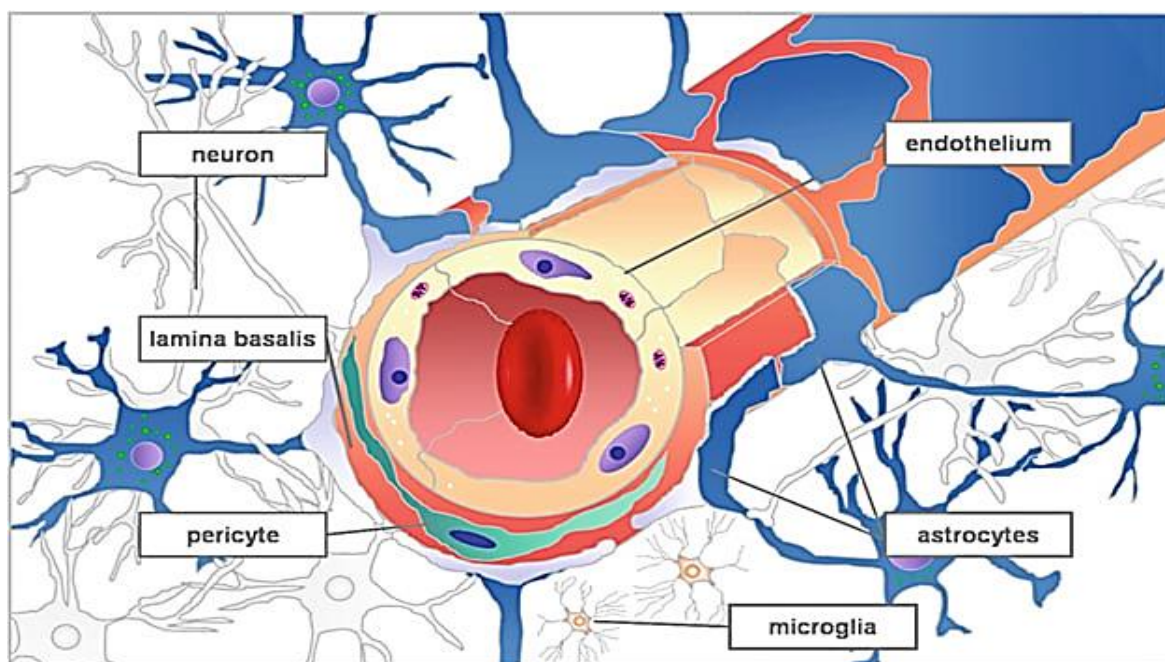


Figure 2. The endothelial cells which makeup the blood brain barrier (Source; <https://images.app.goo.gl/LQo64dghU7fUGRU17>)

2.2.2 Drugs used to treat gliomas brain cancer.

Many of the currently proposed therapies for malignant brain tumor fail to provide long-term management because they target both tumor cells, healthy and vital normal brain cells (Zhou et al., 2007). Carmustine and temozolomide have been used widely in treatment of malignant

glioma (Mody and Wheelhouse, 2014) due to their ability to cross the blood brain barrier. Carmustine (BCNU) is an alkylating agent which has been demonstrated to have anticancer activities against brain tumor, malignant melanoma, and certain other neoplasms (O'Driscoll et al., 1990). One characteristic that makes the drug essential in brain cancer treatment is its lipophilicity, which enables it to cross the BBB. The drug however has been shown to have limitations such as sensitivity to aqueous solutions with short serum half-life of 15 min, and cause lung fibrosis within three years of treatment (Haque et al., 2006).

Temozolomide has received enhanced attention and approval by the FDA following lapsing of patients after treatment with nitrosourea drug such as carmustine (Friedman and Kerby, 2000). Temozolomide is a derivative of imidazotetrazine which is administered orally. Following consumption, the drug is converted to 5-(3-methyl)-1-triazen-1-yl-imidazole-4--carboximide (MTIC), which is responsible for the antitumor activity (Reid et al., 1997). This drug has been shown to be distributed to all brain tissues, including penetration into the CNS with relatively low toxicity (Stevens et al., 1987).

2.3 Medicinal Plants in cancer research

Many cancer patients, especially in developing countries encounter financial burden for treatment with drugs such as carmustine and temozolomide (William et al., 2011). Plants are an accessible source of medicaments (Farnsworth et al., 1985). Naturally, plants exhibit chemical defence mechanism against predators (War et al., 2012) by releasing secondary metabolites. These secondary metabolites possess various pharmacological properties and are often utilized as alternative treatments for diseases such as diabetes, inflammation, and cancer (Ashokkuma and Ramaswamy, 2014), to mention a few. Phytochemicals such as flavonoids,

tannins, curcumin, resveratrol and gallacatechins have been identified in medicinal plants and demonstrated to have some anticancer properties (Azmi et al., 2006).

2.3.1 Plants as antioxidants

The diverse bioactive compounds synthesized in plants have been demonstrated to be beneficial supplements that can be potentially used as antioxidants by the human body (Boots et al., 2008). Antioxidants are defined as chemicals or substances with a potential to prevent the oxidation stress in human cells by scavenging initiating reactive oxygen species (ROS) and decreasing localized oxygen concentrations (Miguel, 2010). A variety of antioxidants which include carotenoids, phenolic compounds, flavonoids, lignans, and many more have been identified in plants (Suffredini et al., 2004). Polyphenols such as phenolic acids and flavonoids have been shown in vitro studies to exert higher antioxidant action in contrast to antioxidants that are found in fruits and vegetables such as vitamins (Fresco et al., 2010). Many methods have been implemented to assay the presence of these antioxidants in plants, these include the 2, 2-diphenyl-1-picrylhydrazyl (DPPH) assay, which involves the fast transfer of electron from the sample to DPPH, the FRAP (ferric reducing antioxidant power) assay method which involves the reduction of the complex ferric ion-2,4,6-tri(2-pyridyl)-1,3,5-triazine (TPTZ) by the antioxidants (Thaipong et al., 2006).

2.4 Use of plants in nanotechnology

The application of nanotechnology has been widely used in medicine for delivery of drugs to target organs and tissues (De Jong et al., 2008). This field focuses on understanding and controlling matter in the range of 1-100 nm, with characteristics that range from small size,

large surface to mass ratio, high reactivity, and unique interaction with biological systems (Adams et al., 2014). Some of the advantages of nanocarriers include improved serum solubility of the active compound, prolonged circulation time, drug release control and simultaneously delivery of multiple therapeutic agents to a cell for combined therapy (Lee et al., 2015).

In cancer research, a variety of nanoparticles designs have been proposed for diagnosis and treatment of cancer due to some of the characteristic such as the small size and architecture of the nanoparticles, which promote diffusion within the cell (Brigger et al., 2012). Nanoparticles as seen in figure 3 range from liposomes, polymer nanoparticles, micelles, dendrimers, quantum dots, and metal oxide nanoparticles (Mura et al., 2013). Different methods, including physical, chemical, and biological methods, have been successfully used to produce nanoparticles (Zhang et al., 2016). However, the challenge encountered while applying some of the methods is the release of hazardous by-products into the environment and the expense required to apply these methods (Reijnders, 2008).

Thus, it has become quite important to exploit more environmentally friendly, cheap, and easy methods for synthesis of nanoparticles (Kathiravan et al., 2014). Green synthesis aims to combat the negative aspects encountered by many methods used for synthesis of nanoparticles (Hutchison, 2008). In green synthesis, biological materials such as plant material are used to reduce noble metals into nanoparticles (Marslin et al., 2018).

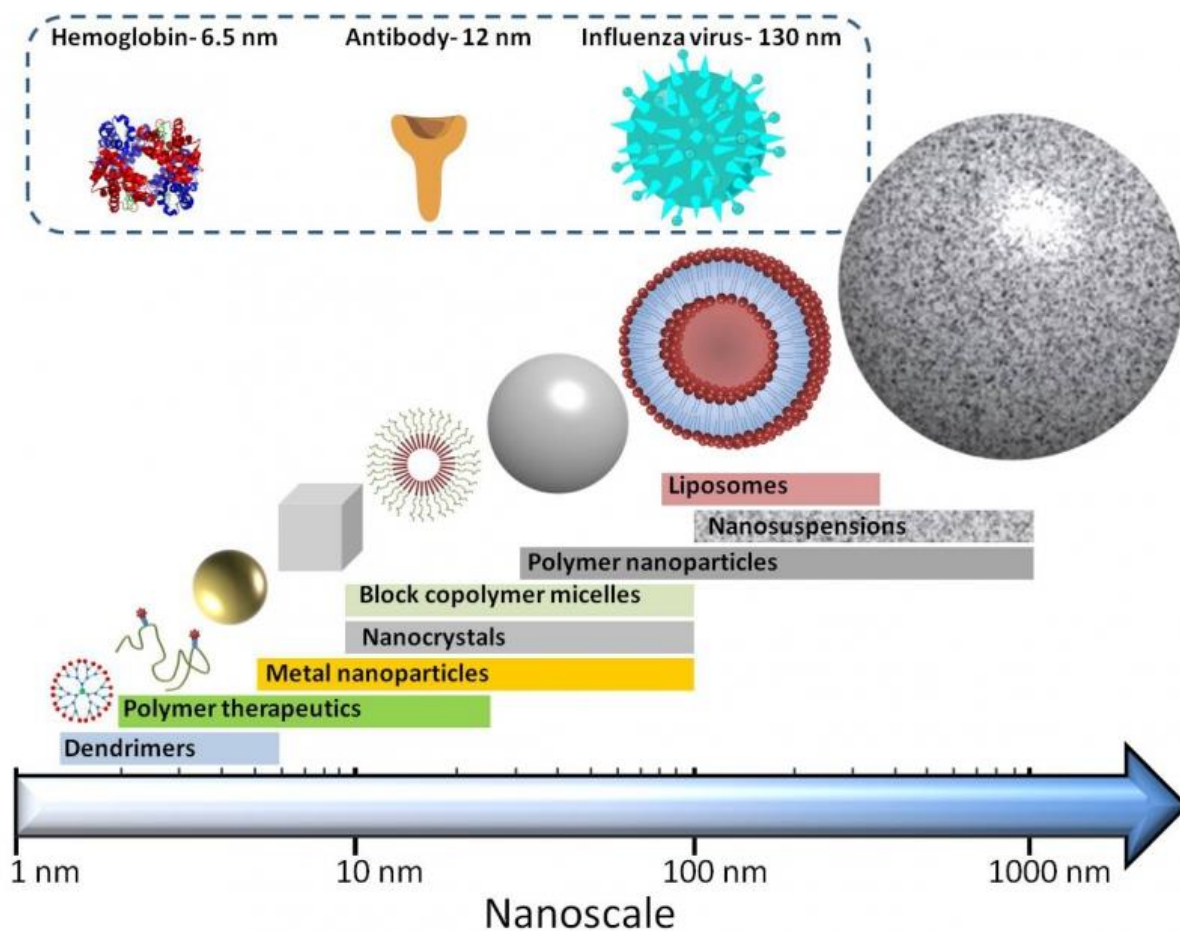


Figure 3. The different nanoparticles according to the nanoscale. Source (<http://www.britishsocietynanomedicine.org/what-is-nanomedicine/>).

2.4.1 Metal oxide: silver nanoparticles

More recently, silver nanoparticles (AgNPs) have been introduced as innovative alternative applications in areas such as diagnostic medicine, disinfection, and most importantly for drug delivery to the target cell (Zhang et al., 2016). The cytotoxicity of silver nanoparticles has been investigated in cancer research, due to their capacity to induce the expression of genes associated with impaired cell cycle progression, DNA damage, and apoptosis in human cancerous cells (Asharani et al., 2009). According to Urbańska and colleagues, AgNPs induced DNA damage leading to cell cycle arrest in G2/M phase and enhanced apoptosis of tumor cells,

including glioblastoma multiform (Urbańska et al., 2015). However, when considering the neurotoxic effects of silver nanoparticles, research has shown that exposure to AgNPs inhibits extension of neurites and results in degeneration of neurons (Xu et al., 2013), thus requiring the stabilization of these nanoparticles.

2.4.2 Liposomes nanocarriers

Liposomes are spherical lipid vesicles with a bilayer membrane structure consisting of amphiphilic lipid molecules (Alberts et al., 2002). Liposomes are often selected to stabilize metal nanoparticles due to their unique structure, which allows them to carry both hydrophilic and hydrophobic compounds without changing the compounds. Studies have shown that when liposomes aggregate, the lipid bilayers become extremely impermeable to ionic and polar substances, which consequently increase with their solubilities in nonpolar solvents. In a previous study done by Castangia et al (2017), silver nanoparticles were successfully stabilized in phospholipid vesicles. The most used lipids in preparation of liposomes are phosphatidylcholine, which are best known to mimic the cell membrane and can fuse with microbes (He et al., 2019).

2.4.2.1 Advantages of encapsulating with liposomes

Some of the advantages of using liposomes as nanocarriers is their ability to passively accumulate in tumors and exploit the overexpression of fenestrations in cancer neovasculature, thus increasing drug concentration at tumor sites (Li. et al., 2015). The target liposomes, cationic liposomes, consist of natural neutral phospholipids and positively charged lipids. Cationic liposomes have been selected in this study due to their electrostatic interaction with

membrane anionic microdomains of the brain's capillary endothelial cells and the enhanced affinity for angiogenic endothelial cells and the subsequent anticancer effect (Schnyder and Huwyler, 2005).

2.5 Plants of interest

The study focused on three plants: *Dieffenbachia camilla*, *Adenium multiflorum* and *Pechuel-leosche leibnitzae*. The selected plants have been historically used for treatment of different alignments, however there is limited information of the use of these selected plant in cancer, specifically brain cancer, and in using these plants in the green synthesis of nanoparticles.

2.5.1 *Dieffenbachia camilla*



Figure 4. *D. camilla* leaves (source- <https://www.ourhouseplants.com/plants/dieffenbachia>,

The dieffenbachia species belongs to the family *Araceae*. *Dieffenbachia*, also known as dumb cane, is one of the most diverse families with more than 97 species including hybrids. Morphologically, the family has monocotyledonous flowering plants with flowers that are

borne on a spadix, and prefers shady, moist lowlands of many parts of tropical places (Fochtman et al., 1969). Majority of *Dieffenbachia* species were identified to contain a diversity of calcium oxalate crystals differing in morphology, size, and tissue localization (Cote, 2009; Arditti and Rodriguez, 1982). The current study focuses on *Dieffenbachia mutala* “*camilla*” (figure 4).

2.5.1.1 Historical uses

Historically, the genus was used for treatment of conditions such as gout, dropsy, sexual impotence, and frigidity (Fochtman et al., 1969). The plants such as *Dieffenbachia seguine* belong to the *Dieffenbachia* family were used in the Caribbean Islands to bring about male sterility. Research has been conducted to evaluate the possibility of using the plants in cancer treatment (Arditti et al., 1982).

2.5.1.2 Bioactive chemicals of the genus

Alkaloids were identified to be amongst the toxic and poisonous chemicals in this family (Burkil, 1985). One of the most researched bioactive chemicals is the needle-shaped calcium oxalate crystals called raphides, which is a toxic chemical known to cause kidney stones in humans, and can potentially cause fatality (Fochtman et al., 1969). Another identified chemical is the eugenol (4-alil-2-metoxiphenol) and this was reported to cause buccal ulcerations and tongue hypertrophy (Dip et al., 2004).

2.5.2 *Adenium multiflorum*



Figure 5. The flowers of *Adenium multiflorum* obtained from safari nursery (source-<https://worldofsucculents.com/adenium-multiflorum-impala-lily/>)

Adenium multiflorum also known as impala lily (figure 5) in South Africa, belongs to the population *Nerieae* of the subfamily *Apocynoidae* (Plaizier, 1980). *A. multiflorum* is a succulent shrubby tree which grows in open forest. The plant and others in its genus are most known for their potential toxic effects mediated by digestive disturbances and cardiac insufficiency (Burrows and Tyrl, 2013).

2.5.2.1 Historical use

Adenium multiflorum was used historically for many ethnoveterinary medicinal uses, and as an arrow poison in game hunting and fishing (Bradfield et al., 2015). The plant was used for years in Zimbabwe to manage warts and ectoparasites by small-holder farmers (Marandure, 2016).

2.5.2.2 Bioactive chemicals

The phytochemical analysis of *A. multiflorum* family contained different groups of chemicals, which included the cardiac glycoside, flavonoid, prenylated flavonoids, and terpenoids amongst others (Akhtar et al., 2017). Some of these chemicals were identified to have different biological activities like antiviral, antitumor, and cytotoxic activities (Hossain et al., 2014). *Adenium obesum* a plant belonging to the *Adenium* family, for instance contained various bioactive molecules which exhibited cytotoxic property against epidermoid carcinoma of the nasopharynx system in human beings (Paul Dipak et al., 2015).

2.5.3 *Pechuel-Loeschea leibnitziae*



Figure 6. The plant *P. leibnitziae* (source: https://www.kyffhauser.co.za/Plants3/Pechuel-Loeschea_leibnitziae/Image1.htm)

The plant *P. leibnitziae* which is commonly known as the bitterbrush, stink bush, and bitterbos, is a chamaephyte belonging to the family Asteraceae (Roodt, 1998). *P. leibnitziae* is the only

existing species known and reported so far in this research. The plant is indigenous to Southern Africa. It is also found in areas that include Botswana, southern Angola, Swaziland, Zimbabwe, and Namibia (Le Roux et al., 2009, Foden and Potter, 2005). It mostly inhabits riverbeds throughout the whole of Namibia except in the far north-eastern part. Morphologically the plant looks greyish, due to the fine pubescence covering all plant parts (figure 6). The linear stems have an aromatic smell and contain aromatic oils (Le Roux et al., 2009).

2.5.3.1 Historical use

The root extracts of the plant were used to treat diseases such as gonorrhoea, fever, colds, stomach pains, while the dried stems were used to treat wounds (Le Roux et al., 2009). The people of Namibia reportedly use *P. leibnitziae* to delay menstruation by administering steam baths with leaf decoctions of the plant, which are used for thorough washing of the abdomen and for treatment of skin disorders using the heat vapour of the plant extracts (Koenen, 1996).

2.5.3.2 Bioactive chemicals

Phytochemical analysis of *P. leibnitziae*'s roots and stem extracts showed the presence of the saponins which are steroids or triterpenoid glycosides (Francis et al., 2002). The anthraquinones, an important class of natural and synthetic compounds with a wide range of applications, such as antioxidant activity (Malik et al., 2016), were also identified in the plant. Other research showed the presence of flavonoids and polyphenols in the plant (Ndongo, 2017).

CHAPTER 3

MATERIAL AND METHODS

3.1 Introduction

The chapter outlines general methods and procedures used for the plant extraction, phytochemical analysis, and antioxidant activity of the selected plants.

3.2 Plant extraction

The plant *D. camilla* was collected from Pretoria, South Africa, during summer season, while *A. multiflorum* was collected from the Safari Garden. The powdered root part of the *P. leibnitziae* was donated by Dr Pauline Kadhila from the University of Namibia. The voucher number of *P. leibnitziae* is 13, the identity was confirmed by the curator from National Herbarium at the National Botanical Research Institute of Namibia.

The plant materials of *A. multiflorum* (whole plant) and *D. camilla* (leaves, roots) were dried at room temperature in a dark place, and then pulverized. The powdered plant material of each plant was weighed (10g), immersed in solvent (100 ml), and left on a shaker (FMH instruments, sep sci, speed 100 pr) for 48 hours, then filtered using a filter paper (whatman® Maidstone).

Extraction was performed sequentially using organic solvents in their increasing order of polarity; hexane (HEX), dichloromethane (DCM), DCM: Methanol (MeOH) (1:1) and MeOH for *D. camilla*. The plants *P. leibnitziae* and *A. multiflorum* were extracted using HEX, DCM, and MeOH. An additional solvent, ethyl acetate, was included for extraction of *A. multiflorum* to ensure full recovery of both extract both polar and nonpolar compounds. The extraction process was done in the decreasing polarity of the selected solvents. The filtrates were concentrated using a rotary evaporator (Buchi, labotech Switzerland) and concentrated extracts were further dried in pre-weighed vials under the fume hood, then stored at -4 °C until further use.

3.3 Phytochemical analysis

The powdered material of the roots and leaves of *D. camilla* and whole plant of *A. multiflorum* were screened for selected phytochemicals according to the protocols of Bhandary et al (2012) and Yusuf et al (2014). The plants were screened for the presence of phytosterols, pentose, tannins, alkaloids, glycosides, triterpenoids, anthraquinones, saponins, flavonoids, and alkaloids:

3.3.1 Determination of phytosterols

Powdered material was weighed (50 mg) and 10 mL of chloroform was added to the test tube with the material. From the solution, 0.5 mL was placed in a separate tube and 2 mL of concentrated sulphuric acid was cautiously added and mixture was heated for 5 minutes. The tube was monitored for presence of reddish-brown colour in the chloroform layer.

3.3.2 Determination of pentose, tannins and saponins

In a test tube 40 mL of distilled water was added and 2 g of powdered plant material. For pentose determination, 2 mL filtrate was collected into a separate tube and 2 mL of hydrochloric acid containing a drop of phloroglucinol was added, then heated for five minutes. The appearance of a red colour change was observed as positive. The distilled water extract was further analysed for tannins. A volume of 20 mL was collected into a separate tube, boiled, and filtered while still hot. The mixture was then treated with 3 drops of 0.1% of ferric chloride and presence of a blue colour change was indicated as presence of tannins. From the remaining distilled water extract, 5 mL water extract was collected, boiled, and filtered. Total volume of 3 mL of distilled water was added to the filtrate and the mixture was shaken vigorously for 5 minutes. Frothing was an indicator for presence of saponins.

3.3.3 Determination of glycosides

A total of 0.5 g grounded plant powder was weighed and added into a separate tube with 2 mL acetic acid. The mixture was further treated with 1 drop of 0.1 % of ferric chloride. To the mixture, 1 mL of concentrated sulphuric acid was cautiously added, and appearance of a brown ring was indicative of glycosides.

3.3.4 Determination of triterpenoids

The grounded powder was weighed (2 g), mixed with 1 mL of chloroform and 3 mL of concentrated sulphuric acid was added. The presence of a reddish-brown colouration in between the chloroform layer and sulphuric acid was an indicator for triterpenoids in the mixture.

3.3.5 Determination of anthroquines

The plant material was weighed (1g); 12 mL of hydrochloric acid was added into a test tube and boiled for 5 minutes. The mixture was filtered and cooled down, and then 10 mL of chloroform was added to the filtrate. The two different layers were separated into two tubes, and to the test tube containing chloroform layer; 10 mL of 10% ammonia solution was added to the mixture and then shaken. The presence of anthroquines was monitored for the formation of a rose-pink colour when the two layers were separated.

3.3.6 Determination of flavonoids

In a test tube, 0.5 g of the plant powder was mixed with 10 mL of ethyl acetate, heated for 3 minutes, and allowed to cool. The mixture was filtered, and 1 mL of diluted ammonia solution was then added to 5 mL of the filtrate. The mixture was shaken, and presence of a yellow precipitate was an indicator of presence of flavonoids.

3.3.7 Determination of alkaloids

A weight of 0.2 g of the powdered plant material was placed in a separate test tube and 2 mL of 1 % hydrochloric acid was added. To the mixture, 1 mL of Meyer's reagent was added, followed by addition of 1 mL of dragendorff reagent.

3.4 The MTT assay

Cytotoxicity of all three plants (*D. camilla*, *A. multiflorum* and *P. leibnitziae*) was assessed using MTT assay against the CHO and Vero cells. An additional cell line: U87 glioma was added to test the plant *A. multiflorum* and *P. leubnitzia*. The additional cell line was added due to the high scavenging activity and previous cytotoxic properties, respectively, observed in the two plants.

Briefly, the cells were seeded in a 96 well plate at a concentration of 1×10^5 cells/ml and provided with Dulbecco's Modified Eagle Medium (DMEM) supplemented with 10% Fetal Bovine Serum (FBS). The plate was left for 24 hours in an incubator (NÜVE EC 160, Ankara, Turkey) at 37 °C, 5% CO₂ to allow attachment. The cells were then treated with different concentrations (0.1-100 µg/mL) of each of the four plant extracts in triplicates. After 48 hours of incubation, 25 µL of MTT was added to all the wells and the plate was incubated for a further 4 hours. The medium was removed and 100 µL of Dimethyl sulfoxide (DMSO) was added for colour development. Absorbance was measured at 540 nm using a spectrophotometer (Multiskan GO).

3.5 Antioxidant activity

The HEX and DCM extracts of *D. camilla*, and MeOH extract of *A. multiflorum* were further selected for analysis of the total flavonoid content, based on the cytotoxicity results.

3.5.1 Total flavonoids

The assay was done using the method reported by Sakanaka et al. (2005). Briefly, 100 μL of each HEX/DCM/MeOH extract at a concentration of 240 $\mu\text{g}/\text{ml}$ or different concentrations of quercetin standard (3.75 – 240 $\mu\text{g}/\text{mL}$ in reaction mixture), and 400 μL of ethanol, were mixed with 500 μL of a 2% solution of AlCl_3 diluted in distilled water. After 1 h incubation at room temperature, the absorbance was measured at 430 nm. The flavonoid content of the extracts at a concentration of 240 $\mu\text{g}/\text{mL}$ were computed from the standard curve and expressed as mg/g of quercetin equivalents (QE) using the following formula:

$$\text{Flavonoid content (mg/g GAE)} = \frac{C \times SV}{M} \quad \text{Equation 1}$$

Where, “C” is the concentration (μM) extrapolated from standard curve; “SV” is the sample volume (mL), and “M” is the mass (g) of the sample in SV (mL) of the sample solution.

3.5.2 Total phenolic content

The total phenolic content was measured using the Folin-Ciocalteu colorimetric assay as previously described by Ainsworth and Gillespie (2007) with slight modifications. The HEX/DCM/MeOH extract at a concentration of 240 $\mu\text{g}/\text{mL}$, or different concentrations of gallic acid standard (3.75 – 240 $\mu\text{g}/\text{mL}$ in reaction mixture) was incubated with 125 μL of 10 times diluted Folin-Ciocalteu reagent (Merck, South Africa) and 100 μL of 0.7 M Na_2CO_3 . The absorbance was read at 765 nm after 30 min of incubation at room temperature in the dark. The

total phenol content was computed from the standard curve and expressed as mg/g of gallic acid equivalents (GAE) using the “Equation 1” formula.

$$\text{Phenol content (mg/g GAE)} = \frac{C \times SV}{M} \quad \text{Equation 1}$$

Where, “C” is the concentration (μM) extrapolated from standard curve; “SV” is the sample volume (mL), and “M” is the mass (g) of the sample in SV (mL) of the sample solution.

3.5.3 DPPH radical scavenging assay

The DPPH (2, 2-diphenyl-1-picrylhydrazyl) radical scavenging activity of HEX/DCM/MeOH extracts was done using the method by Erukainure et al. (2019), with slight modification. Volume of 75 μL of the extract (7.5, 15, 30, 60, 120, 240 $\mu\text{g/mL}$) or standards (ascorbic acid and Trolox) at different concentrations (7.5, 15, 30, 60, 120, 240 $\mu\text{g/mL}$ in reaction mixture) or their solvents (control) and 37.5 μL of 0.1 mM DPPH were mixed in a 96 well plate and incubated at room temperature (RT) in the dark. The absorbance was read at 517 nm, and free radical scavenging activity calculated using the formula:

$$\begin{aligned} & \text{Scavenging activity (\%)} \\ & = \frac{\text{Absorbance of control} - \text{Absorbance of test}}{\text{Absorbance of control}} \times 100 \quad \text{Equation 2} \end{aligned}$$

3.5.4 Ferric reducing antioxidant power.

The assay was performed using methods reported by Benzie and Strain (1996), with slight modifications. Aliquots of 25 μL HEX/DCM/MeOH extract (240 $\mu\text{g/mL}$ in reaction mixture) or 25 μL of different concentrations of standards; gallic acid, ascorbic acid and Trolox (3.75 – 240 $\mu\text{g/mL}$ in reaction mixture) were incubated with 25 μL 0.2 M phosphate buffer (pH 6.6)

and 25 μL 1% potassium ferricyanide at 50°C for 30 min. Thereafter, 25 μL of 10% TCA was added to the mixture. Immediately, 10 μL of distilled water and 50 μL of 0.1% ferric chloride were consecutively added and the absorbance of each mixture was measured at 700 nm. The FRAP of the extracts was determined from gallic acid, ascorbic acid and Trolox standard curves (3.75 – 240 $\mu\text{g}/\text{mL}$) and computed as mg/g equivalent of the standards using the “Equation 1” formula.

$$FRAP (mg/g GAE) = \frac{C \times SV}{M} \quad \text{Equation 1}$$

Where, “C” is the concentration (μM) extrapolated from standard curve; “SV” is the sample volume (mL), and “M” is the mass (g) of the sample in SV (mL) of the sample solution.

3.6 Statistical analysis

The assays MTT, total flavonoid content, phenolic content, and antioxidants assays (DPPH and FRAP) were done in triplicates, and values were expressed as the mean \pm standard deviation (SD) using Microsoft Excel. The results were analysed using one-way analysis of variance (ANOVA) and Tukey's multiple range post hoc tests. To test for multiple comparisons, $p < 0.05$ was considered statistically significant (IBM, SPSS, version 23). The IC_{50} was calculated using GraphPad prism 8 software.

CHAPTER 4

Dieffenbachia camilla

4.1 Introduction

Exposure to toxicants and normal aerobic processes such as respiration, leads to the production of reactive oxygen species (ROS) in mammalian cells. These reactive species are known for damaging the cell mitochondria (Murphy, 2009), stimulate cell proliferation, promote mutations, and modify the sensitivity of cancerous cell to anticancer agents (Pelicano et al., 2004). The destructive mechanism of ROS is attributed to the presence of free radicals such as superoxide, and hydroxyl radicals (Altemimi et al., 2017). A wide range of diseases such as: cancer, diabetes mellitus, neurodegenerative disease to mention a few, initiate due to increased levels of ROS (Ray et al., 2012; Manton et al., 2004) in cells and body tissue. Previous reports have shown that some synthetic antioxidants and plant derived antioxidants can protect the human body from ROS (Je et al., 2005; Hamid et al., 2010). In this study *D. camilla* was selected for investigation due to the historical uses of the *dieffenbachia* family in medicine, having been used to treat a variety of ailments. There is, however, not enough information about the anticancer properties, i.e., antioxidant and cell cytotoxicity on record about *D. camilla*. The aim of the study was to investigate the cytotoxicity, antioxidant activity, and the total flavonoid and phenolic content of *D. Camilla*, and to further identify chemical constituents present in the selected plant extracts.

4.2 Methodology

4.2.1 Extractions, phytochemical analysis and MTT assay

The extraction and phytochemical analysis were performed according to section 3.2 and 3.3 respectively. For cytotoxicity, normal epithelial cells CHO and one metabolic cell lines (Vero

cells), which represent organs that are important in metabolism and excretion of xenobiotics were selected. The assay was performed according to section 3.4.

4.2.2 GC-MS of HEX and DCM extracts

The GC-MS (Gas chromatography/mass spectrometry) analysis of HEX and DCM extracts of *D. camilla* were carried out on a ThermoElectron Trace 1310 gas chromatograph (GC) coupled with an ISQ 7000 mass spectrometer (MS). The two extracts; HEX and DCM were selected due to the observed inhibitory activity against the Vero and CHO cell lines. The GC-MS system was equipped with Agilent FactorFour VF-5 ms capillary column (60 m Length x 0.32 mm Inner diameter x 0.25 μm film thickness) for separation. Injection was carried out in split mode with a ratio of 1:10. Carrier gas was helium (99.99%) at a flow of 5 ml/min, at the following temperatures: 60°C for 1 min to 300°C and held for 5 min. The GC injection port temperature was 250 °C, flame ionization detector (FID) base temperature was 280 °C and MS transfer line temperature was set to 280 °C. The samples were dissolved in MeOH: chloroform (4:1) and transferred to chromatography vials. Electron impact ionization fragmentation was employed. Data were collected with ThermoElectron Xcalibur 4 software and mass spectrometric spectrum searches were carried out on the NIST 17 library.

4.3 Results

The obtained results for the phytochemical analysis showed presence the of alkaloids, glycosides, triterpenoids, anthroquines, saponins, flavonoids and phytosterols. The MTT results showed that HEX extract of *D. camilla* exhibited high cytotoxicity with low IC_{50} values against CHO (1.41 $\mu\text{g}/\text{mL}$) and Vero (0.31 $\mu\text{g}/\text{mL}$) cell lines, respectively. The DCM extract exhibited cytotoxic activity against the CHO and Vero cell lines, with IC_{50} values of 2.72

$\mu\text{g/mL}$ and $0.29 \mu\text{g/mL}$, respectively. The HEX extract exhibited a higher value of the total flavonoid content, $145 \pm 16.70 \text{ mg/g GAE}$, compared to the DCM ($86.62 \pm 11.25 \text{ mg/g GAE}$). However, DCM extract was shown to have more total phenolic content ($13.64 \pm 1.2 \text{ mg/g GAE}$) compared to the HEX extract ($5.51 \pm 4.6 \text{ mg/g GAE}$). The DPPH antioxidant activity results showed that DCM extract exhibited the lowest IC_{50} ($10.61 \mu\text{g/mL}$) compared to HEX extract which had an IC_{50} $27.45 \mu\text{g/mL}$. The FRAP values for DCM were 6.25 ± 0.15 , $51 \pm 0.39 \text{ mg/g GAE}$ and $16.18 \pm 0.65 \text{ mg/g GAE}$ and for HEX; $7.88 \pm 2.12 \text{ mg/g GAE}$, $55.46 \pm 5.78 \text{ mg/g GAE}$ and $23.54 \pm 9.57 \text{ mg/g GAE}$, ascorbic acid equivalence and trolox equivalence, respectively. The GC-MS analysis of HEX and DCM extracts showed the presence of n-hexadecanoic acid, Bis-(2-ethylhexyl) phthalate, tri-(2-ethylhexyl) trimellitate, hexadecanoic acid, and 1-(+)-Ascorbic acid 2,6-dihexadecanoate.

4.3.1 The MTT assay results

Cytotoxicity results are shown in figure 7. The IC_{50} value were compared to the Council for Scientific and Industrial Research (CSIR), standard criteria (Table 1).

Table 1. CSIR standard criteria for anticancer and cytotoxicity. (Supplementary table)

Anticancer activity		Cytotoxicity	
IC_{50} [$\mu\text{g/mL}$]	Status	IC_{50} [$\mu\text{g/mL}$]	Status
> 100	Inactive	> 100	Low Hazard
< 100 >15	Weak	< 100 >30	Weak hazard
< 15 >6.25	Moderate	< 30 >5	Moderate Hazard
< 6.25	Potent	< 5	High Hazard

The cytotoxic activity of the different extract was selected based on the criteria of CSIR. The extracts included DCM extract against CHO ($IC_{50} = 2.72$) and Vero ($IC_{50} = 0.29 \mu\text{g/mL}$) cells (Table 2 and Figure 7), along with the HEX extract which had activity of 1.41 and $0.31 \mu\text{g/mL}$, against the CHO and Vero cells respectively.

The MeOH extract showed moderate activity against the CHO cell line and weak hazardous activity against the Vero cell line. The DCM: MeOH showed weak to moderate cytotoxic effect as seen in table 2. Further analysis of the two potent plant extracts (HEX and DCM) was done on section 4.3.3-4.3.6.

Table 2. Antioxidant and cytotoxicity activities [$\mu\text{g/mL}$] exhibited by organic extracts of *D. camilla*.

Parameters or assays	IC_{50} values ($\mu\text{g/mL}$) of <i>D. camilla</i> extracts							
	HEX	DCM	DCM: MeOH	MeOH	Gallic acid	Ascorbic acid	Trolox	
CHO	1.41	2.72	22.82	5.80	ND	ND	ND	
Cytotoxicity activity	Vero	0.31	0.29	30.04	8.75	ND	ND	ND
DPPH scavenging activity	27.45	10.61	ND	ND	9.94	15.32	13.55	

ND= Not done

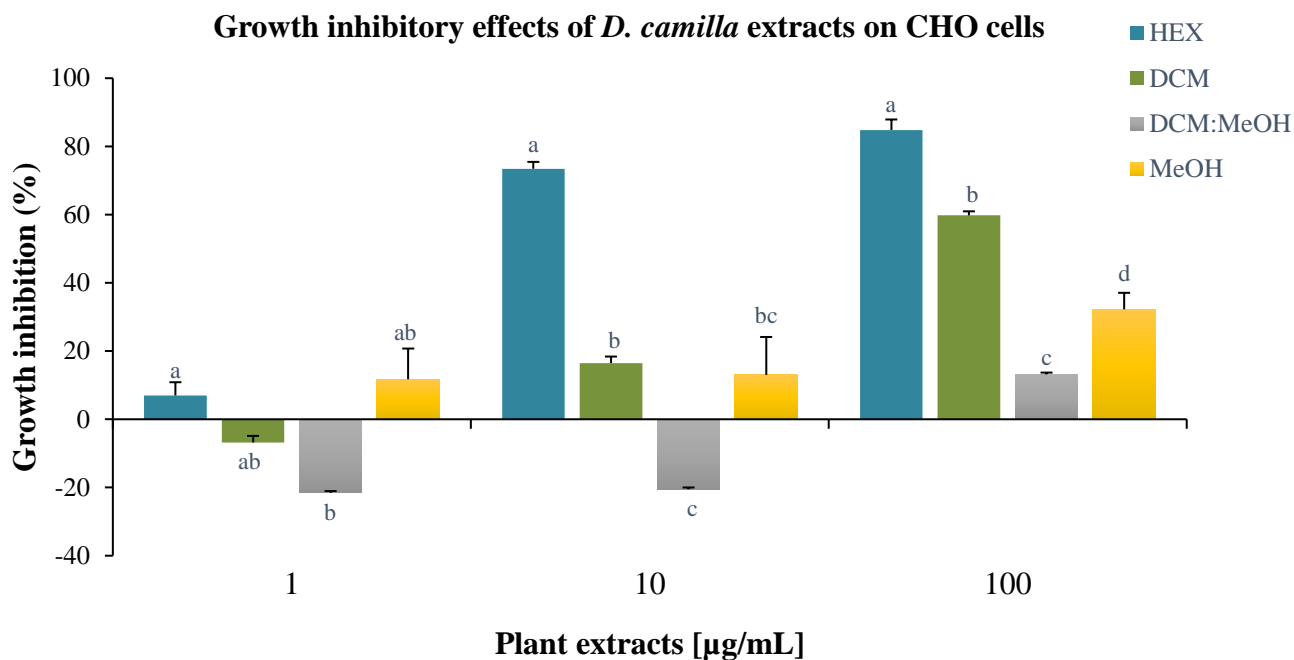


Figure 7. Growth inhibitory effects of *D. camilla* extracts on CHO cells. Each of the values represents the mean of three independent experiments \pm SD.

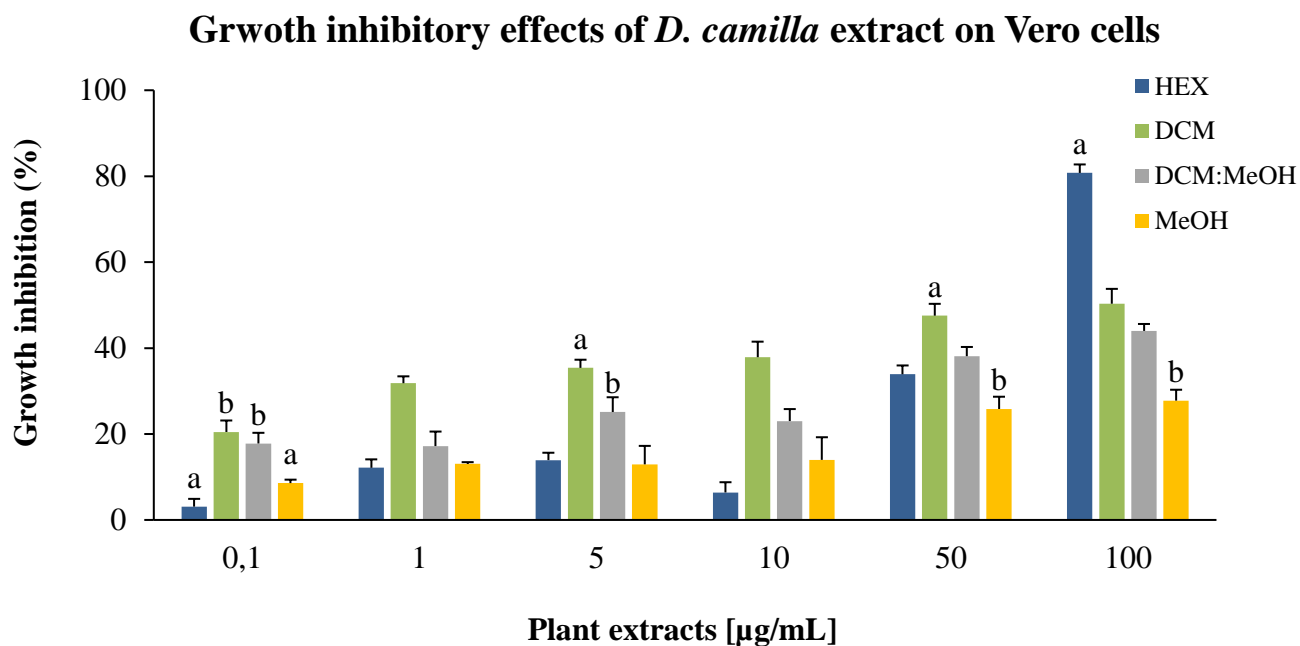















Figure 8. Inhibitory effects of *D. camilla* extract on Vero cells. Each of the values represents the mean of three independent experiments \pm SD.





4.3.2 Phytochemical analysis

The phytochemical analysis of the root and leaf parts of the plant *D. camilla* were recorded in table 3. The analysis showed presence of phytosterols, glycosides, triterpenoids, and alkaloids in both parts of the plant. The appearance of a reddish-brown colour in the chloroform indicated the presence of phytosterols, the appearance of a brown ring indicated the presence of glycosides, the formation of an interface with reddish brown coloration indicated the presence of triterpenoids, the formation of a rose-pink colour indicated the presence of anthraquinones, a yellow precipitate indicated the presence of flavonoids, an organic precipitate indicated the presence of alkaloids. Pentose and tannins were not detected.

Table 3. The phytochemical analysis of the roots and leaf plant parts *D. camilla*.

Phytochemical	Roots	Leaves
Phytosterols	 (+)	 (+)
Pentose	 (-)	 (-)







<p>Tannins</p>	 <p>(-)</p>	 <p>(-)</p>
<p>Glycosides</p>	 <p>(+)</p>	 <p>(+)</p>
<p>Triterpenoids</p>	 <p>(+)</p>	 <p>(+)</p>
<p>Anthroquines</p>	 <p>(+)</p>	 <p>(+)</p>
<p>Saponins</p>	 <p>(+)</p>	 <p>(+)</p>

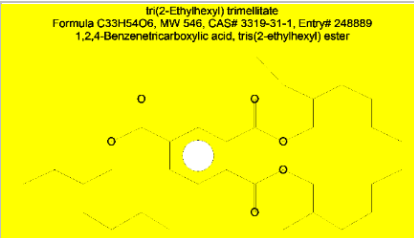
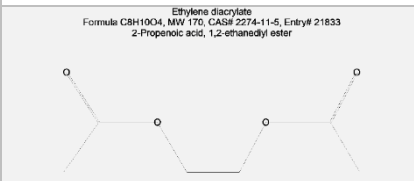
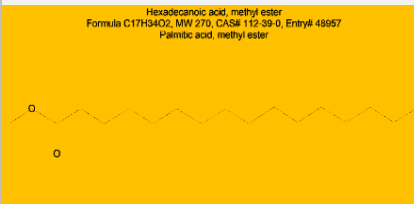
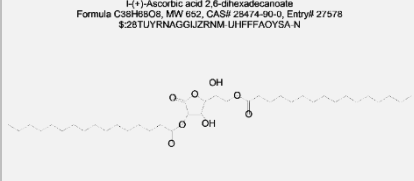
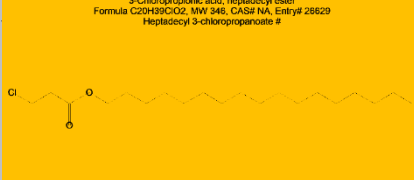
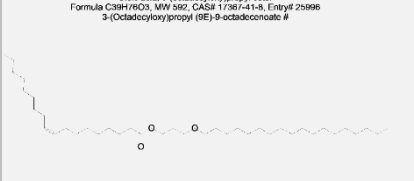
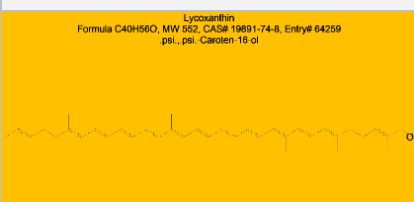
<p>Flavonoids</p>	 (+)	 (+)
<p>Alkaloids</p>	 (+)	 (+)

4.3.3 GC-MS analysis of *D. camilla*

The GC-MS analysis of *D. camilla* was carried on HEX and DCM extracts, as they showed highest cell growth inhibitory activity. From the two plants extracts, five of the obtained peaks had 50% or more composition: n hexadecanoic acid, Bis (2-ethylhexyl) phthalate, tri(2-ethylhexyl) trimellitate, Hexadecanoic acid, methyl ester and 1-(+)-Ascorbic acid 2,6-dihexadecanoate, as shown in table 4 and figure 9.

Table 4. The GC-MS analysis of the extracts HEX and DCM of the plant *D. camilla*.

The HEX Extract				
No	Compound	RT	% Composition	Compound Structure
1	Tetradecane	13.55	10.19	<p>Tetradecane Formula C₁₄H₃₀, MW 198, CAS# 629-59-4, Entry# 26185 n-Tetradecane</p> 
2	Hexadecane	16.60	13.53	<p>Hexadecane Formula C₁₆H₃₄, MW 226, CAS# 544-76-3, Entry# 26289 n-Cetane</p> 
3	3-chloropropionic acid, heptadecyl ester	17.97	10.48	<p>3-Chloropropionic acid, heptadecyl ester Formula C₂₀H₃₉ClO₂, MW 346, CAS# NA, Entry# 26629 Heptadecyl 3-chloropropionate #</p> 
4	n hexadecanoic acid	21.56	52.60	<p>n-Hexadecanoic acid Formula C₁₆H₃₂O₂, MW 256, CAS# 57-10-3, Entry# 9946 Hexadecanoic acid</p> 
5	3-chloropropionic acid heptadecyl ester	25.19	9.40	<p>3-Chloropropionic acid, heptadecyl ester Formula C₂₀H₃₉ClO₂, MW 346, CAS# NA, Entry# 26629 Heptadecyl 3-chloropropionate #</p> 
6	Bis (2-ethylhexyl) phthalate	27.69	64.84	<p>Bis(2-ethylhexyl) phthalate Formula C₂₄H₃₈O₄, MW 390, CAS# 117-81-7, Entry# 152160 Phthalic acid, bis(2-ethylhexyl) ester</p> 

7	tri(2-ethylhexyl) trimellitate	35.63	95.74	<p>tri(2-Ethylhexyl) Trimellitate Formula C33H54O6, MW 546, CAS# 3319-31-1, Entry# 248889 1,2,4-Benzenetricarboxylic acid, tris(2-ethylhexyl) ester</p> 
DCM Extract				
No	Compounds	RT	% Composition	
1	Ethylene diacrylate	17.97	9.16	<p>Ethylene diacrylate Formula C8H10O4, MW 170, CAS# 2274-11-5, Entry# 21833 2-Propenoic acid, 1,2-ethanediyl ester</p> 
2	Hexadecanoic acid, methyl ester	20.98	80.01	<p>Hexadecanoic acid, methyl ester Formula C17H34O2, MW 270, CAS# 112-39-0, Entry# 48957 Palmitic acid, methyl ester</p> 
3	l-(+)-Ascorbic acid 2,6-dihexadecanoate	21.60	36.60	<p>l-(+)-Ascorbic acid 2,6-dihexadecanoate Formula C38H66O8, MW 662, CAS# 28474-90-0, Entry# 27578 #28TUVRNAGGLZRNH UHFFFAOYSA N</p> 
4	3-chloropropionic acid heptadecyl ester	25.21	13.31	<p>3-Chloropropionic acid, heptadecyl ester Formula C20H39ClO2, MW 346, CAS# NA, Entry# 28629 Heptadecyl 3-chloropropionate #</p> 
5	oleic acid 3-(octadecyloxy)propyl ester	28.55	6.53	<p>Oleic acid, 3-(octadecyloxy)propyl ester Formula C39H76O2, MW 562, CAS# 1791-41-8, Entry# 25998 3-(Octadecyloxy)propyl (9E)-9-octadecenoate #</p> 
6	Lycoxanthin	37.60	7.29	<p>Lycoxanthin Formula C40H56O, MW 562, CAS# 19891-74-8, Entry# 64259 psi., psi. Caroten-16-ol</p> 

*See supplementary picture 1-11 for clear pictures.

The two plant extracts, HEX and DCM, showed different compounds at the retention time of 17.97. These were identified as Ethylene diacrylate and 3 chloropropionic acid heptadecyl ester. The extracts both showed the presence of 3-chloropropionic acid heptadecyl ester, however the retention times differed slightly (figure 9).

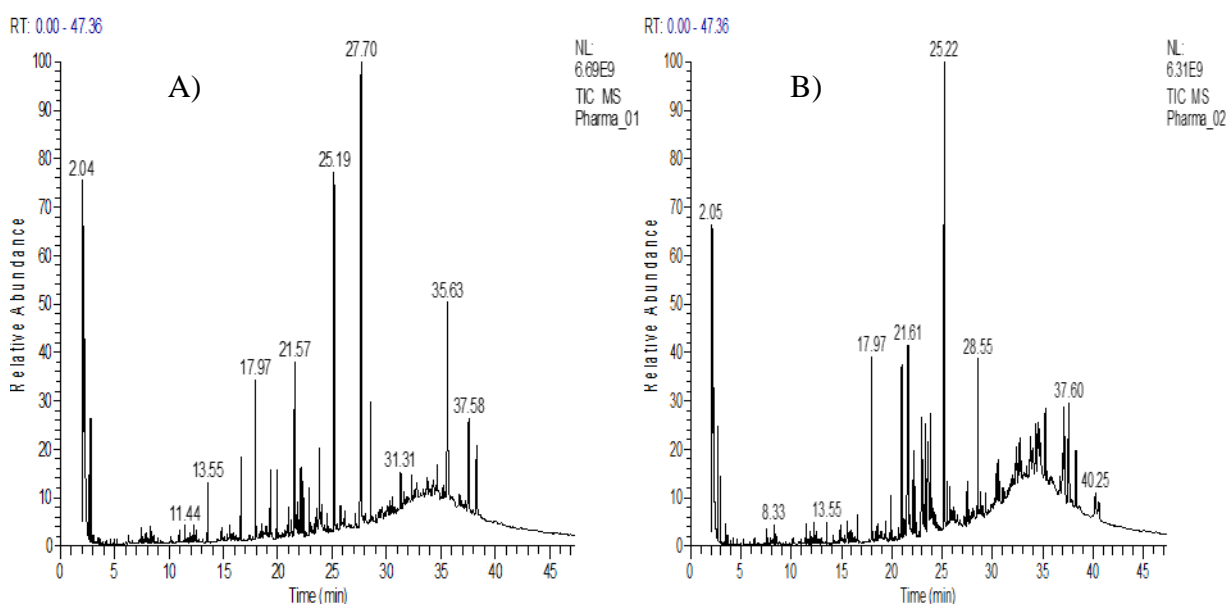


Figure 9. The MS spectra of the (a) HEX and (b) DCM extracts.

4.3.4 The total phenolic content and total flavonoid content

Table 5. A summary of the FRAP results, the total flavonoid and phenolic content results, represented in mean \pm SD.

Test Performed		<i>D. camilla</i>	
		HEX	DCM
TFC	[mg/g QE]	145 \pm 16.70	86.6 \pm 11.25
TPC	[mg/g GAE]	5.51 \pm 3.58	13.64 \pm 1.15

FRAP	[mg/g GAE]	7.88± 2.12	6.25± 0.15
	[mg/m AE]	55.46±5.78	51±0.39
	[mg/g TE]	23.54±9.57	16.18±0.65

The abbreviations QE= quercetin equivalence, GAE= gallic acid equivalence, AE= ascorbic acid equivalence, TE=trolox equivalence, TPC= total phenolic content, TFC=total flavonoid content.

The HEX and DCM extracts of *D. camilla* were tested for the total phenolic and flavonoid content (table 5). Phenols are very important constituents of plants and have been demonstrated to act as free radical terminators. The total phenolic content results showed that DCM extract, extrapolated from $R^2 = 0.9966$, had a high value of 13.64 ± 1.15 mg/g while the HEX extract showed a value of 5.51 ± 3.58 mg/g. Interestingly, the opposite was observed when the total flavonoid content was extrapolated from $y = 0.0016x - 0.0144$, $R^2 = 0.9976$. The results for the TPC showed that the HEX extract had the highest flavonoid value, 145 ± 16.7 mg/g. In contrast to HEX, DCM extract showed a low value of the total flavonoid (86.62 ± 11.25 mg/g).

4.3.5 The ferric reducing antioxidant power results.

The ferric reducing antioxidant power (FRAP) was used to assay the ability of the plant extracts to reduce ferric ions. The assay used three antioxidants: gallic acid ($R^2 = 0.9998$), ascorbic acid ($R^2 = 0.9889$) and trolox ($R^2 = 0.9933$) to extrapolate the concentrations. It was observed that the HEX extract had higher FRAP values; 7.88 ± 2.12 mg/g, 55.46 ± 5.78 mg/g, 23.54 ± 9.57 mg/g, for gallic acid, ascorbic acid and trolox equivalence, respectively. The DCM extract showed lower FRAP values when compared to the HEX; 6.25 ± 0.15 mg/g, 51 ± 0.39 mg/g, 16.18 ± 0.65 mg/g for gallic acid, ascorbic acid and trolox equivalence, respectively (table 5).

4.3.6 The DPPH assays.

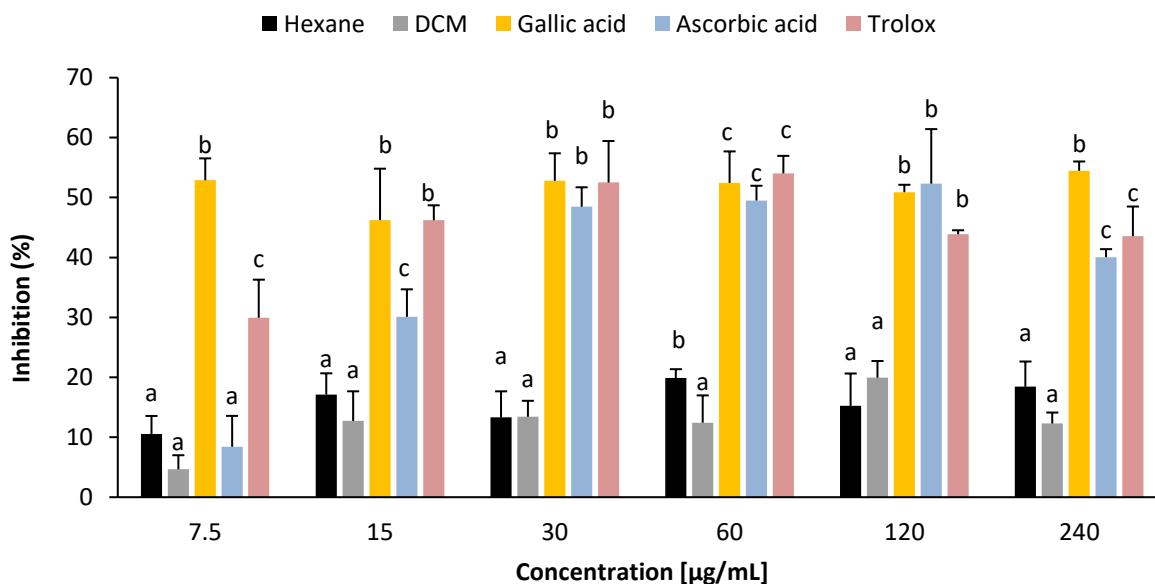


Figure 10. The DPPH results of four samples at a range of concentrations [µg/mL]. Each of the values represents the mean of three independent experiments \pm SD. The values with different letter are considered significantly different ($P < 0.05$, one-way analysis of variance (ANOVA) followed by Tukey-Kramer test) from each other.

The free radical scavenging ability of the HEX and DCM extracts are shown in figure 10. The extracts were observed to have the lowest scavenging activity at all the concentration, exhibiting the percentage inhibition $< 50\%$ for in all the concentrations for both extracts. The free radical scavenging ability of the HEX gave a DPPH value in the range between 10.6% and 19.9%, while the DCM extract showed a value in the range between 4.66% and 19.9% (figure 10). The extracts showed an IC_{50} value of 27.45 and 10.61 µg/mL, HEX and DCM, respectively (table 2). When compared to the antioxidant standards, the extracts exhibited significantly low DPPH values at all concentrations.

4.4 Discussion

There has been an increasing interest in the search of novel bioactive compounds for the treatment of reactive oxygen species and cancer cells. In this study, the dry powdered material of *D. camilla* was analysed for the presence of a variety of phytochemicals considered essential for the scavenging of reactive oxygen species in cancer cells. Phytochemicals such as flavonoids and triterpenoids which in previous studies were shown to have anticancerogenic and antitumor properties (Liby et al., 2007 and Sufferdini et al., 2004), were positively identified in *D. camilla* plant. Furthermore, analysis by GC-MS revealed the presence of L-(+)-Ascorbic acid 2,6-dihexadecanoate, a derivative of ascorbic acid, present in moderate quantities (36%) in DCM extract (Table 4). This compound was previously reported to have antimicrobial and anti-tumor properties (Sharma et al., 2015). In relation to our study, it was observed that the DCM extract showed some inhibitory effect against the two selected normal cells which could potentially implicate that the presence of L-(+)-Ascorbic acid 2,6-dihexadecanoate might have similar inhibitory effects as observed in the study done by Sharma and colleagues. In this reported study, the presence of n-hexadecanoic acid and lycoxanthin were confirmed present, and these two compounds which were previously shown to have antioxidant activity (Hema and Alagusundaram, 2011), anti-inflammatory, and anticancer activities (Tamilselvan et al., 2014), respectively.

Studies have shown that phytochemicals in medicinal plants can be utilized as natural antioxidants that can potentially scavenge free radicals in mammals, which has relevance in the treatment of cancer, diabetes, and many diseases. In this study, the HEX and DCM extracts showed the presence of phenolic compounds, which are notorious for their ability to donate

electrons (Bendary et al., 2013) and scavenge free radicals. DCM, which is known to extract polar flavonoids such as flavanones, methylated flavones and flavonols (Brglez et al., 2016) showed a rather significantly low TFC values compared to HEX, which is known to extract less polar compounds (oils, wax and many more). According to a study done by Ganiyat et al (2011), the plant *D. camilla* was shown to contain essential oils with antioxidant activity, which could have contributed to the high TFC values observed in the HEX extract. The phytochemicals such as phenolics and flavonoids have been shown to contribute for antioxidant activities exhibited by plants, therefore the scavenging activity of *D. camilla* can be attributed to both the presence of flavonoids and phenolic in the plant extracts (Oloyede and Ayanbadejo, 2014). Although it was noted that antioxidant analysis using the DPPH assay indicated low activity of the DCM and HEX extracts when compared to experimental results of methanol extracts done by Line-Edwige and colleagues.

It is thus further possible that some of the phytochemicals/compounds that are found in the DCM extracts such as lycoxanthin, have contributed to the high observed cytotoxic effect of the extract against Vero cells as shown in figure 8. Our study showed that the HEX extract exhibited less cytotoxicity against the Vero cells and had some antioxidant activity. This indicates that less polar extracts such as HEX can also be used as antioxidants due to their potent DPPH radical scavenging activity, which is in agreement with other studies that focused more on the polar extracts of the *dieffenbachia* family (Line-Edwige et al., 2009 and Oloyede and Ayanbadejo, 2014).

CHAPTER 5

Adenium multiflorum

5.1 Introduction

The study investigated the phytochemical constituents of the root and leaf parts of *A. multiflorum*, and the antioxidant activity of the plant using two antioxidant assays. We further investigated the cytotoxicity, of the different plant extracts of *A. multiflorum* against only one metabolic cell line: Vero cell line and against the glioblastoma (U87) cell line. The aim of the research was to use different assays to help select plant extracts with potential antineoplastic properties for further studies. The methods were followed as outlined in Chapter 3.

5.2 Results

5.2.1 Summary of the results



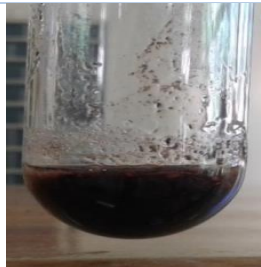
The results for the phytochemical analysis revealed the presence of phytosterols, pentose, glycosides, triterpenoids, flavonoids, and alkaloids in both the leaf and root plant material. For this part of the research only one metabolic cell line, Vero cell line and U87 cell line were selected to monitor the inhibitory effect of the plant extracts. The MTT assay showed that the leaf DCM extract was cytotoxic with an IC_{50} of 3.91 and 0.14 $\mu\text{g/mL}$ for Vero and U87 cell, respectively. The MeOH leaf extract was cytotoxic with IC_{50} of 0.50 $\mu\text{g/mL}$ against the Vero cell line. Interestingly the HEX root extract had reduced cytotoxicity against for the Vero cell line (27.07 $\mu\text{g/mL}$) and stronger inhibitory effect against the U87 cells (4.92 $\mu\text{g/mL}$). Similarly, the DCM root extract showed lower activity ($IC_{50} = 4.42$ and 1.49 $\mu\text{g/mL}$, Vero and U87, respectively) compared to the leaf extract. Ethyl acetate showed low inhibitory effect in the leaves (18,71 $\mu\text{g/mL}$) compared to roots (1.51 $\mu\text{g/mL}$) against Vero cells, while the opposite was observed against the U87 cell line; leaves showed an $IC_{50} = 2.57$ $\mu\text{g/mL}$ and roots had an $IC_{50} = 15.45$ $\mu\text{g/mL}$.

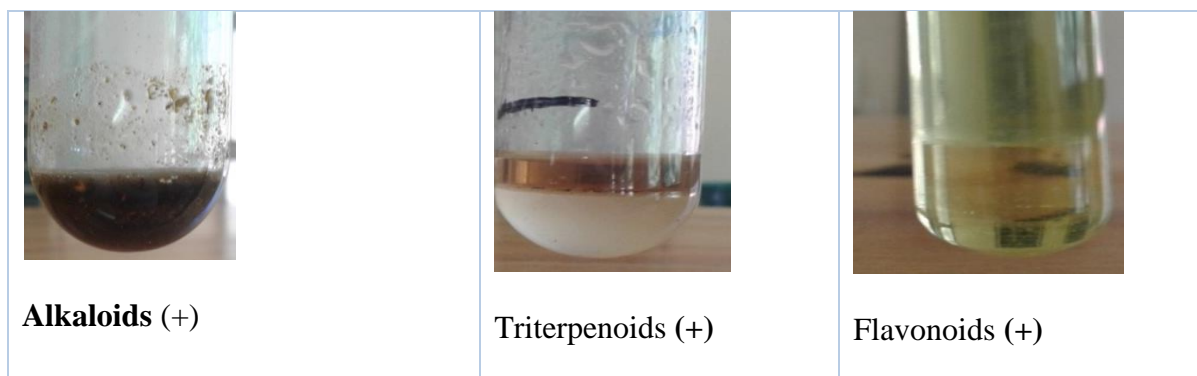
The total phenolic content was identified as 267.98 ± 10.63 mg/m which was higher than the value of the total flavonoids content 27.51 ± 0.40 mg/m. The antioxidant results showed that the MeOH extract has an IC_{50} value of 13.37 mg/m, while FRAP values were identified as 116.30 ± 14.71 mg/m, 351.33 ± 40.15 mg/m and 513.27 ± 66.45 mg/m, for gallic acid, ascorbic acid and trolox respectively.

5.2.2 Phytochemical analysis

The results for the *A. multiflorum* plant showed the presence of phytosterols, pentose, glycosides, triterpenoids, and alkaloids in both the stem and roots of the plant, (table 6). The stem part of the plant when tested for flavonoids, showed a rather more concentrated colour. Both parts showed the absence of tannins, anthroquines and saponins.

Table 6. The phytochemical analysis *A. multiflorum* plants

Phytochemical analysis of whole (roots and stem) plant of <i>Adenium multiflorum</i>		
Saponin (-)	Anthroquines (-)	Tannins (-)
		
Phytosterols (+)	Pentose (+)	Glycoside (+)



5.2.3 The total phenolic content and total flavonoid content

The MeOH extract of the plant *A. multiflorum* were tested for the total phenolic and total flavonoid content (table 6). The MeOH extract was selected due to extract availability and due to the ability of MeOH to be more efficient in extracting phenols and flavonoids (Jahromi, 2019). The total phenolic content as extrapolated from the calibration curve ($R^2 = 0.9966$), identified as 267.9812 ± 10.6321 mg/g and the total flavonoids ($R^2 = 0.9976$) was 27.5065 ± 0.4048 mg/g. These results indicated that the total phenolic content was higher than the total flavonoid in the MeOH extract.

Table 7. Total phenolic content, total flavonoid content and antioxidant activity using the MeOH plant extract of *A. multiflorum*.

Test Performed	Extracts (MeOH)
Total flavonoid content (mg/g)	27.51 ± 0.40
Total phenolic content (mg/g)	267.98 ± 10.63
IC ₅₀ (µg/mL)	13.37
FRAP (mg/g GAE)	116.30 ± 14.71

(mg/m AE)	351.33±40.15
(mg/g TE)	513.27±66.45

5.2.4 The ferric reducing antioxidant power (FRAP) results.

The reducing potential of the plant was determined by the ferric reducing antioxidant power (FRAP) method and the results were compared to three antioxidant standards: gallic acid ($R^2 = 0.9998$), ascorbic acid ($R^2 = 0.9889$) and trolox ($R^2 = 0.9933$). Values obtained were: 116.3 ± 14.71 , 351.332 ± 40.146 and 513.269 ± 66.448 , for gallic acid, ascorbic acid and trolox respectively, as summarized in table 7. The highest concentration, $513.269 \pm 66.448 \mu\text{g/mL}$, was observed when the absorbance of the plant extract was expressed as trolox equivalent.

5.2.5 The Free radical scavenging activity of the plant extract activity using the MeOH plant extract of *A. multiflorum* and antioxidant standard.

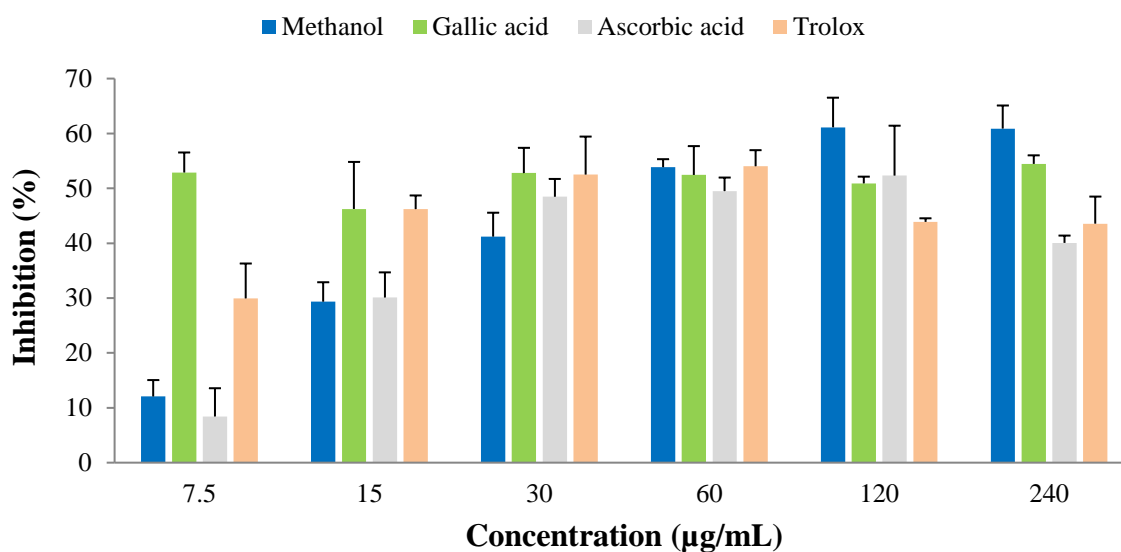


Figure 11. Free radical scavenging activity of the MeOH extracts of *A. multiflorum*, and antioxidant standards.

The results indicate that gallic acid had the highest scavenging activity at the lowest concentration of 7.5 µg/mL when compared to ascorbic acid (table 7 and figure 11). The scavenging activity of the MeOH extract was shown to be concentration dependent, exhibiting the highest scavenging activity at concentration of 120 and 240 µg/mL. Ascorbic acid generally exhibited the lowest activity in comparison to the other three standards.

Table 8. The Summary of Percentage inhibition of DPPH using four different samples.

Concentration (µg/mL)	Inhibition of DPPH (%)			
	Plant extract	Gallic acid	Ascorbic acid	Trolox
7,5	12.06±2.27	52.89±3.65	8.42±5.15	29.94±6.36
15	29.34±4.18	46.24±8.47	30.12±4.58	46.22±2.48
30	41.20 ± 2.54	52.78±4.60	48.47±3.24	52.51±6.92

60	53.86±1.34	52.44±5.26	49.50±2.46	54.01±2.92
120	61.12±2.20	50.90±1.22	52.32±9.09	43.88±0.66
240	60.89±2.31	54.46±1.56	40.06±1.33	43.56±4.94

5.2.6 The MTT assay results

Extracts of the root and leaf parts of *A. multiflorum* were tested for cytotoxicity against the Vero cells and U87 gliomas cells and results are graphically represented in figure 12-15. The DCM leaf extract had an IC_{50} 3.91 $\mu\text{g/mL}$ against the Vero cell line, which was shown to be the only cytotoxic extracts. The other extracts had weak inhibitory effect according to the CSIR criteria (table 1), with IC_{50} of 27.07, 30.05 and 18.71 $\mu\text{g/mL}$, HEX, MeOH and ethyl acetate, respectively (table 9) against the Vero cell line.

However, against the U87 cell line, the leaf extracts displayed potent activity for all the extracts, in the range of 0.14-4.92 $\mu\text{g/mL}$. All extracts displayed increased cytotoxicity activity against the Vero cell line with IC_{50} values; 4.42, 3.00, 0.92, and 1.51 $\mu\text{g/mL}$, HEX, DCM, MeOH and ethyl acetate, respectively as seen in table 9. Against the U87 cell line, the roots extracts also exhibited potent activity for DCM (IC_{50} =1.49 $\mu\text{g/mL}$) and HEX (IC_{50} =2.30 $\mu\text{g/mL}$). The other two extracts; MeOH (IC_{50} =6.50 $\mu\text{g/mL}$) and ethyl acetate (IC_{50} =15.45 $\mu\text{g/mL}$), had moderate activity according to the CSIR criteria (table 1 and 9).

Growth inhibitory effects of leave extracts of *A. Multiflorum* on Vero cells

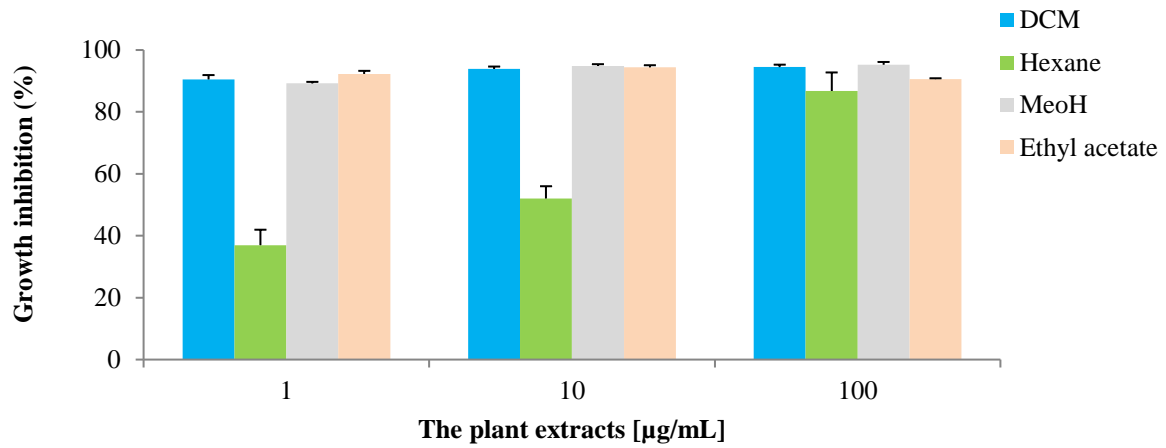


Figure 12. Inhibitory effects of leave extracts [1, 10 and 100 µg/mL] of *A. multiflorum* on Vero.

Inhibitory effects of roots extracts of *A. Multiflorum* on Vero

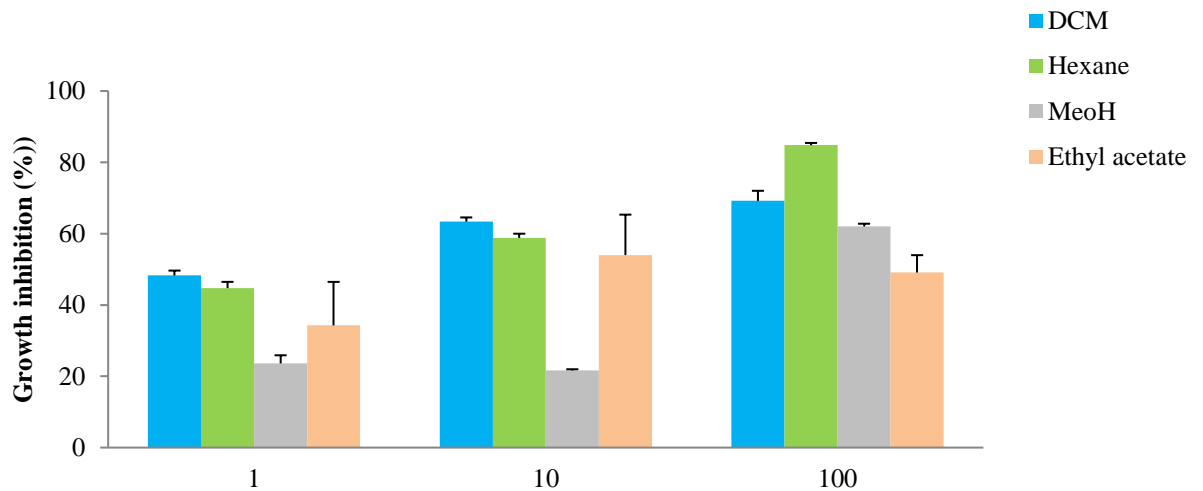


Figure 13. Inhibitory effects of roots extracts [1, 10 and 100 µg/mL] of *A. multiflorum* on Vero cells.

Growth inhibitory effects leave extract of *A. Multiflorum* on U87 cells

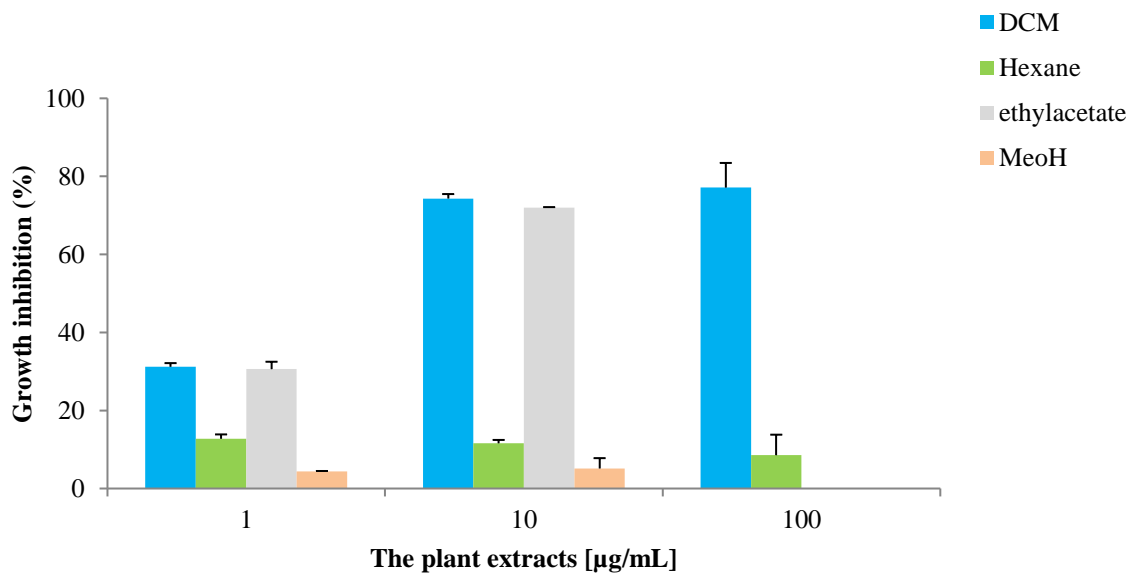


Figure 14. Inhibitory effects of leave extracts [1, 10, and 100 µg/mL] of *A. Multiflorum* on U87 cells.

Growth inhibitory effect of roots of *A. Multiflorum* on U87 cells

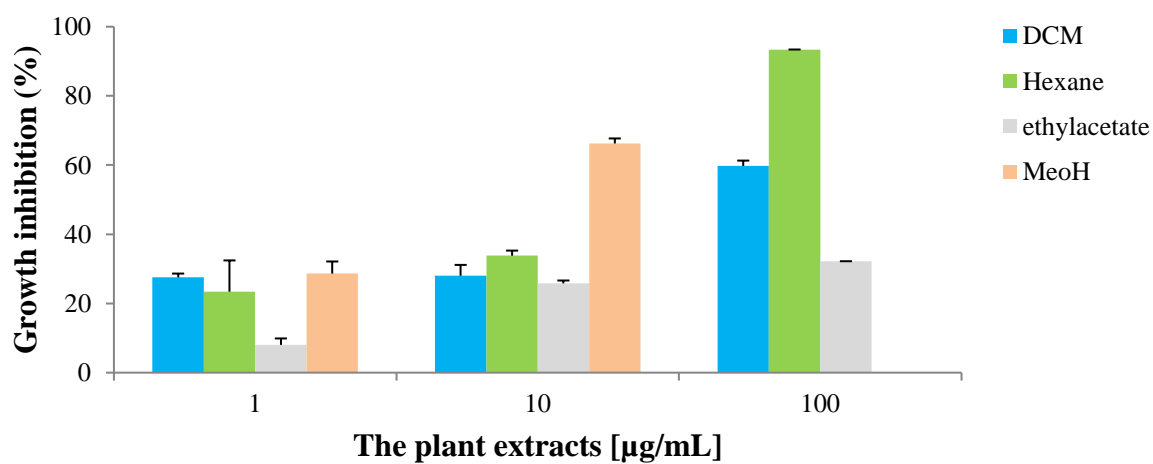


Figure 15. Inhibitory effects of leaves extract [1, 10, and 100 µg/mL] of *A. multiflorum* on U87.

Table 9. The IC₅₀ values of the root and leaf extracts against the Vero and U87 cells.

Test Performed		Extracts							
		Leaves				Roots			
		DCM	HEX	MeOH	EA	DCM	HEX	MeOH	EA
IC ₅₀ (µg/mL)	Vero	3.91	27.07	30.05	18.71	4.42	3.00	0.92	1.51
	U87	0.14	4.92	0.50	2.57	1.49	2.30	6.5	15.45

5.3 Discussion

Phytochemicals are responsible for the chemical defence of a plant against predators and diseases (Bradford and Awad, 2007). Flavonoids are phenolic compounds with a variety of chemical structure and are known to act as antioxidants (Pietta, 2000) in humans. In cancer research, it is suggested that plants taken as part of the dietary meal such as flavonoids may reduce the risk breast cancer, cancer of the pancreas amongst other types of tumors (Ramognolo and Selmin, 2012). In this research the total flavonoid content showed a low yield, in contrast to the total phenolic content of the MeOH extract, which gave a high yield. Phenolic compounds are subdivided in groups which include tannins, coumarins, phenolic acids, lignans, quinones, curcuminoids, stilbens and flavonoids. The high yield of total phenolic content could mean that some of the phytochemicals that were not tested such as lignans, could have possibly contributed to the observed yield. This high yield of phenolic content means the plant probably has good antioxidant activity and can act as either a reducing agent or hydrogen donors (Rice et al., 1995). Phenolic have been demonstrated to have anticancer effects, by

modulating cellular mechanisms such as cell apoptosis and cell signalling cascades (Wahle et al., 2010).

The ferric ion reducing antioxidant power assay was achieved to evaluate the ion reducing capacity of the MeOH extract through the ability of polyphenols present in the extracts to reduce ferric (III) ions. The yellow colour test solution was shown to change to green and this was dependent on the extract. Thus, the FRAP values indicated a correlation between the observed values of total phenolic content and FRAP values. The cytotoxicity results further showed that the three leaf extracts (HEX, MeOH and EA) exhibited approximately similar activity on Vero cells (figure 12 and 13).

CHAPTER 6

Pechuel-loeschea leibnitziae

6.1 Introduction

Nanotechnology has advanced the synthesis of silver at the nanoscale with a variety of unique morphologies and characteristics (Silver, 2006). Different methods such as, physical, chemical, and biological method, have been successfully used to produce silver nanoparticles (Zhang et al., 2016). The challenge encountered while applying some of these methods, however, is the release of hazardous by-products into the environment and the expense required to apply these methods (Reijnders, 2008). Green synthesis aims to combat the negative aspects encountered by majority of the methods used for synthesis of nanoparticles. It is environmentally friendly, cost effective and easy to follow (Kathiravan e al., 2014).

Silver nanoparticles, instead of bulky metallic silver, are considered suitable theranostic agents in cancer research due to their anticancer properties against some cancer cells, including human glioblastoma cells U251 and MDA-MB-231 human breast cancer cells (De Matteis et al., 2108, Asharani et al., 2009, Gurunathan et al., 2013).

While silver nanoparticles have shown anticancer properties, their general toxicity is however, a great concern. Literature has shown that silver nanoparticles induce blood brain dysfunction in *in vivo* studies (Sharma et al.,2009). Prolonged bio-distribution of silver nanoparticles has been shown to result in increased toxicity in a variety tissue's such as the spleen and liver (Xue et al., 2012). To decrease some of these negative side effects and to ensure safe delivery of silver nanoparticles across the blood brain barrier when treating brain tumors, encapsulation, and stabilization of silver nanoparticles in liposomes is essential for the purpose of safe delivery (Sercombe et al., 2015).

This part of the project aimed to investigate the cytotoxicity of *P. leibnitziae* extracts against the brain U87, Vero and fractions against CHO cell lines, synthesis of silver oxide nanoparticles using the plant extract, and to determine the cytotoxicity of the synthesised silver oxide nanoparticles against the U87 glioma cell line. The project further aimed to design a nano drug delivery carrier by entrapping the silver nanoparticles in cationic liposomes for the hypothesised increased effectiveness of delivery into the brain cancer cells.

6.2 Methodology

6.2.1 Phytochemical analysis

The phytochemical analysis of *P. leibnitziae* was conducted following a spraying method previously done by Kadhila (2019). Freshly prepared Liebermann Burchard reagent (LBr) was used for the detection of terpenoids and saponins. The reagent was prepared by carefully adding 5 mL of concentrated H_2SO_4 to 50 mL of absolute ethanol on ice. The TLC plates were prepared by adding and sprayed with 5-10 mL of LBr reagent, warmed at 100 °C for 5 to 10 minutes. The anthraquinones and coumarins were evaluated using freshly prepared KOH; the TLC plates were sprayed with 10 mL of a 10% (w/v) KOH in 96% ethanolic and dried. The flavonoids were detected using aluminium Chloride; the TLC plate was sprayed with 5-10 mL of 1% (w/v) $AlCl_3$ in 95% ethanolic solution. The dragendorff reagent was prepared and used for the detection of alkaloids. The reagent was prepared by dissolving 8.00 g of KI in 20 mL of distilled water. This solution was then added to a second solution containing 0.85 g of basic

bismuth nitrate in 40 mL of distilled H₂O and 10 mL of glacial acetic acid. Each TLC plate were sprayed with 10 mL of the reagent and allowed to dry. The Presence of all the screened phytochemicals was evaluated under UV light at 365 nm.

6.2.2 Silver nanoparticle (AgNP) synthesis

Silver nitrate (AgNO₃) was purchased from Sigma–Aldrich Chemicals, South Africa. Five grams (5g) of silver nitrate (10mM) and 1 g of MeOH extract were dissolved in 100mL of distilled water. The mixture was left on a magnetic stirrer overnight at 60 °C to favour the reduction of AgNO₃ to Ag⁺ ions. The mixture was then dried in the oven at 70°C (Castangia et al., 2017). The dry sample was stored at room temperature in closed vials for future use.

6.2.3 Characterization of silver nanoparticles

The synthesised silver oxide nanoparticles (AgNPs) were confirmed and characterised by several technologies; Preliminary characterization of the AgNPs was carried out using PerkinElmer Lambda 950 UV/Vis Spectrophotometer. UV–vis spectroscopy confirmed the presence of a peak at 300 nm. The Fourier-Transform Infrared (FTIR) spectrum was recorded in the range of 4000- 400 cm⁻¹ using Thermo Nicolet Nexus 670 spectrometer in the diffuse reflectance mode operating at resolution of 4 cm⁻¹ (Mallikarjuna et al., 2011). FTIR spectroscopy confirmed presence of peaks from 500-4000 cm⁻¹. The presence of silver, carbon and oxygen was confirmed by X-ray photoelectron spectroscopy and Energy-dispersive X-ray spectroscopy (EDAX). The AgNP sample was also then annealed in oxygen atmosphere at 500 °C temperatures. The structural property of the nanoparticles was investigated by X-ray diffraction (XRD, Bruker D8. The X-ray source was 3 kW with a Cu target; high-resolution

XRD patterns were measured using a scintillation counter ($\lambda=1.5406 \text{ \AA}$). The XRD data were collected over a 2θ range of 15° - 80° with steps of 0.034° .

The morphology of nanoparticles was investigated by scanning electron microscopy (SEM); JEOL JEM 2010 UHR equipped with a Gatan Imaging Filter, with a 15-eV window and a 794 slow scan CCD camera, operating at 2.00 kV. Transmission electron microscopy (TEM) (Philips 100 transmission electron microscope) was used to obtain high resolution images of the nanoparticle. X-ray photoelectron spectroscopy (XPS) was performed at A 100 μm diameter monochromatic Al $K\alpha$ x-ray beam ($h\nu = 1486.6 \text{ eV}$) generated by a 25 W and 15 kV electron beam. The pass energy was set to 11 eV to give an analyser resolution $\leq 0.5 \text{ eV}$. The Multipack version 9 software was used to analyse the spectra to identify the chemical compounds and their electronic states using Gaussian–Lorentz fits. Furthermore, the compounds present were identified using EDAX (JEOL JEM 2010 UHR).

6.2.4 Liposome Synthesis

The liposomes were prepared and modified using the thin film method. Briefly, in a round-bottom flask, cationic liposomes composed of Dimyristoylphosphatidylcholine (DMPC): dioleoyl-trimethylammonium-propane (DOTAP): Cholesterol (Chol): non-exchangeable dialkyl carbocyanine membrane label DiIc18(5) (DiD) (2.75:5:4.5:1.1 mole % each) were dissolved in 10 mL of chloroform. The mixture was poured into two round bottom flasks each containing 5ml. The organic solvent was evaporated using a rotary evaporator (Castangia et al., 2017) and left overnight covered with parafilm. The dry lipid was hydrated with 2 mL of Tris buffer in one flask and Tris buffer containing silver nanoparticles in a second flask, and both flasks were vortexed for 10 seconds on maximum speed three times to suspend

the lipid materials in the solution. The solutions were allowed to stand overnight at 4 °C to efficiently hydrate the lipid materials.

6.2.5 Characterization of Liposomes; Transmission electron microscopy

Liposomes were analysed on negative stain electron microscopy using a JEM 1200 EXII electron microscope (Jeol, Tokyo, Japan). A drop of liposome suspension (5 µmol/mL) was applied to carbon-coated grids, and, after 2 min, the excess was drawn off with filter paper. A saturated uranyl acetate aqueous solution was used as a staining agent. The excess stain was washed-off with distilled water and the sample was analysed by TEM at 80 kV.

6.2.6 Isolation of cytotoxic compounds

The DCM extract of *P. leibnitziae* showed the highest cell growth anti-proliferative activity and was selected for further studies. The *P. leibnitziae* DCM extract was fractionated using column chromatography. Briefly, slurry was made using silica (0.063-0.200mm) and HEX, the mixture was poured into a glass column (60 x 4 cm) and then left to settle. The extract was dissolved in 5 mL DCM: HEX (9:1) added gently to the column and washed with 50 mL HEX to remove any excess amount of DCM. The mobile phase: DCM: Hex (60:40) was added slowly to the stationary phase. The flow rate was adjusted to 65 drops per minute. A total of 117 fractions of 10 mL each were collected.

6.2.7 Thin Layer Chromatography

The phytochemical profiles of the fractions that eluted from column chromatography run were determined using TLC. TLC was performed on Whatman aluminium sheets coated with a 0.2 mm layer of silica (Si gel 60). The TLC plates for the first 30 samples were immersed in a DCM: HEX: solvent (6:3:1) mobile phase tank. The polarity of the mobile phase was increased

to a DCM: HEX: MeOH (6:2:2) to analyse the last 87 fractions. The TLC plates were viewed under 254 nm and 365 nm UV light. Fractions with similar TLC profile were pooled together.

6.3 Results

6.3.1 Phytochemical analysis

The TLC plates indicated the presence of brown and grey zones under UV light at 365 nm, and weak grey in visible light, which are attributed to the presences of terpenoids and saponins. The anthraquinones and coumarins compounds were confirmed by the presence of yellow zones on the TLC plate under the UV light and visible light. The flavonoids were confirmed by the presence of blue, green, and purple zones on the TLC plate. The alkaloids were confirmed by the presence of orange to red colour and yellow zones (table 10).

Table 10. Summary of Phytochemical analysis for the DCM extract of *P. leibnitziae*, where (+) means the presence and (-) means the absence of the tested phytochemical.

Phytochemical	Presence/absence
Terpenoids	+
Saponins	+
Anthraquinones	+
Coumarins	+
Flavonoids	+
Alkaloids	+

6.3.2 Characterization of AgNPs

6.3.2.1 UV-vis spectroscopy and XDR analysis

The formation of AgNPs was confirmed by the colour change from clear brown plant-silver nitrate salt mixture to dark grey under visible light. The characterization of AgNPs was monitored using the UV-vis. Results showed the presence of peak at 400 nm which was assigned to the presence AgNPs and 350 was attributed to the presence of AgO in the samples.

Figure 16 shows the UV-vis spectra of the AgNPs.

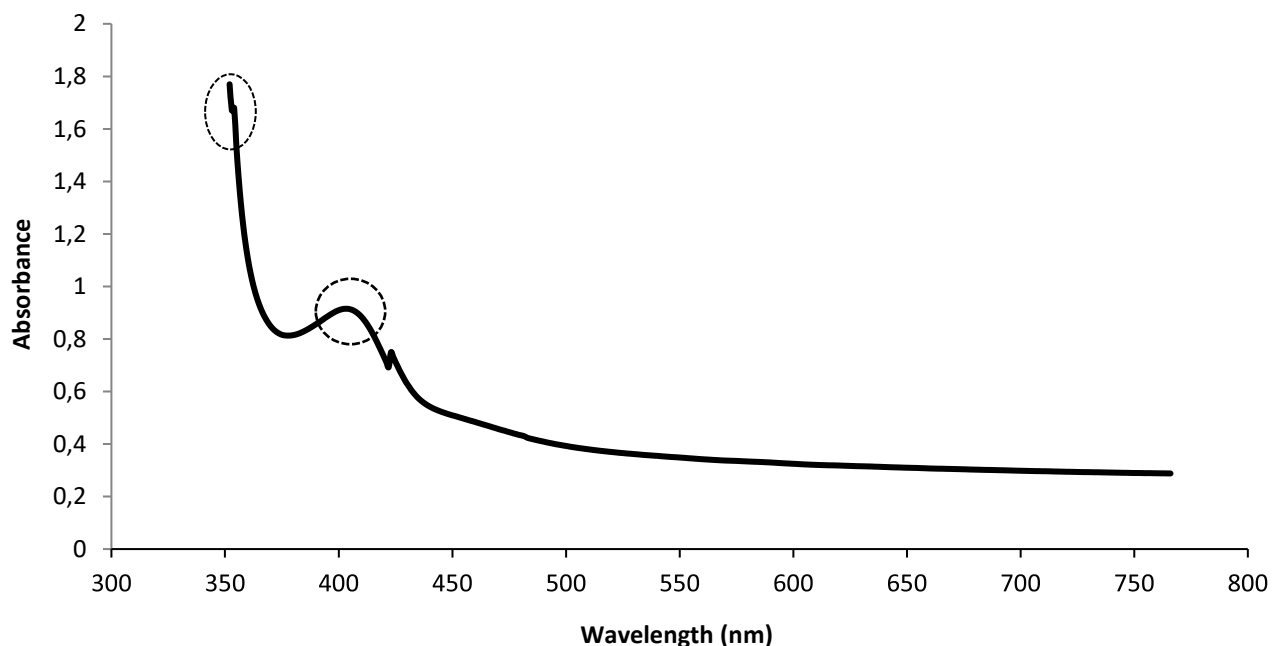


Figure 16. The UV-vis absorption spectra of silver nanoparticles synthesised using the MeOH extract of *P. leibnitziae*.

Further characterization of silver oxide was confirmed by XDR, figure 16. The results showed prominent peaks at $2\Theta = 40.0, 43.43, 64.55$ and 77.44° , which according to literature correspond to the (111), (200), (220) and (311) planes of silver, respectively (Raj et al., 2018).

The other observed peaks are possibly due to the plant extract used in the synthesis. The $2\theta = 19.56, 21.68, 24.26, 29.57, 32.76$ and 35.44° , were detected in the sample and attributed to the presence of AgNO_3 (Figure 17). Furthermore, impurities of AgO were detected at peaks $2\theta=54.6$ and 31.8° .

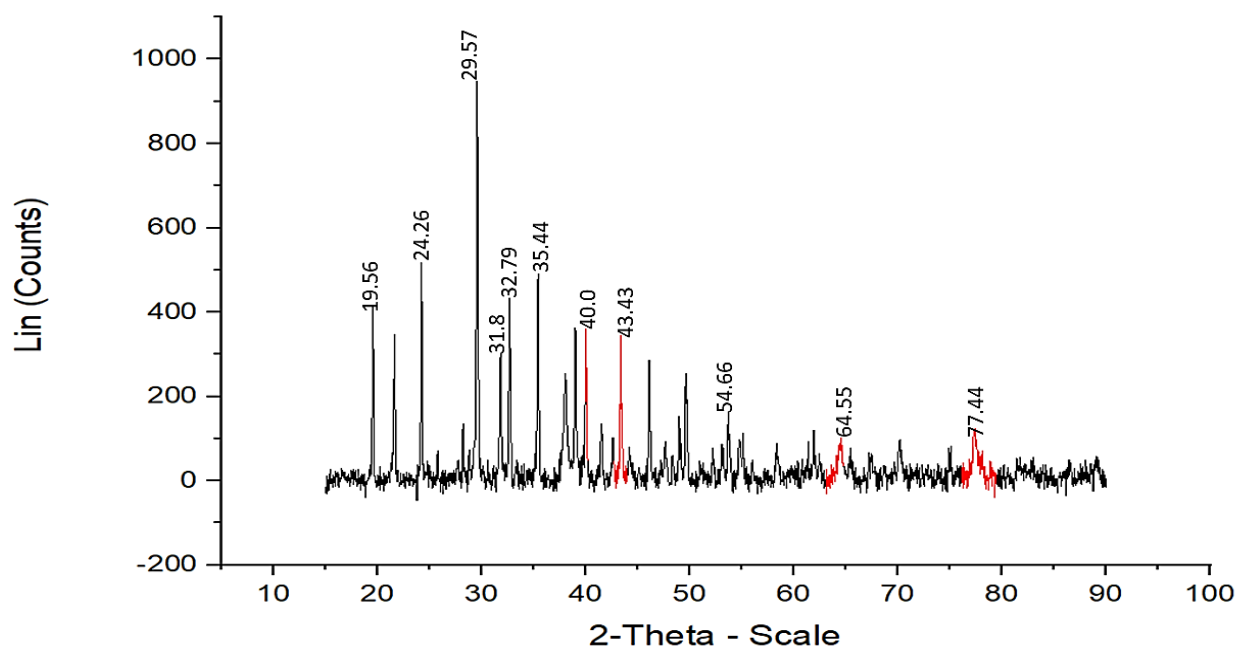


Figure 17. The XRD pattern of silver oxide nanoparticle synthesized using MeOH extract of *P. leibnitziae*.

6.3.2.2 Fourier-transform infrared spectroscopy spectral analysis

The FTIR spectra results showed possible functional groups for the reduction of AgNO_3 by *P. leibnitziae* (Figure 18). A band at about 2991 cm^{-1} was attributed to stretching of C-H alkane and the O-H stretch of carboxylic acids. The presence of the band at 2354 cm^{-1} was correlated to the possible presence of the C=C group, presence of alkynes, N-C and N=C groups. Furthermore, observed bands at $1774\text{--}1753\text{ cm}^{-1}$ can be attributed to the presence of C=O. The

band at 1593 cm^{-1} was an indicator of the bending of O-H, which indicates carboxylate. The weak band at 1278 cm^{-1} was assigned to C-N stretching and confirmed the presence of carboxylic acid group. The bands at $1040\text{--}732\text{ cm}^{-1}$ were attributed to the presence of =CH found in aromatic compounds of plant extracts, and bands at 599 cm^{-1} were attributed to the AgNPs.

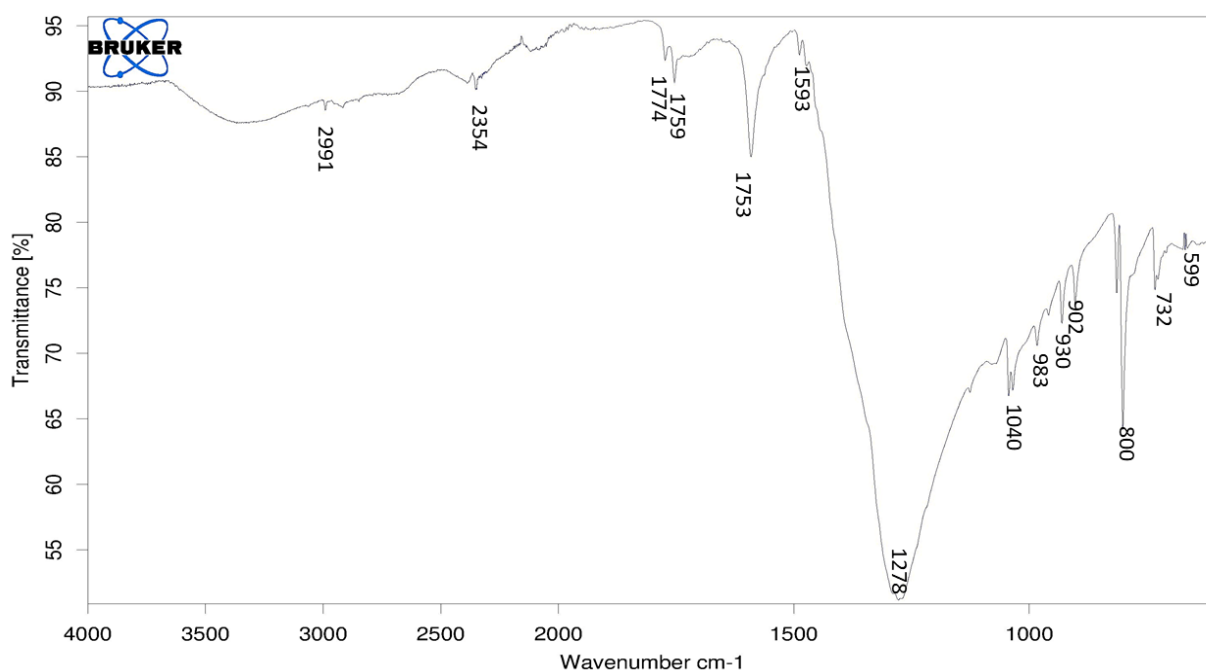


Figure 18. The FTIR spectra of the silver oxide nanoparticles.

6.3.2.3 Transmission electron microscopy and Scanning electron microscope.

The figure 19a shows the morphology and size of the synthesized AgNPs observed at 100 nm using transmission electron microscopy results. The shape of the nanoparticles appeared spherical and opaque at different locations of the grid, indicating that the NPs are stable (Figure 19a) and uniform in the size of 100nm, with no visible aggregations or agglomeration.

Furthermore, the morphology of the nanoparticle was also observed using the scanning electron microscope at the magnification of 100 mm. The morphology of the AgNPs was observed to be a uniform spherical shape of aggregated nanoparticles (Figure 19b), which correlated with the observed morphology under TEM.

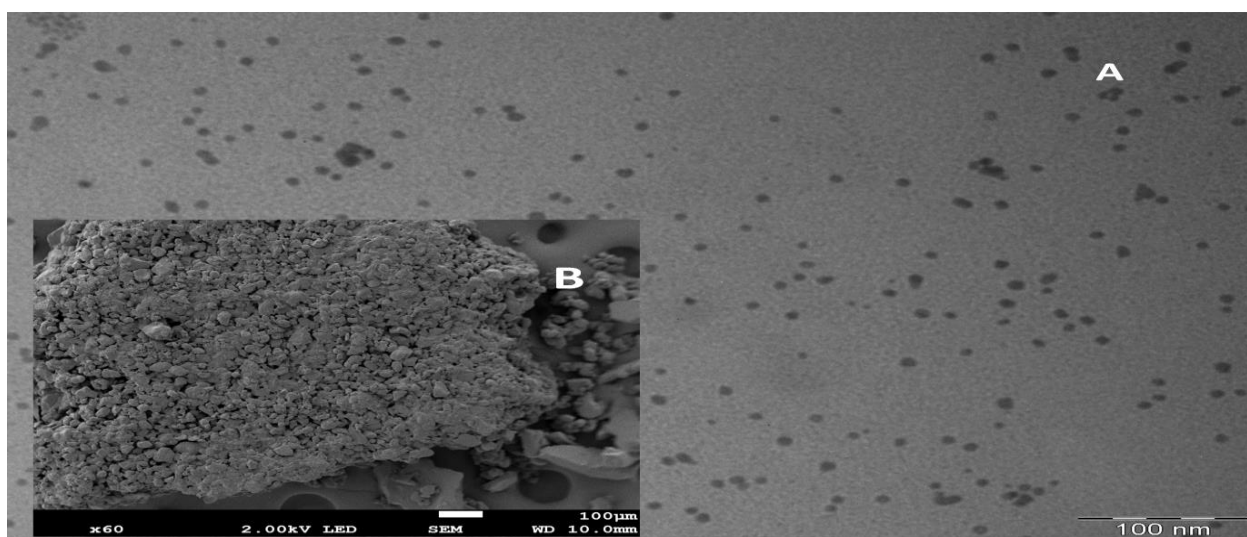


Figure 19. (A), the TEM results of silver oxide nanoparticles observed at 100 nm. (B) SEM results of silver oxide nanoparticles observed at 100 μm .

6.3.2.4 The X-ray photoelectron spectroscopy results

The XPS results (fig 20) revealed the presence of Ag, C and O atoms according to their binding energies as shown in figure 20. The peaks shifted according to C1s – 284.5 eV. The results indicate low peaks of C and O and the high peaks of Ag. In general, the presence of C1 s and O1 s peaks are indicative of high and low electrochemical activity regions, respectively.

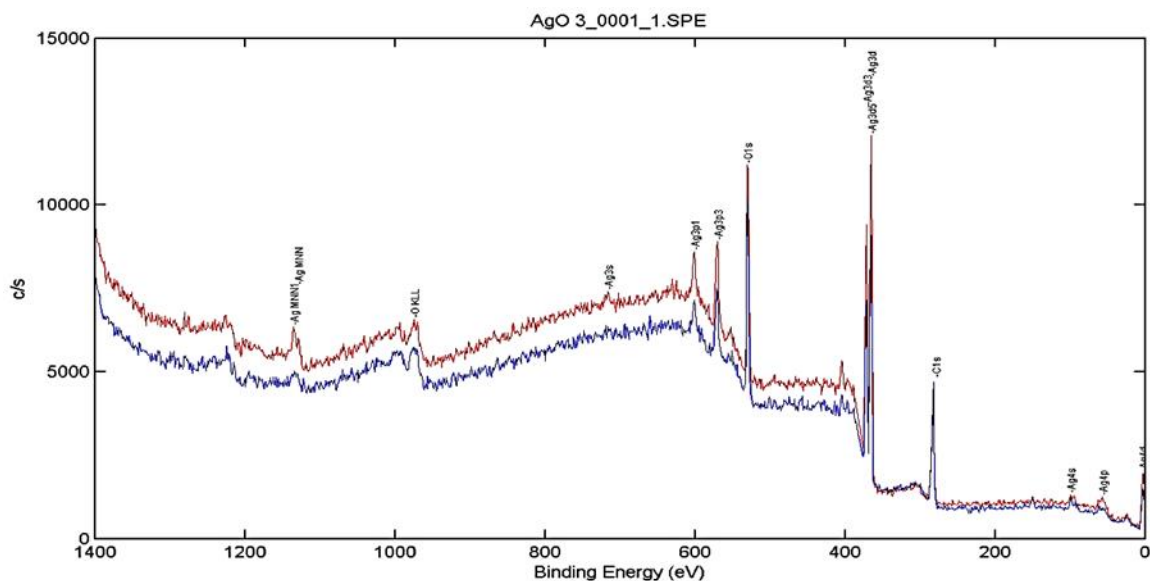


Figure 20. X-ray photoelectron spectroscopy spectrum of silver oxide nanoparticles. The red line represented before annealing and blue line represents after annealing of the sample.

The most prominent signal in the XPS spectrum, Ag3d, in figure 21, consists of two spin-orbit components at 368 (Ag3d_{5/2}) and 374 (Ag3d_{3/2}) eV, the two orbits were separated by ~6.0 eV binding energy. These observed results are correlated to the standard Ag3d binding energies, 3d_{5/2} = 368.3 eV, 3d_{3/2} = 374.3 eV tabulated earlier (Chastain, 1992), which are characteristic for Ag⁰. In each side of the Ag3d_{5/2} and Ag3d_{3/2} energy loss was observed at 366 eV and 372 eV respectively. When the samples were annealed, the peak positions showed no significant change, however the intensities of the peak changed and indicated a change in the material at the surface. The binding energy of O1s was identified to be 532 eV and that of C1s was indicated to be 285 eV.

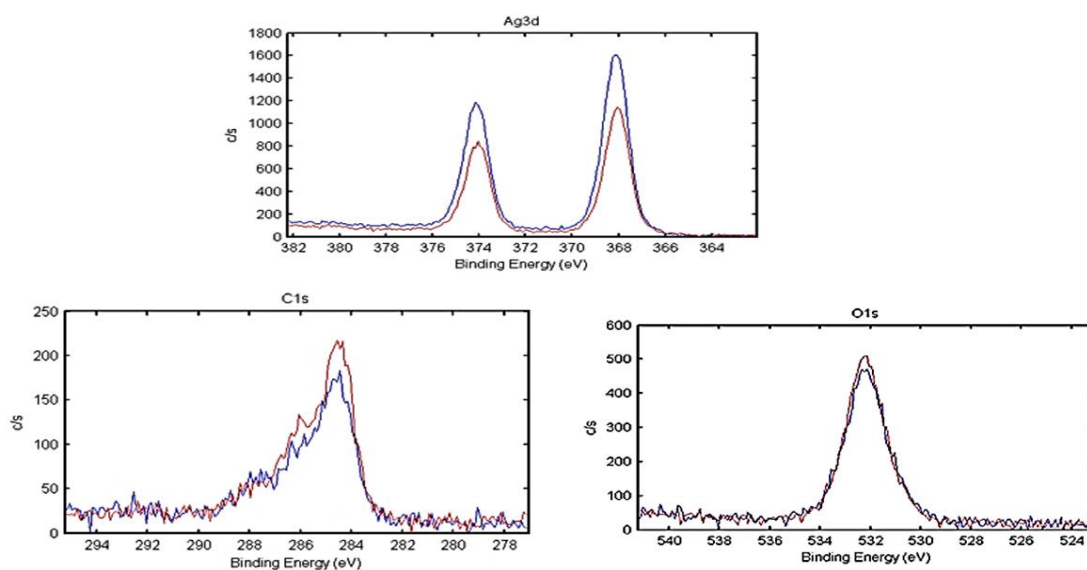


Figure 21. The XPS spectra of components present in the silver oxide nanoparticle sample. Red line represents before annealing and blue line after annealing of sample.

6.3.2.5 EDAX analysis of silver oxide nanoparticles

The silver oxide nanoparticles were further analysed for the presence of elements using EDAX in figure 22. The absorption of metallic nanoparticle was observed at 3 keV which was in alignment with the literature (Andreescu et al., 2007). The horizontal axis represented the energy in Kev, while vertical axis represented the x-ray counts. The results confirmed the presence of silver oxide nanoparticle and other elements, nitrogen, carbon and oxygen.

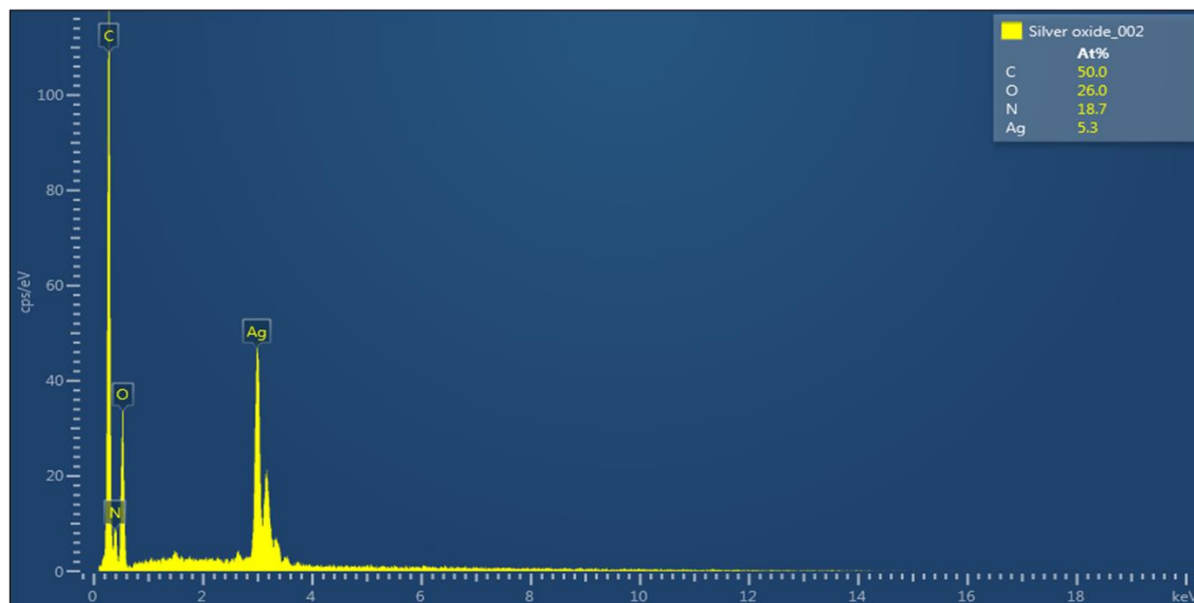


Figure 22. The EDAX spectrum showing peaks of elements present in the sample. Carbon (50%), Oxygen (26%), Nitrogen (18.7%) and Silver (5.3%) were detected. The organic elements could be from functional groups of the phytochemical components present in the plant.

6.3.3 Characterization of Liposomes

The successful synthesis of liposome was confirmed using TEM analysis (figure 23-24). The analysis method was performed using a saturated uranyl acetate aqueous solution as staining agent, and one experiment without any staining agent. When the results were compared, it was observed that both encapsulated silver, and empty cationic liposomes nanoparticles were present (figure 23). However only a small proportion of silver nanoparticles was entrapped in the liposomes.

Results from the unstained grid showed that many of the observed liposomes were empty vesicles and appeared quite stable. Only a few vesicles appeared to have entrapped silver nanoparticles as indicated by the red circles. The liposomes had uniform size and roughly a circular shape.

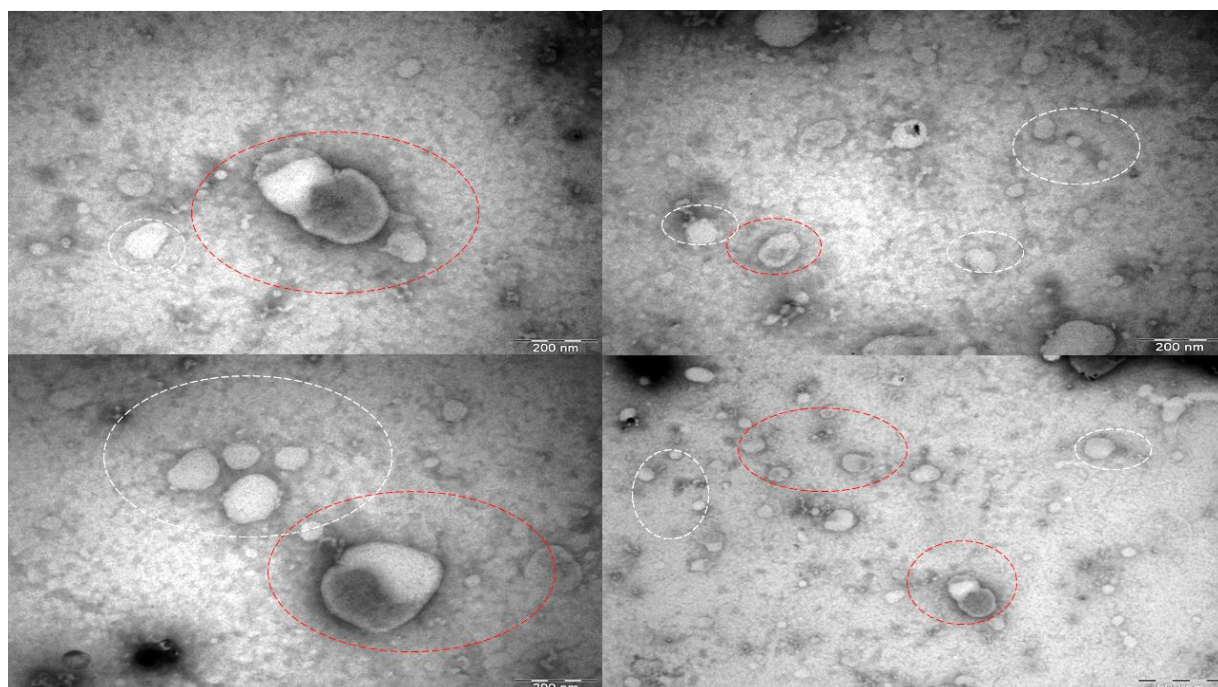


Figure 23. TEM analysis of stained liposomes. The white circles show empty liposomes, while red circles indicate silver encapsulated liposome. The liposomes were stained with saturated uranyl acetate aqueous solution.

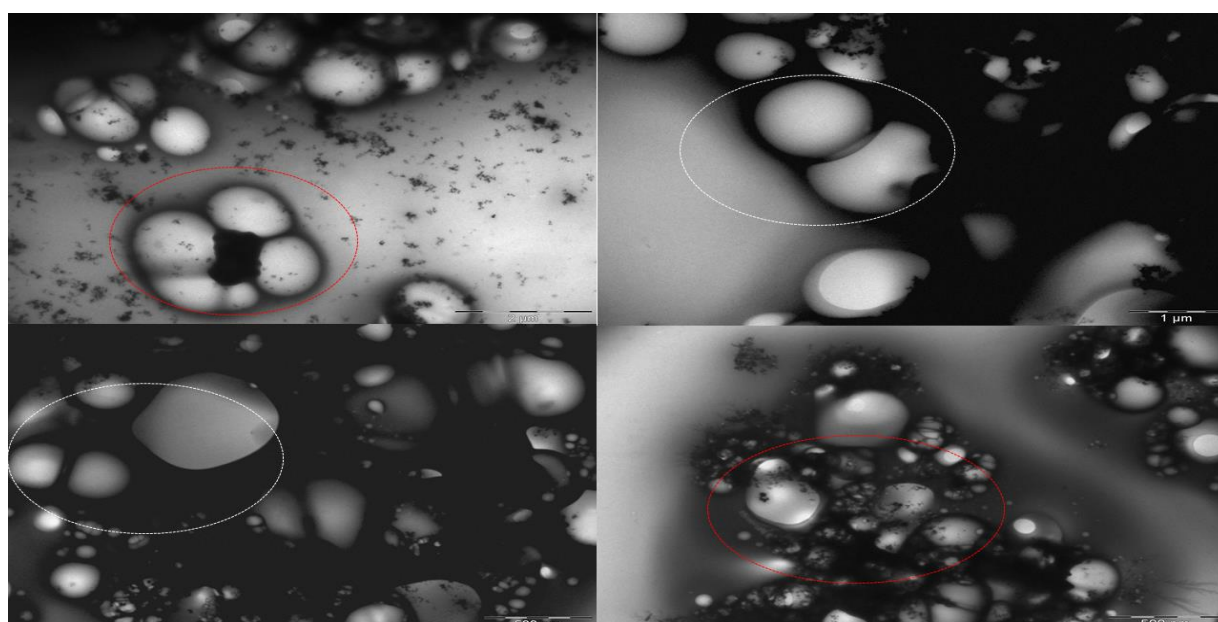


Figure 24. TEM analysis of unstained liposomes. White circles indicate empty liposomes and red circles indicated liposomes encapsulating silver nanoparticles (i.e., AgNPs inside of the liposomes).

6.3.4 The MTT assay results

6.3.4.1 Cell growth inhibition activity of plant extracts and AgNPs.

The cytotoxicity of the plant extracts and synthesized AgNPs were assayed by MTT against Vero and U87 glioma cell lines as outlined in section 3.4. The cells were treated with concentrations of 100-0.001 $\mu\text{g/mL}$ of the test samples. Emetine was used as positive control.

All the samples showed activity at the concentration of 100 $\mu\text{g/mL}$ (figure 25), while growth inhibition activity of the DCM extract and AgNPs was observed at 1 $\mu\text{g/mL}$. Some overgrowth of the cells was observed at the lowest concentration of 0,001 $\mu\text{g/mL}$ for three of the test samples, due to non-activity.

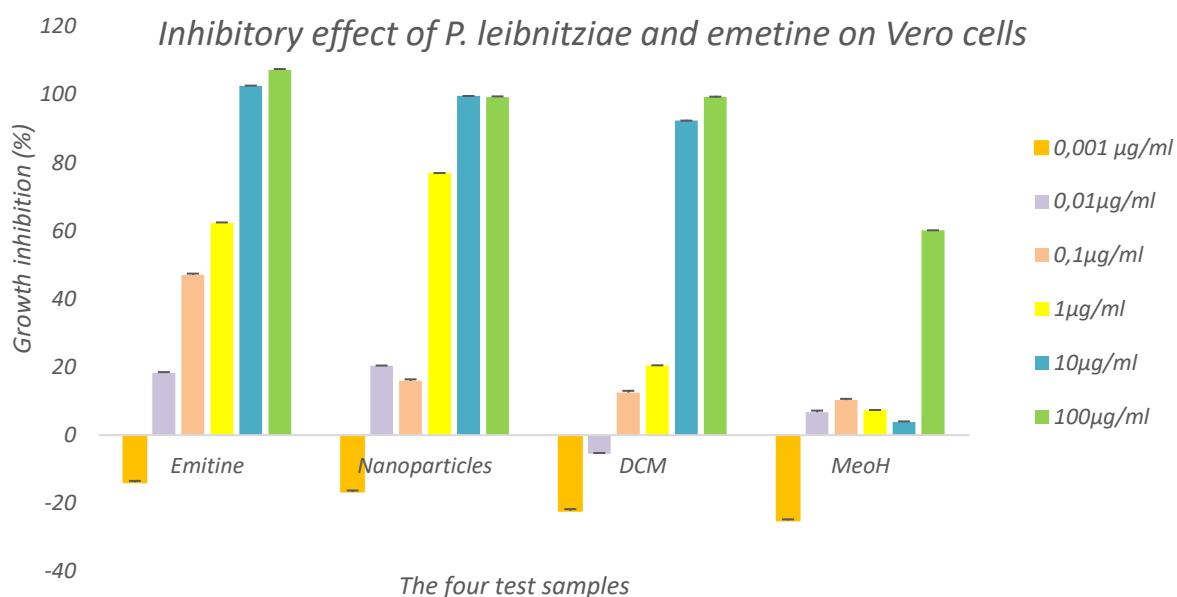


Figure 25. The inhibitory effect of the DCM and MeOH extracts of *P. leubnitziae*; AgNPs, and emetine on Vero cells.

The DCM extract and AgNPs showed the highest activity and were for further testing against the U87 cell line. The U87 cell line showed neurospheres like appearance after 48 hours of incubation (figure 26). This confirms that the cell line mimicked the microenvironment of the

brain. The U87 cell lines are shown to form a network in stressful conditions, this is the time when nutrients are becoming depleted and as a survival mode these tumor cells form a network. The live cell count results showed that a larger portion of the cells survived even when nutrients were becoming depleted.

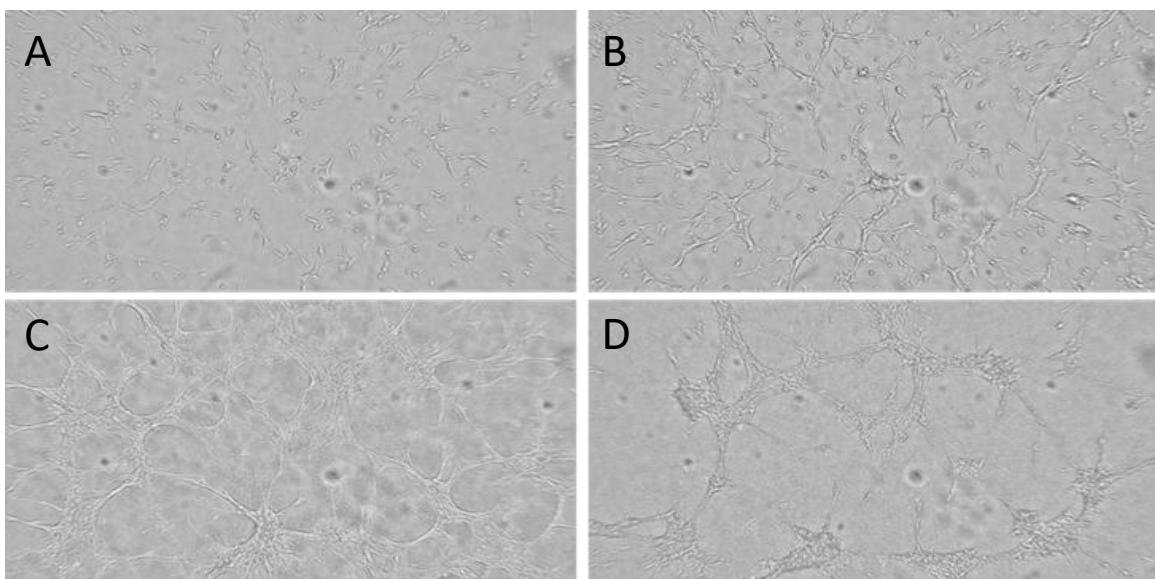


Figure 26. The growth pattern of the U87 Glioma over a period of 48 hours; A) The U87 glioma cells on the first day after thawing of the cells, before incubation B) The cells after an hour of incubation, C) The cells after 24 hours of incubation, and D) the cells after 48 hours of incubation.

When the cell culture medium was supplemented with silver nanoparticles, it was observed that the culture had reached more than 50% cell death as indicated by the red colour after 12 hours of medium supplementation (figure 27).

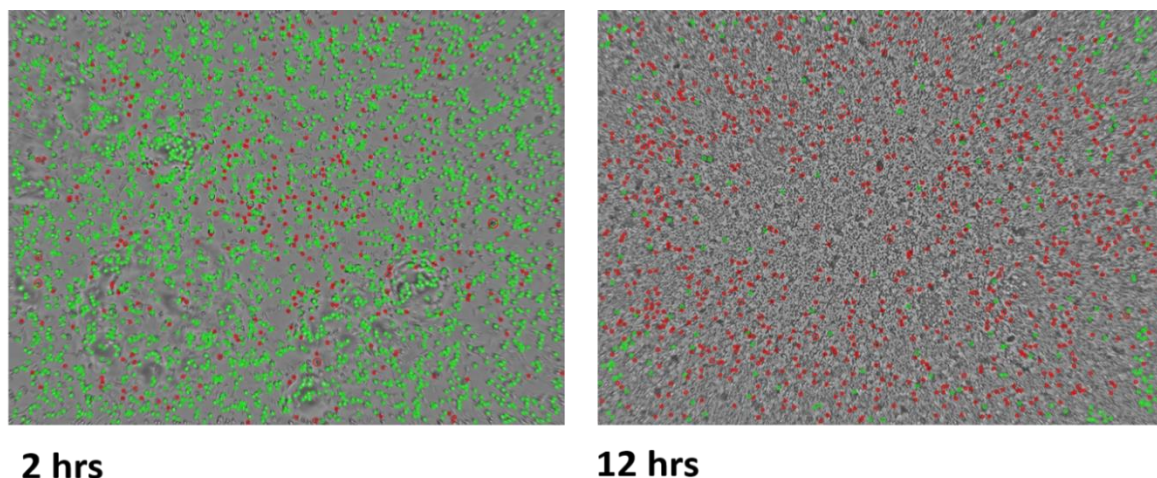


Figure 27. The cell viability count results of the cell culture after 2 hours and 12 hours of incubation with medium containing silver nanoparticles at a concentration of 1 $\mu\text{g/ml}$.

6.3.4.2 Cell growth inhibition of U87 cells by extracts of *P. leibnitziae* and AgNPs.

Based on the obtained cytotoxicity results, the anticancer activity of the DCM extract and silver nanoparticles was investigated further against the U87 cell line (figure 28). The results revealed that the DCM extract had inhibitory activities against the U87 glioma cell line, with IC_{50} value in the range of 3 $\mu\text{g/mL}$ as shown in table 10. Silver oxide nanoparticles exhibited enhanced cell inhibitory effect with IC_{50} values in the range of 0, 64-0, 71 $\mu\text{g/mL}$, while emetine exhibited activity with an IC_{50} in the range of 3,47 $\mu\text{g/mL}$. According to CSIR criteria for anticancer and cytotoxicity, an $\text{IC}_{50} > 100$ is considered inactive and less hazard, thus these low IC_{50} values suggest the strong inhibitory activity of the test samples against U87 cell line, particularly that of the AgNPs, which exceeded the activity of the positive control drug. The data showed that R-square values, which indicates the closeness of data to the regression line, was in the range of 0.61- 0.95.

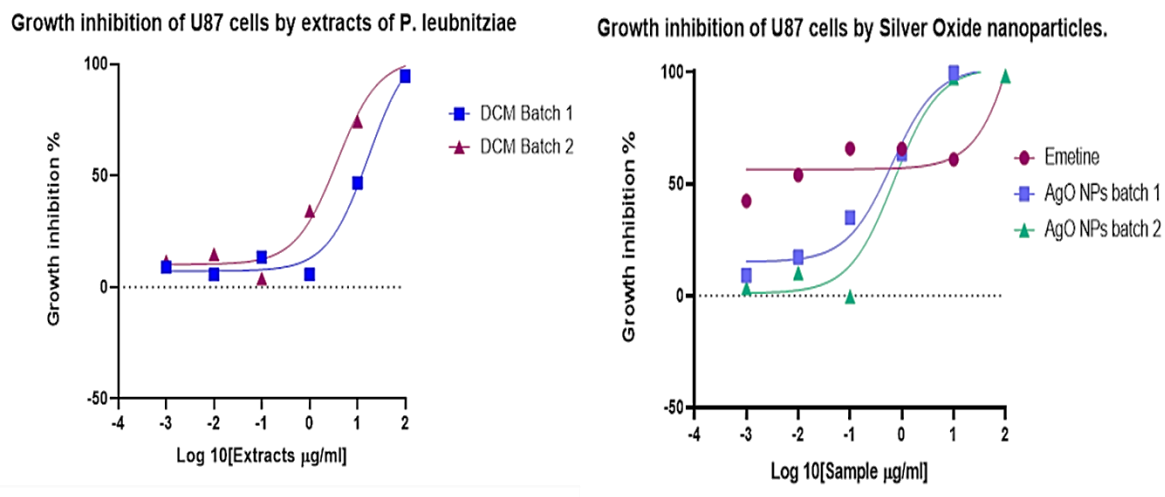


Figure 28. The cell growth inhibitory effects of test samples against the U87 cell line, a) batch 1= DCM extracts, batch 2= DCM extract from Namibia. b) Cytotoxic standard drug emetine used as positive control; nanoparticles synthesised using plant material. The synthesis experiment was repeated twice to produce batch 1 and batch 2 of the nanoparticles.

Table 11. The IC₅₀ [µg/mL] values of cell growth inhibitory effect of the DCM extracts of *P. leibnitziae*, the AgNPs and emetine drug

	<i>The plant extracts</i>		<i>Standard drug</i>	<i>Silver nanoparticles</i>	
	DCM batch 1	DCM batch 2	Emetine	Batch 1	Batch 2
IC₅₀ [µg/mL]	3,26	3,74	3,47	0,64	0,71
R squared	0,61	0,83	0,69	0,95	0,93

The results were obtained from Prism GraphPad Prism version 8.0 software for Windows.

6.3.5 Fractionation of the DCM extract and isolation of active compound

The DCM extract was selected for fractionation due to the observed high cell growth inhibitory activity against both the Vero and U87 cell lines (figure 25). The fractionation by column chromatography gave a yield of 117 fractions of 10 ml each. The fractions were labelled Npk1

and followed by order of collection. The fractions Npk1 F70-77 and Npk1 F78-90 showed crystallization immediately after collection and drying (figure 29).

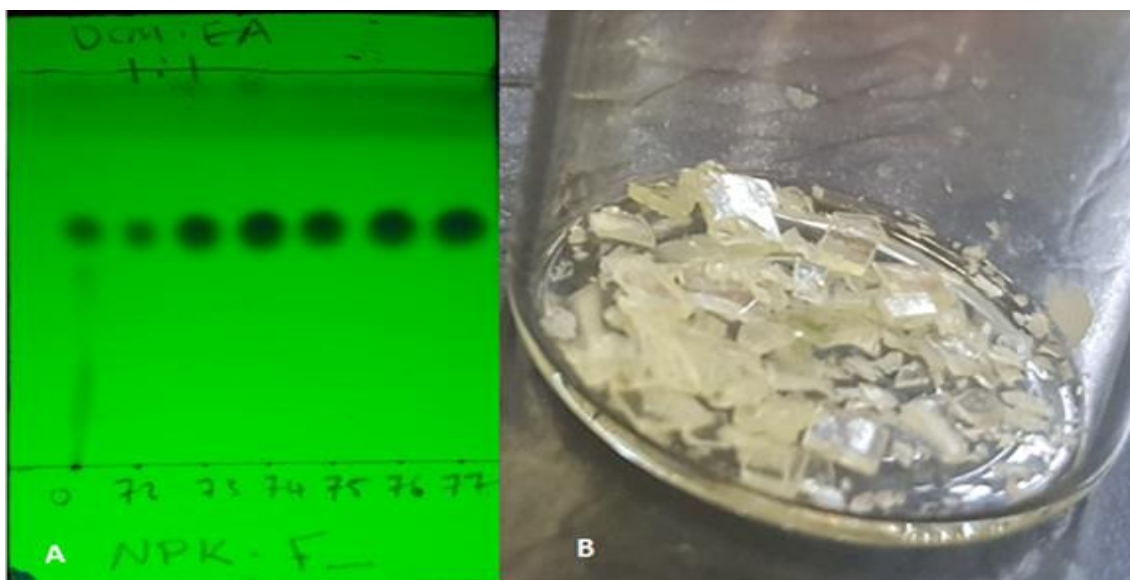


Figure 29. Fractionation of the DCM extract by column chromatography, A) the TLC plate with the different fractions (F70-F77), and B) the crystallized fractions F70-77 and F78-90 after being combined based on their similar profile on TLC plate.

6.3.5.1 Identification of the chemical structure of the isolated compound

The structural analysis of the crystallized fraction in figure 29 revealed a molecular weight of 246.3042 g/mol. The compound was further identified as Xerantholide (figure 30) using the ¹H-NMR Spectrum, ¹³C-NMR Spectrum and FTIR (Kadhila P., 2018). The compound Xerantholide was identified to belong to the sesquiterpene lactones.

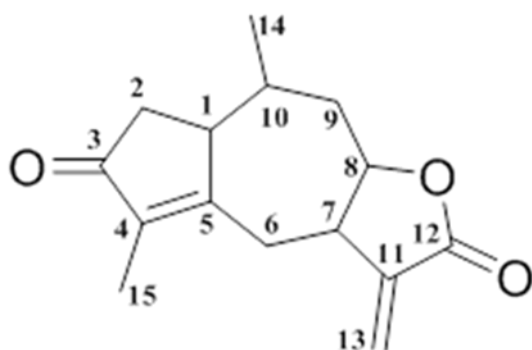


Figure 30. The structural characterization of a C13 compound with molecular weight 246.3042 g/mol

6.3.5.2 Cell growth inhibition of CHO cells by *P. leibnitziae* fractions.

The pure crystallized compounds were tested for cytotoxicity against Vero, U87 and CHO cell lines (figure 31-33). The results showed that the fraction 78 inhibited CHO cells by over 50% at all tested concentrations of 0.001-100 $\mu\text{g/mL}$ in comparison to emetine. Fraction 70 reached over 50% cell growth inhibition only at concentrations of 10 $\mu\text{g/mL}$ and 100 $\mu\text{g/mL}$ (figure 31). Further analysis showed that fraction 78 inhibited U87 cell by over 50% from 10-100 $\mu\text{g/mL}$, while fraction 70 had 50% inhibitory activity from a concentration of 5-100 $\mu\text{g/mL}$ (figure 32). When compared to the Vero cell line, fraction 70 and 78 showed decreased inhibitory activity, with 50% inhibitory activity only been observed at 50 and 100 $\mu\text{g/mL}$ (figure 33).

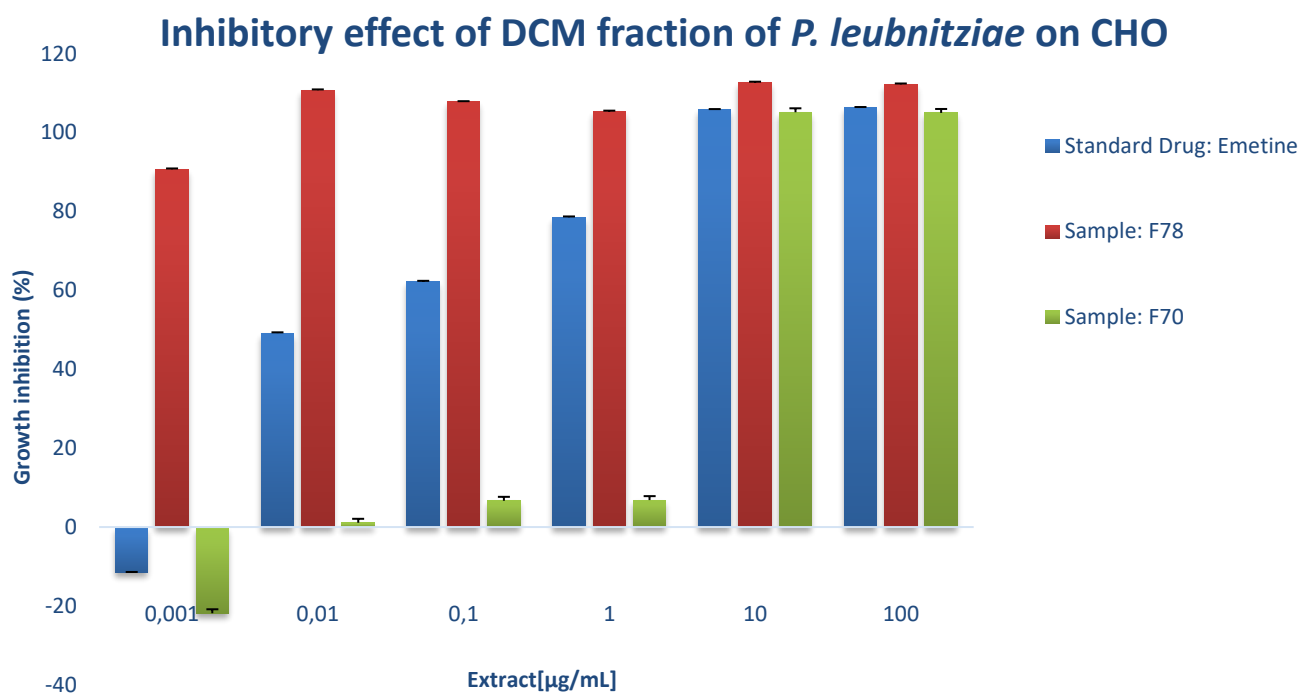


Figure 31. Inhibitory effect of DCM fractions of *P. leubnitziae* and Emetine on CHO cells.

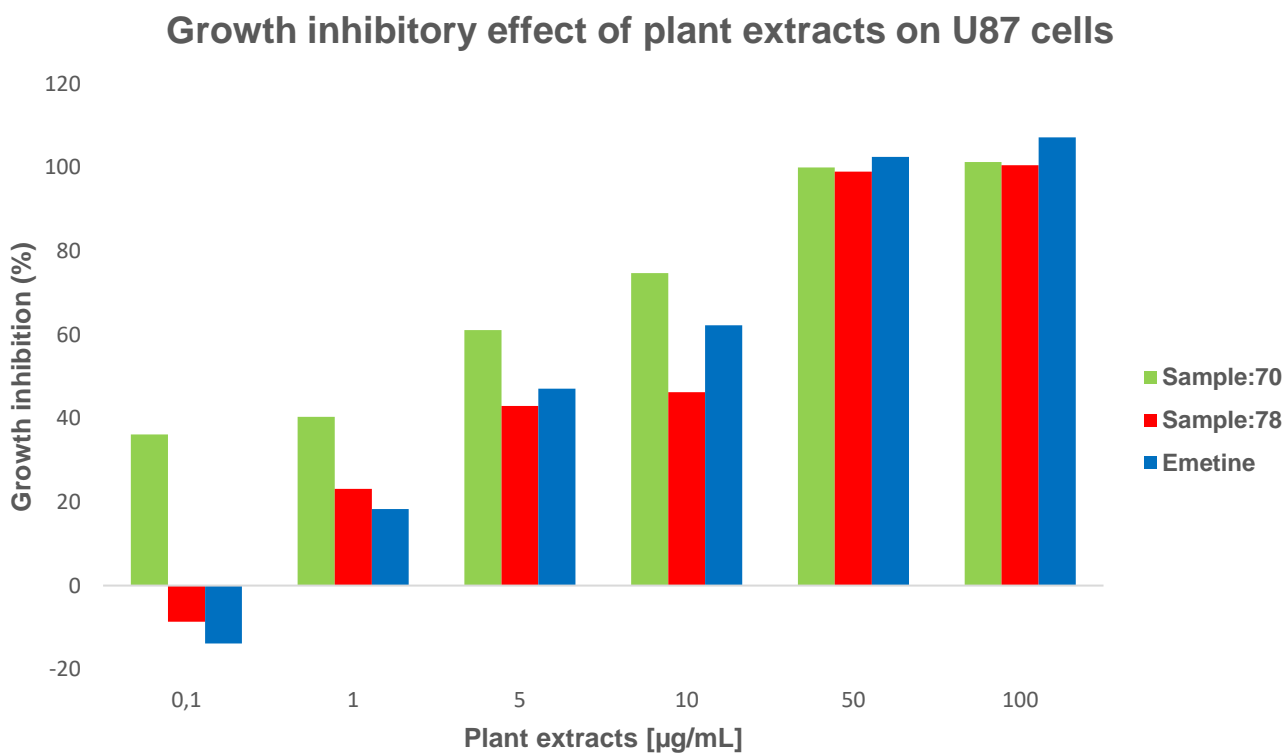


Figure 32. Inhibitory effect of DCM fractions of *P. leubnitziae* and Emetine on U87 cells.

Growth inhibitory effect of DCM fraction of *P.leubnitziae* on Vero cells

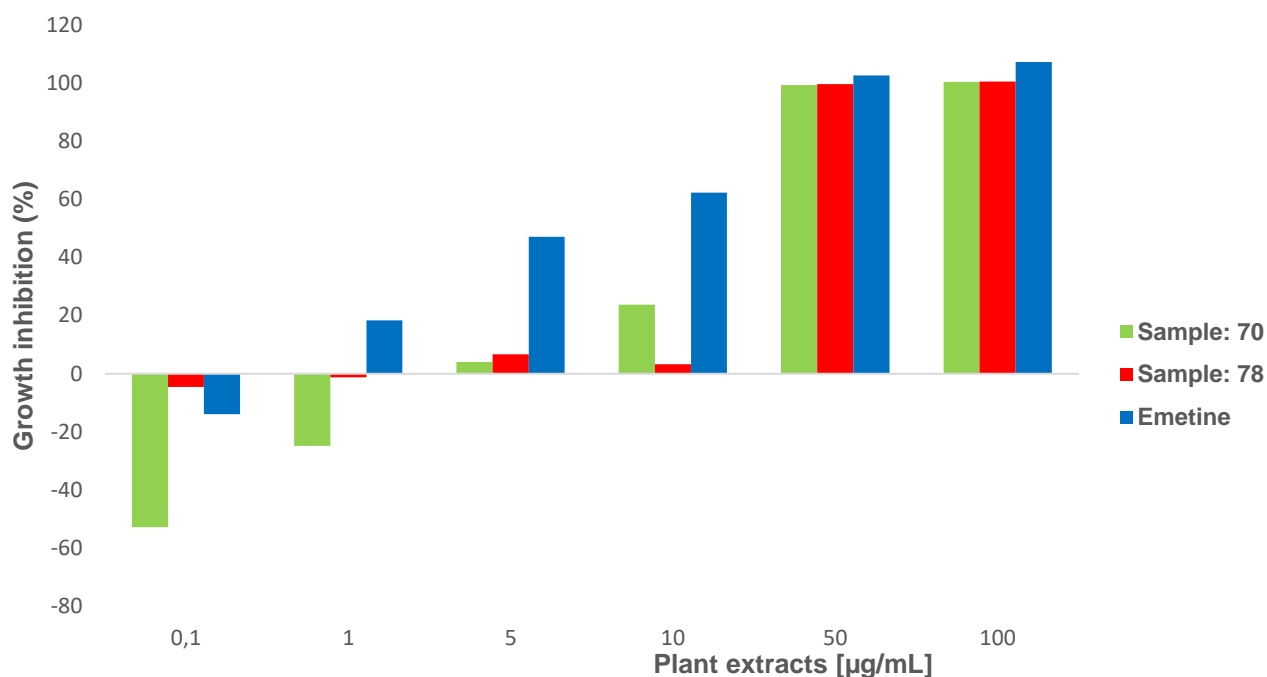


Figure 33. Inhibitory effect of DCM fractions of *P. leubnitziae* and Emetine on Vero cells.

6.4 Discussion

Phytochemical analysis in this study showed the presence of terpenoids, saponins, anthroquinones, coumarins, flavonoids and alkaloids. The FTIR results of the silver oxide nanoparticle revealed peaks that according to literature, correlate to the presence of classes of compounds such as phenolic, tannins and those identified in our studies; flavonoids and saponins as major functional groups for the formation of the silver oxide nanoparticle (Kumar et al., 2010). Mixture of the plant extract and silver nitrate showed a change in colour from brown to dark greyish blue occurred, indicating the reduction of Ag^+ ions to silver oxide by

the plant metabolites. This was further confirmed by the UV-vis spectroscopy with a peak which correlated to the formation of silver nanoparticles aggregation (Lu et al., 2005). The XDR also indicated the presence of peaks that correlate to the face-centred cubic (fcc) crystal structure of metallic silver. The aggregation of silver nanoparticle was further confirmed by SEM at 100 μm , and a uniform stable silver oxide nanoparticle was shown to be in alignment with a study done on the synthesis of silver oxide nanoparticles by Li Kai et al., (2012) at room temperature. The components identified from XPS and EDAX confirmed the presence of silver as part of the constituents in the sample, together with other constituents e.g., carbon, oxygen etc.

The cytotoxicity results showed the DCM extract, which is known to extract low polarity compounds, exhibited the highest inhibitory activity against both the Vero cell line and U87 cell line, in contrast to the MeOH extracts. Further investigation of the DCM extract against the U87 cell line, showed the extract to have some potential anti-cancer activity properties. Further fractionation of the DCM extract yielded 117 fractions, with fractions 70 and 78 showing increased growth inhibition against the CHO cell line. Furthermore, the synthesized nanoparticles showed activity in a concentration dependent manner, with high inhibitory activity at the highest concentration. The increased inhibition of the silver nanoparticles in comparison to the plant extract against the U87 cells suggests that the nanoparticles have potential anti-proliferative activities and are potent anticancer agents. According to the CSIR criteria, $IC_{50} < 6.25 \mu\text{g/mL}$ against cancer cells is considered a potent anticancer activity (Mariri, 2017).

The use of AgNPs in *in vitro* studies continues to show the toxicity of the nanoparticles towards cancer cells, suggesting the importance of stabilizing the AgNPs for treatment of human cancers. Liposomal nanoparticles have unique characteristics that make them efficient drug delivery systems. Characteristics such their ability to mimic the lipid bilayer of the cell membrane (Yusuf and Casey et al., 2017), and to carry both hydrophobic and hydrophilic molecules has made them very essential for the study. The study aimed at designing a nano carrier system using liposomes, which could be used to deliver silver nano particles into the brain for treatment of Glioblastoma. The study showed successful entrapment of AgNPs in liposomes, which has fulfilled the intended design of a nano carrier system predictably suitable for delivery of chemotherapy into the brain.

The compound Xerantholide was identified to belong to the sesquiterpene lactones, which are well known for the high diversity in their structures and biological activities (Zhang et al., 2005). Their functional group, α -methylene- γ -lactone ring, has been identified as a lead promising anticancer effect. In a study related to the plant *P. leibnitziae*, the DCM extract was also shown to have *in vitro* activity against malaria parasite, *Plasmodium falciparum*. The antimalarial properties were potentially attributed to the presence of Xerantholide (Castangia et al., 2017). It is therefore possible that this molecule is responsible for the cell inhibitory activity observed in the DCM extract.

CHAPTER 7

GENERAL DISCUSSION AND CONCLUSION

7.1 The relevance of the study

Glioblastoma, a type of tumor that arises from glia within the central nervous system, has been shown to be one of the most aggressive type of astrocytoma tumors (Béduneau et al., 2007). In African populations, traditional medicine, particularly medicinal plants, has been historically used for the treatment of different diseases including cancer (Cunningham, 1993). These medicinal plants possess secondary metabolites like polyphenols, terpenes and alkaloids which have anti-mutagenic and anticancer properties. Despite the wide use of medicinal plants, there is still insufficient information with regards to their antioxidant activity, active phytochemicals, selectivity for cancerous cells, and the safety towards normal human cells. Antioxidant and cytotoxicity are two of the major evaluations in cancer. Antioxidants play an important role when reactive oxygen species are activated in cells. Reactive oxygen species in cancer research have been demonstrated to activate cell progression, inflammation, invasion, and many more pathways (Sabharwal and Schumacker, 2014). Antioxidants, however, counteract by chelating ROS and maintain redox equilibrium in cells (Fuchs-Tarlovsky, 2013).

Furthermore, some phytochemicals have potential to reduce metal precursors to nanoparticles, which can be used in treatment of brain tumors (Marstin et al., 2018; Leela and Vivekanandan, 2008). The investigation of medical plants in cancer research seems important and relevant in three aspects which are explored in this study:

- It is important to identify plants with phytochemicals that have potential to inhibit cancerous cells in a selective manner, either through high antioxidant activity or potent cytotoxicity.

- It is technologically and scientifically useful to identify and use phytochemicals found in plants to synthesise nanoparticles that have cell anti-proliferation activity
- It is important to purify and identify the chemical structures of compounds or plant constituents responsible for the cell antiproliferation, so that these can be further developed into anticancer drugs should they have satisfactory safety and efficacy profiles.

Chemotherapeutic treatment for brain tumors, which involves the use of chemical molecules, has been drastically hindered by the presence of the blood brain barrier, which is very selective of the types of drugs that can enter the brain. Nanoparticles presents high probability to cross the BBB due to their small size, which is in the range of 1-100 nm. Silver nanoparticles have demonstrated to cross the blood brain barrier and inhibit cancerous cells *in vivo* studies (Mahringer et al., 2013). These however, also affected the non-cancerous normal brain cells.

In this study, to synthesise the AgNPs, green synthesis method was employed using the plant *P. leubnitziae* to synthesize silver nanoparticles. While silver nanoparticles are shown to have anticancer properties, they have also been demonstrated to have some equal and similar effect on normal cells. The delivery of these nanoparticles into the brain to treat glioblastoma would be detrimental to normal brain cells, hence the need to encapsulate them in liposomal nanoparticles as a nano-delivery system which is hypothesised to be safer and more efficient, as it mimics the brain environment better. Stabilization of the silver nanoparticles which was one of the most important objectives of the study is very crucial in maintaining the integrity of the blood brain barrier while ensuring safe and efficient delivery of anticancer components to the brain tumor. The selection of cationic liposomes is important due to their ability to mimic and fuse the cell membrane, which then allows the silver nanoparticles to cross the blood brain

barrier. The relevance of this mechanism in cancer treatment, as hypothesised by the study, is that the encapsulated nano-delivery system would increase the bioavailability of anticancer agents in the brain tumors which currently is a huge challenge facing successful treatment of brain tumors by chemotherapy.

7.2 The extent to which objectives have been met.

The study investigated three medicinal plants specie's: *D. camilla*, *A. multiflorum* and *P. leibnitziae*. The study aimed to evaluate their cancer cell antiproliferative activity, to assess their selectivity for cancers when compared to normal, their antioxidant activity, identification of their active constituents, and lastly, select one plant to use in the green synthesis to silver nanoparticles.

Objective 1

To achieve these; the plants were collected, dried and ground to fine power. Plant materials were extracted using organic solvents; HEX, DCM, and MeOH. Furthermore, ethyl acetate and a combination of DCM: MeOH (1:1) were also added to the list of solvents used for the extraction of *D. camilla* and *A. multiflorum*, respectively. The cytotoxicity of the extracts was tested against CHO and Vero cell lines. Further cytotoxic analysis was done only for the plant *P. leibnitziae* and *A. multiflorum* against U87 cell line.

The plant showed strong inhibitory effects against Vero cells, and moderated activity against U87 glioma cell line. *P. leibnitziae* showed strong inhibitory effects against Vero, and U87 glioma cell lines. *P. leibnitziae* showed rather significantly stronger inhibitory effect in comparison to the other two plants, hence its selection for further fractionation. Its fractions showed increased activity against the CHO cell lines.

Objective 2

The plants extract that showed considerable cell antiproliferation activity.

The three plants; *P. leibnitziae*, *D. camilla* and *A. multiflorum* showed the presence of flavonoids and alkaloids. These identified phytochemicals amongst other phytochemicals such as terpenoids and phenolic compounds have been demonstrated to act as capping or reducing agents in synthesis of nanoparticles (Hashemi et al., 2016). Furthermore, *D. camilla* tested positive for phytosterols, glycosides, anthroquines and saponins were identified positive. Although this plant possessed a variety of phytochemicals, it exerted moderate cytotoxic activity on selected cell lines. In addition to presence of phytosterols and glycosides, only *A. multiflorum* contained pentose sugars.

GC-MS analysis further revealed the presence of compounds such as *n* hexadecanoic acid, Bis (2-ethylhexyl) phthalate, tri(2-ethylhexyl) trimellitate, Hexadecanoic acid, methyl ester and l-(+)-Ascorbic acid 2,6-dihexadecanoate amongst many other compounds from *D. camilla*. These compounds that have been recorded to possess inflammatory effect, antitumor and antioxidant activity (Tamilselvan et al., 2014, Sufferdini et al., 2004, and Tamilselvan et al., 2014).

As mentioned above, *P. leibnitziae* showed stronger inhibitory hence its selection for further fractionation. Fractionation of the DCM extract of *P. leibnitziae* yielded fraction 70-78, which formed clear crystals, suggesting it was a pure compound. The compound was identified to be Xerantholide (Zhang et al., 2005).

Objective 3

The plant, *P. leibnitziae* was further used in synthesis of silver nanoparticles, using the green synthesis method (Marslin et al., 2018). The synthesised silver nanoparticles exhibited increased inhibitory effects when tested against the U87 cell line which correlated with studies done of the cell line by Urbańska and colleagues (Urbańska et al., 2015). As elaborated in the literature, silver nanoparticles also and equally negatively affect normal cells. Thus, encapsulation of silver nanoparticles in liposomes was conducted as a possible solution to combat the general cytotoxicity of silver nanoparticles.

Objective 4

Some of the methods used to synthesize liposomes are shown to be complex and require mass production (Lujan et al., 2019). Thin-film hydration, a method elaborated to synthesize small and uniform particle was selected for the purpose of the research (Ai et al., 2014). Although, in this project we observed different sizes of the liposomes, using TEM analysis, it was shown that the cationic liposomes were successfully synthesized and able to entrap silver nanoparticles and different shapes of the liposomes were observed. This part of the project satisfied the fourth and last objective of the project. Empty liposomes that were observed from the study could simply imply that for further studies the concentration of liposomes must be increased and a separation method between the empty and silver entrapped liposomes should be implemented.

7.3 Challenges and limitation

The main challenge experienced in the study was that the plants used for synthesis of the AgNPs is seasonal. Also, the plant *P. leibnitziae* was collected from another country (Namibia), making recollection, and transportation of plant material across border difficult. This affected the momentum of the research especially when extracts ran out during cell culture analysis.

The size of the liposomes encapsulating the AgNPs is important to ensure that liposomes successfully cross the blood brain barrier. The study could not produce the uniform size nor determine the size of the liposomal vesicles formed. This was due to the expensive price of the filter membrane for liposomes, which were unattainable. We recommend that these be done in future studies. It is important that *in vitro* testing and analysis precede *in vivo* experimentation. Due to time limitation, liposomes were successfully synthesized, however the efficiency of the liposomes was not assayed against U87 cell line *in vitro*, which means that the efficacy and safety aspects of our AgNPs-liposomes nano carrier was not determined *in vitro* and its effect in *in vivo* cannot be extrapolated from *in vitro* results.

7.4 Conclusions

The plant *P. leubnitziae* showed strong inhibitory effect and phytochemicals with abilities to reduce metal salt into nanoparticles. Furthermore, the other plants, *D. camilla* and *A. multiflorum*, also demonstrated presence of phytochemicals with anticancer and antioxidant actives. The *A. multiform*, has been shown to have potent antioxidant activity and inhibitory activity against the U87 cell line. No reports have been shown for using this plant in cancer

research. The results obtained in this study suggest that based on the phytochemicals, potent antioxidant activity and cell cancer growth inhibitory activity, this plant, *A. multiform*, can be considered for use with caution for cancer treatment in primary and home-based care in communities where traditional medicine is the main if not the only treatment option available. The selected plants were able to produce experimental results and leave room for further studies to be done.

FUTURE WORK

Future work includes testing or the cytotoxic effect of the developed nano-carrier delivery system and testing their ability to cross the blood brain barrier of Sprague rats. This future work forms part of my PhD proposal, which is a continuation of this work, with additional innovative technological advances relevant to development of nanomedicine for brain cancer treatment.

REFERENCE

1. A. Yusuf1, A. Brophy, B. Gorey, A. Casey, Liposomal encapsulation of silver nanoparticles enhances cytotoxicity and causes induction of reactive oxygen species independent apoptosis.
2. Adams, C.P., Walker, K.A., Obare, S.O. and Docherty, K.M., 2014. Size-dependent antimicrobial effects of novel palladium nanoparticles. *PLoS One*, 9(1), p.e85981.
3. Ainsworth, E.A. and Gillespie, K.M., 2007. Estimation of total phenolic content and other oxidation substrates in plant tissues using Folin–Ciocalteu reagent. *Nature protocols*, 2(4), p.875.
4. Alberts, B., Johnson, A., Lewis, J., Walter, P., Raff, M. and Roberts, K., 2002. *Molecular Biology of the Cell 4th Edition: International Student Edition*.
5. Alekshun, M.N. and Levy, S.B., 2007. Molecular mechanisms of antibacterial multidrug resistance. *Cell*, 128(6), pp.1037-1050.
6. Andreescu, D., Eastman, C., Balantrapu, K. and Goia, D.V. A simple route for manufacturing highly dispersed silver nanoparticles. *Journal of materials research* 2007. 22(9), pp.2488-2496. DOI: 10.1557/jmr.2007.0308
7. Anti-Angiogenic Effect of Nelumbo nucifera Leaf Extracts in Human Umbilical Vein Endothelial Cells with Antioxidant Potential Jong Suk Lee1, Shruti Shukla1, Jung-Ae Kim2, Myunghee Kim1*
8. Apel, K. and Hirt, H., 2004. Reactive oxygen species: metabolism, oxidative stress, and signal transduction. *Annu. Rev. Plant Biol.*, 55, pp.373-399.

9. Ardittiaad, J and Rodriguez, E. (1982). Dieffenbachia uses abuses and toxic constituents. *A Review Journal of Ethno Pharmacology*. Pp 293-302.
10. Asharani, P.V., Hande, M.P. and Valiyaveetil, S. Anti-proliferative activity of silver nanoparticles. *BMC cell biology* 2009, 10(1), p.65. DOI: 10.1186/1471-2121-10-65
11. Asharani, P.V., Hande, M.P. and Valiyaveetil, S., 2009. Anti-proliferative activity of silver nanoparticles. *BMC cell biology*, 10(1), p.65.
12. Ashokkumar, R. and Ramaswamy, M. Phytochemical screening by FTIR spectroscopic analysis of leaf extracts of selected Indian medicinal plants. *Journal of Current Microbiology and Applied Sciences* 2014, 3(1), pp.395-406.
13. Bagchi, K. and Puri, S., 1998. Free radicals and antioxidants in health and disease: A review.
14. Becker, E.M., Nissen, L.R. and Skibsted, L.H., 2004. Antioxidant evaluation protocols: Food quality or health effects. *European Food Research and Technology*, 219(6), pp.561-571.
15. Béduneau, A., Saulnier, P. and Benoit, J.P., 2007. Active targeting of brain tumors using nanocarriers. *Biomaterials*, 28(33), pp.4947-4967.
16. Behin, A., Hoang-Xuan, K., Carpentier, A.F. and Delattre, J.Y., 2003. Primary brain tumours in adults. *The Lancet*, 361(9354), pp.323-331.
17. Bendary, E.; Francis, R.R.; Ali, H.M.G.; Sarwat, M.I.; El Hady, S. Antioxidant and structure–activity relationships (SARs) of some phenolic and anilines compounds. *Ann. Agric. Sci.* 2013, 58, 173–181.

18. Benzie, I.F. and Strain, J.J., 1996. The ferric reducing ability of plasma (FRAP) as a measure of “antioxidant power”: the FRAP assay. *Analytical biochemistry*, 239(1), pp.70-76.
19. Berg JM, Tymoczko JL, Stryer L. *Biochemistry*. 5th edition. New York: W H Freeman; 2002. Section 15.5 Defects in Signalling Pathways Can Lead to Cancer and Other Diseases. Available from: <https://www.ncbi.nlm.nih.gov/books/NBK22359/>
20. Berg JM, Tymoczko JL, Stryer L. *Biochemistry*. 5th edition. New York: W H Freeman; 2002. Section 15.5 Defects in Signalling Pathways Can Lead to Cancer and Other Diseases. Available from: <https://www.ncbi.nlm.nih.gov/books/NBK22359/>
21. Bhandary, S.K., Kumari, S.N., Bhat, V.S., Sharmila, K.P. and Bekal, M.P., 2012. Preliminary phytochemical screening of various extracts of Punica granatum peel, whole fruit and seeds. *J Health Sci*, 2(4), pp.35-8.
22. Boots, A.W.; Haenen, G.R.; Bast, A. Health effects of quercetin: From antioxidant to nutraceutical. *Eur. J. Pharmacol.* 2008, 585, 325–337.
23. Borek, C., 2004. Dietary antioxidants and human cancer. *Integrative cancer therapies*, 3(4), pp.333-341.
24. Bosch, C.H. Siemonsma, J.S., Lemmens, R.H.M.J. and Oyen, L.P.A (2002). *Plant Resource of Tropical Africa. Basic List of species and commodity groupings* Pp. 341.
25. Bozzuto, G. and Molinari, A., 2015. Liposomes as nanomedical devices. *International journal of nanomedicine*, 10, p.975.
26. Bradfield, J., Lombard, M. and Wadley, L., 2015. Southern African arrow poison recipes, their ingredients and implications for Stone Age archaeology. *Southern African Humanities*, 27(1), pp.29-64.

27. Bradford, P.G. and Awad, A.B., 2007. Phytosterols as anticancer compounds. *Molecular nutrition and food research*, 51(2), pp.161-170.
28. Brglez Mojzer, E., Knez Hrnčič, M., Škerget, M., Knez, Ž. and Bren, U., 2016. Polyphenols: extraction methods, antioxidative action, bioavailability and anticarcinogenic effects. *Molecules*, 21(7), p.901.
29. Brigger, I., Dubernet, C. and Couvreur, P., 2012. Nanoparticles in cancer therapy and diagnosis. *Advanced drug delivery reviews*, 64, pp.24-36.
30. Cai, Y., Luo, Q., Sun, M. and Corke, H., 2004. Antioxidant activity and phenolic compounds of 112 traditional Chinese medicinal plants associated with anticancer. *Life sciences*, 74(17), pp.2157-2184.
31. Castangia, I., Marongiu, F., Manca, M.L., Pompei, R., Angius, F., Ardu, A., Fadda, A.M., Manconi, M. and Ennas, G. Combination of grape extract-silver nanoparticles and liposomes: a totally green approach. *European Journal of Pharmaceutical Sciences* 2017, 97, pp.62-69. DOI: 10.1016/j.ejps.2016.11.006
32. Cerrano C, Bavestrello G, Arillo A, Benatti U, Bonpadre S, et al. 1999. Calcium oxalate production in the marine sponge *Chondrosia reniformis*. *Mar. Ecol.-Prog. Ser.* 179:297–300
33. Chang, H.J., Burke, A.E. and Glass, R.M., 2010. Gliomas. *JAMA*, 303(10), pp.1000-1000.
34. Charles P. Davis, MD, PhD. 2016. Brain Tumor Symptoms, Signs, Types, Causes, Treatments, and Survival Rates. [ONLINE] Available at: https://www.medicinenet.com/brain_tumor/article.htm.

35. Chastain, J. Handbook of X-ray photoelectron spectroscopy. Perkin-Elmer Corporation 1992, 40, p.221.
36. Cheney, R.H. (1931). Geographic and Taxonomic Distribution of American Plant Arrow Poisons. American Journal of Botany, 6:136-145.
37. Cheng, Y., Morshed, R.A., Auffinger, B., Tobias, A.L. and Lesniak, M.S., 2014. Multifunctional nanoparticles for brain tumor imaging and therapy. Advanced drug delivery reviews, 66, pp.42-57.
38. Chinsembu, K.C. Plants as antimalarial agents in Sub-Saharan Africa. Acta tropica 2015, 152, pp.32-48. DOI: 10.1016/j.actatropica.2015.08.009
39. Cunningham, A.B., 1993. African medicinal plants. United Nations Educational, Scientific and Cultural Organization: Paris, France.
40. Davson H, Oldendorf WH (1967) Proc R Soc Med 60:326–329
41. De Jong, W.H. and Borm, P.J., 2008. Drug delivery and nanoparticles: applications and hazards. International journal of nanomedicine, 3(2), p.133.
42. De Matteis, V., Cascione, M., Toma, C. and Leporatti, S. Silver nanoparticles: Synthetic routes, in vitro toxicity and theranostic applications for cancer disease. Nanomaterials 2018, 8(5), pp.319. DOI: 10.3390/nano8050319
43. Dizaj, S.M., Lotfipour, F., Barzegar-Jalali, M., Zarrintan, M.H. and Adibkia, K., 2014. Antimicrobial activity of the metals and metal oxide nanoparticles. Materials Science and Engineering: C, 44, pp.278-284.
44. Dushimemaria, F. and Mumbengegwi, D.R. Proposition of a low-cost field assay to determine antiproliferative properties of indigenous plants using *Dugesia*

- dorotocephala (brown planaria). *Scientific Research and Essays* 2015, 10(4), pp.144-149. DOI: 10.5897/SRE2014.6112
45. Duthie, G.G., Duthie, S.J. and Kyle, J.A., 2000. Plant polyphenols in cancer and heart disease: implications as nutritional antioxidants. *Nutrition research reviews*, 13(1), pp.79-106.
46. Fabi, A., Felici, A., Metro, G., Mirri, A., Bria, E., Telera, S., Moschetti, L., Russillo, M., Lanzetta, G., Mansueto, G. and Pace, A., 2011. Brain metastases from solid tumors: disease outcome according to type of treatment and therapeutic resources of the treating center. *Journal of Experimental and Clinical Cancer Research*, 30(1), p.10.
47. Farnsworth, N.R., Akerele, O., Bingel, A.S., Soejarto, D.D. and Guo, Z., 1985. Medicinal plants in therapy. *Bulletin of the world health organization*, 63(6), p.965.
48. Fochtman FW, Manno JE, Winek CL, Cooper JA. 1969. Toxicity of the genus *Dieffenbachia*. *Toxicology and Applied Pharmacology* 15: 38-45.
49. Franceschi VR. 2001. Calcium oxalate in plants. *Trends Plant Sci.* 6:331
50. Fresco, P.; Borges, F.; Marques, M.P.M.; Diniz, C. The Anticancer Properties of Dietary Polyphenols and its Relation with Apoptosis. *Curr. Pharm. Des.* 2010, 16, 114–134.
51. Furnari, F.B., Fenton, T., Bachoo, R.M., Mukasa, A., Stommel, J.M., Stegh, A., Hahn, W.C., Ligon, K.L., Louis, D.N., Brennan, C. and Chin, L., 2007. Malignant astrocytic glioma: genetics, biology, and paths to treatment. *Genes and development*, 21(21), pp.2683-2710.
52. Goodenberger, M.L. and Jenkins, R.B., 2012. Genetics of adult glioma. *Cancer genetics*, 205(12), pp.613-621.

53. Gurunathan, S., Han, J.W., Eppakayala, V., Jeyaraj, M. and Kim, J.H. Cytotoxicity of biologically synthesized silver nanoparticles in MDA-MB-231 human breast cancer cells. *BioMed research international*, 2013. DOI: 10.1155/2013/535796
54. Hajhashemi, V., Vaseghi, G., Pourfarzam, M. and Abdollahi, A., 2010. Are antioxidants helpful for disease prevention?. *Research in pharmaceutical sciences*, 5(1), p.1.
55. He, H., Lu, Y., Qi, J., Zhu, Q., Chen, Z. and Wu, W., 2019. Adapting liposomes for oral drug delivery. *Acta pharmaceutica sinica B*, 9(1), pp.36-48.
56. Israelachvili, J.N., Mitchell, D.J. and Ninham, B.W., 1976. Theory of self-assembly of hydrocarbon amphiphiles into micelles and bilayers. *Journal of the Chemical Society, Faraday Transactions 2: Molecular and Chemical Physics*, 72, pp.1525-1568.
57. Jeong, J.H., Kang, S.H., Kim, D.K., Lee, N.S., Jeong, Y.G. and Han, S.Y., 2019. Protective Effect of Cholic Acid-Coated Poly Lactic-Co-Glycolic Acid (PLGA) Nanoparticles Loaded with Erythropoietin on Experimental Stroke. *Journal of nanoscience and nanotechnology*, 19(10), pp.6524-6533.
58. Joshi, D.M., Rana, N.K. and Misra, V., 2010, May. Classification of brain cancer using artificial neural network. In *2010 2nd International Conference on Electronic Computer Technology* (pp. 112-116). IEEE.
59. Kadhila, N.P. Evaluation of indigenous Namibian mushrooms and plants for antimalarial properties (Doctoral dissertation, University of Namibia) 2019.
60. Kathiravan, V., Ravi, S. and Ashokkumar, S. Synthesis of silver nanoparticles from *Melia dubia* leaf extract and their in vitro anticancer activity. *Spectrochimica Acta Part*

- A: *Molecular and Biomolecular Spectroscopy* 2014, 130, pp.116-121. DOI: 10.1016/j.saa.2014.03.107
61. Kumar, G., Karthik, L. and Rao, K.B. Phytochemical composition and in vitro antimicrobial activity of *Bauhinia racemosa* Lamk (Caesalpinaceae). *International Journal of Pharmaceutical Sciences and Research* 2010, 1(11), p.51.
62. Kumar, V. and Yadav, S.K., 2009. Plant-mediated synthesis of silver and gold nanoparticles and their applications. *Journal of Chemical Technology and Biotechnology: International Research in Process, Environmental and Clean Technology*, 84(2), pp.151-157.
63. Lee, J.H. and Yeo, Y., 2015. Controlled drug release from pharmaceutical nanocarriers. *Chemical engineering science*, 125, pp.75-84.
64. Leela, A. and Vivekanandan, M., 2008. Tapping the unexploited plant resources for the synthesis of silver nanoparticles. *African Journal of Biotechnology*, 7(17).
65. Levin, V.A., Leibel, S.A. and Gutin, P.H., 2001. Neoplasms of the central nervous system. *Cancer: Principles and Practice of Oncology*. 6th ed. Philadelphia: Lippincott Williams and Wilkins, pp.2100-60.
66. Li, J., Wang, X., Zhang, T., Wang, C., Huang, Z., Luo, X. and Deng, Y., 2015. A review on phospholipids and their main applications in drug delivery systems. *Asian journal of pharmaceutical sciences*, 10(2), pp.81-98.
67. Li, K., Jia, X., Tang, A., Zhu, X., Meng, H. and Wang, Y. Preparation of spherical and triangular silver nanoparticles by a convenient method. *Integrated Ferroelectrics* 2012, 136(1), pp.9-14. DOI: 10.1080/10584587.2012.686405

68. Lu, J., Bravo-Suárez, J.J., Takahashi, A., Haruta, M. and Oyama, S.T. In situ UV–vis studies of the effect of particle size on the epoxidation of ethylene and propylene on supported silver catalysts with molecular oxygen. *Journal of Catalysis*, 232(1) 2005, pp.85-95. DOI: 10.1016/j.jcat.2005.02.013
69. Mahringer, A., Ott, M. and Fricker, G., 2013. The Blood–Brain Barrier: An Introduction to Its Structure and Function. In *The Blood Brain Barrier (BBB)* (pp. 1-20). Springer, Berlin, Heidelberg.
70. Mallikarjuna, K., Narasimha, G., Dillip, G.R., Praveen, B., Shreedhar, B., Lakshmi, C.S., Reddy, B.V.S. and Raju, B.D.P. Green synthesis of silver nanoparticles using *Ocimum* leaf extract and their characterization. *Digest Journal of Nanomaterials and Biostructures* 2011, 6(1), pp.181-186.
71. Mariri, NG., 2017. In Vitro Evaluation of the Bioactivity of *Gnidia Polycephala* and *Senecio Serratuloides* (master’s dissertation, Bloemfontein: Central University of Technology, Free State).
72. Marslin, G., Siram, K., Maqbool, Q., Selvakesavan, R.K., Kruszka, D., Kachlicki, P. and Franklin, G., 2018. Secondary metabolites in the green synthesis of metallic nanoparticles. *Materials*, 11(6), p.940.
73. Mazid, M., Khan, T.A. and Mohammad, F. Role of secondary metabolites in defense mechanisms of plants. *Biology and medicine* 2011, 3(2), pp.232-249.
74. Miguel, M.G., 2010. Antioxidant activity of medicinal and aromatic plants. A review. *Flavour and Fragrance Journal*, 25(5), pp.291-312.
75. Moody, C.L. and Wheelhouse, R.T., 2014. The medicinal chemistry of imidazotetrazine prodrugs. *Pharmaceuticals*, 7(7), pp.797-838.

76. Mura, S., Nicolas, J. and Couvreur, P., 2013. Stimuli-responsive nanocarriers for drug delivery. *Nature materials*, 12(11), p.991.
77. Murphy, M.P., 2009. How mitochondria produce reactive oxygen species. *Biochemical journal*, 417(1), pp.1-13.
78. Neuwinger, H.D., 1996. African ethnobotany: poisons and drugs: chemistry, pharmacology, toxicology. CRC Press.
79. Newlands, E.S., Blackledge, G.R.P., Slack, J.A., Rustin, G.J., Smith, D.B., Stuart, N.S., Quarterman, C.P., Hoffman, R., Stevens, M.F.G., Brampton, M.H. and Gibson, A.C., 1992. Phase i trial of temozolomide (CCRG 81045: MandB 39831: NSC 362856). *British journal of cancer*, 65(2), p.287.
80. Nieder, Carsten, Anca L. Grosu, and Laurie E. Gaspar. "Stereotactic radiosurgery (SRS) for brain metastases: a systematic review." *Radiation Oncology* 9.1 (2014): 155.
81. Nygren, P., 2001. What is cancer chemotherapy?. *Acta Oncologica*, 40(2-3), pp.166-174.
82. Order, Stanley E., et al. "Improvement in quality of survival following whole-brain irradiation for brain metastasis." *Radiology* 91.1 (1968): 149-153.
83. Pardridge, W.M., 2005. The blood-brain barrier: bottleneck in brain drug development. *NeuroRx*, 2(1), pp.3-14
84. Parisot, S., Darlix, A., Baumann, C., Zouaoui, S., Yordanova, Y., Blonski, M., Rigau, V., Chemouny, S., Taillandier, L., Bauchet, L. and Duffau, H., 2016. A probabilistic atlas of diffuse WHO grade II glioma locations in the brain. *PloS one*, 11(1), p.e0144200.

85. Penn, I., 1981. Depressed immunity and the development of cancer. *Clinical and experimental immunology*, 46(3), p.459.
86. Peppiatt CM, Howarth C, Mobbs P, Attwell D (2006) *Nature* 443:700–704
87. Pietta, P.G., 2000. Flavonoids as antioxidants. *Journal of natural products*, 63(7), pp.1035-1042.
88. Plaizier, A.C., 1980. A revision of *Adenium* Roem. and Schult. and of *Diplorhynchus* Welw. Ex Fic. and Hiern (Apocynaceae) (No. 80-12). Veenman.
89. Reid, J.M., Stevens, D.C., Rubin, J. and Ames, M.M., 1997. Pharmacokinetics of 3-methyl-(triazene-1-yl) imidazole-4-carboximide following administration of temozolomide to patients with advanced cancer. *Clinical cancer research*, 3(12), pp.2393-2398.
90. Reijnders, L. Hazard reduction in nanotechnology. *Journal of Industrial Ecology* 2008, 12(3), pp.297-306. DOI: 10.1111/j.1530-9290.2008.00049.x
91. Rice-evans, C.A., Miller, N.J., Bolwell, P.G., Bramley, P.M. and Pridham, J.B., 1995. The relative antioxidant activities of plant-derived polyphenolic flavonoids. *Free radical research*, 22(4), pp.375-383.
92. Romagnolo, D.F. and Selmin, O.I., 2012. Flavonoids and cancer prevention: a review of the evidence. *Journal of nutrition in gerontology and geriatrics*, 31(3), pp.206-238.
93. Roodt V. 1998. Trees and shrubs of the Okavango Delta: medicinal uses and nutritional value. *Shell Field Guide Series: Part I. Gaborone: Shell Oil Botswana.*
94. Roy, A., Bulut, O., Some, S., Mandal, A.K. and Yilmaz, M.D., 2019. Green synthesis of silver nanoparticles: biomolecule-nanoparticle organizations targeting antimicrobial activity. *RSC advances*, 9(5), pp.2673-2702.

95. Sakanaka S, Tachibana Y, Okada Y. Preparation and antioxidant properties of extracts of Japanese persimmon tea (kakinoha-cha). *Food Chem.* 2005; 89: 569–575.
96. Schnyder, A. and Huwyler, J., 2005. Drug transport to brain with targeted liposomes. *NeuroRx*, 2(1), pp.99-107.
97. Sercombe, L., Veerati, T., Moheimani, F., Wu, S. Y., Sood, A. K., and Hua, S. (2015). Advances and challenges of liposome assisted drug delivery. *Frontiers in Pharmacology*, 6, 286.
98. Shankar, S.S., Rai, A., Ahmad, A. and Sastry, M., 2004. Rapid synthesis of Au, Ag, and bimetallic Au core–Ag shell nanoparticles using Neem (*Azadirachta indica*) leaf broth. *Journal of colloid and interface science*, 275(2), pp.496-502.
99. Sharma, V.K., Yngard, R.A. and Lin, Y., 2009. Silver nanoparticles: green synthesis and their antimicrobial activities. *Advances in colloid and interface science*, 145(1-2), pp.83-96.
100. Silver, S., Phung, L.T. and Silver, G. Silver as biocides in burn and wound dressings and bacterial resistance to silver compounds. *Journal of Industrial Microbiology and Biotechnology* 2006, 33(7), pp.627-634. DOI: 10.1007/s10295-006-0139-7
101. Singh, R. and Lillard Jr, J.W., 2009. Nanoparticle-based targeted drug delivery. *Experimental and molecular pathology*, 86(3), pp.215-223.
102. Soffietti, Riccardo, et al. "Brain metastases." *European Handbook of Neurological Management*. 2nd ed. Oxford: Blackwell Publishing Ltd (2011): 437-45.
103. Sohail, M.F., Rehman, M., Sarwar, H.S., Naveed, S., Salman, O., Bukhari, N.I., Hussain, I., Webster, T.J. and Shahnaz, G., 2018. Advancements in the oral delivery of

- Docetaxel: Challenges, current state-of-the-art and future trends. *International journal of nanomedicine*, 13, p.3145.
104. Sondi, I. and Salopek-Sondi, B. Silver nanoparticles as antimicrobial agent: a case study on *E. coli* as a model for Gram-negative bacteria. *Journal of colloid and interface science* 2004, 275(1), pp.177-182. DOI: 10.1016/j.jcis.2004.02.012
105. Stamatelou KK, Francis ME, Jones CA, Nyberg LM Jr, Curhan GC. 2003. Time trends in reported prevalence of kidney stones in the United States: 1976–1994. *Kidney Int.* 63:1817–23
106. Sudjaroen, Y., 2009. Plant-derived phenolic antioxidants and cancer prevention. *Thai Cancer J*, 29(9), pp. 126-34.
107. Suffredini, I.B.; Sader, H.S.; Gonçalves, A.G.; Reis, A.O.; Gales, A.C.; Varella, A.D.; Younes, R.N. Screening of antibacterial extracts from plants native to the Brazilian Amazon rain forest and Atlantic forest. *Braz. J. Med. Biol. Res.* 2004, 37, 379–384.
108. Tedder, M.J., Kirkman, K.P., Morris, C.D., Trollope, W.S. and Bonyongo, M.C. Determinants of the occurrence of a native encroacher species, *Pechuelloeschea leubnitziae* (wild sage), in the eastern Okavango Delta, Botswana. *African journal of range and forage science* 2015, 32(4), pp.253-259. DOI: 10.2989/10220119.2015.1005668
109. Thaipong K, Boonprakob U, Crosby K, Cisneros-Zevallos L and Byrne DH (2006) Comparison of ABTS, DPPH, FRAP, and ORAC assays for estimating antioxidant activity from guava fruit extracts. *Journal of Food Composition and Analysis* 19: 669–675.

110. Tungmunnithum, D.; Thongboonyou, A.; Pholboon, A.; Yangsabai, A. Flavonoids and other phenolic compounds from medicinal plants for pharmaceutical and medical aspects: An overview. *Medicines* 2018, 5,93.
111. Urbańska, K., Pająk, B., Orzechowski, A., Sokołowska, J., Grodzik, M., Sawosz, E., Szmidt, M. and Sysa, P., 2015. The effect of silver nanoparticles (AgNPs) on proliferation and apoptosis of in ovo cultured glioblastoma multiforme (GBM) cells. *Nanoscale research letters*, 10(1), p.98.
112. Van Damme, P., Van Den Eynden, V. and Vernemmen, P.,. Plant uses by the Topnaar of the Kuiseb Valley Namib desert. *Afrika focus* 1922, 8(3-4), pp.223-252.
113. Von Koenen, E. Medicinal, Poisonous, and Edible Plants in Namibia. Windhoek, Namibia: Klaus Hess Publishers 2001.
114. Wahle, K.W., Brown, I., Rotondo, D. and Heys, S.D., 2010. Plant phenolics in the prevention and treatment of cancer. In *Bio-Farms for Nutraceuticals* (pp. 36-51). Springer, Boston, MA.
115. Walter WG, Khanna PN. 1972. Chemistry of the Aroids. I. Dieffenbachia seguine, amoena, and picta. *Economic Botany* 26: 364-372.
116. War, A.R., Paulraj, M.G., Ahmad, T., Buhroo, A.A., Hussain, B., Ignacimuthu, S. and Sharma, H.C., 2012. Mechanisms of plant defense against insect herbivores. *Plant signaling and behavior*, 7(10), pp.1306-1320.
117. Xu, F., Pielt, C., Farkas, S., Qazzaz, M. and Syed, N.I., 2013. Silver nanoparticles (AgNPs) cause degeneration of cytoskeleton and disrupt synaptic machinery of cultured cortical neurons. *Molecular brain*, 6(1), p.29.

118. Xue, Y., Zhang, S., Huang, Y., Zhang, T., Liu, X., Hu, Y., ... Tang, M. (2012). Acute toxic effects and gender-related biokinetics of silver nanoparticles following an intravenous injection in mice. *Journal of Applied Toxicology*, 32, 890–899.
119. Yusuf, A.Z., Zakir, A., Shemau, Z., Abdullahi, M. and Halima, S.A., 2014. Phytochemical analysis of the MeOH leaves extract of *Paullinia pinnata* linn. *Journal of pharmacognosy and phytotherapy*, 6(2), pp.10-16.
120. Zainol, M.K., Abd-Hamid, A., Yusof, S. and Muse, R., 2003. Antioxidative activity and total phenolic compounds of leaf, root and petiole of four accessions of *Centella asiatica* (L.) Urban. *Food Chemistry*, 81(4), pp.575-581.
121. Zhang X-F, Liu Z-G, Shen W, Gurunathan S. Silver Nanoparticles: Synthesis, Characterization, Properties, Applications, and Therapeutic Approaches. Yan B, ed. *International Journal of Molecular Sciences*. 2016;17(9):1534. doi:10.3390/ijms17091534.
122. Zhou, W., Mukherjee, P., Kiebish, M.A., Markis, W.T., Mantis, J.G. and Seyfried, T.N., 2007. The calorically restricted ketogenic diet, an effective alternative therapy for malignant brain cancer. *Nutrition and metabolism*, 4(1), p.5
123. O'Driscoll, B.R., Hasleton, P.S., Taylor, P.M., Poulter, L.W., Gattamaneni, H.R. and Woodcock, A.A., 1990. Active lung fibrosis up to 17 years after chemotherapy with carmustine (BCNU) in childhood. *New England Journal of Medicine*, 323(6), pp.378-382.
124. Haque, R.M., Amundson, E., Dorsi, M. and Brem, H., 2006. Interstitial chemotherapy and polymer-drug delivery. In *Handbook of Brain Tumor Chemotherapy* (pp. 274-294). Academic Press.

125. Friedman, H.S., Kerby, T. and Calvert, H., 2000. Temozolomide and treatment of malignant glioma. *Clinical cancer research*, 6(7), pp.2585-2597.
126. Stevens, M.F., Hickman, J.A., Langdon, S.P., Chubb, D., Vickers, L., Stone, R., Baig, G., Goddard, C., Gibson, N.W., Slack, J.A. and Newton, C., 1987. Antitumor activity and pharmacokinetics in mice of 8-carbamoyl-3-methyl-imidazo [5, 1-d]-1, 2, 3, 5-tetrazin-4 (3H)-one (CCRG 81045; M and B 39831), a novel drug with potential as an alternative to dacarbazine. *Cancer research*, 47(22), pp.5846-5852.
127. Hashemi, S., Asrar, Z., Pourseyedi, S. and Nadernejad, N., 2016. Green synthesis of ZnO nanoparticles by Olive (*Olea europaea*). *IET nanobiotechnology*, 10(6), pp.400-404.
128. Sabharwal, S.S. and Schumacker, P.T., 2014. Mitochondrial ROS in cancer: initiators, amplifiers or an Achilles' heel?. *Nature Reviews Cancer*, 14(11), pp.709-721.
129. Fuchs-Tarlovsky, V., 2013. Role of antioxidants in cancer therapy. *Nutrition*, 29(1), pp.15-21.
130. Lujan, H., Griffin, W.C., Taube, J.H. and Sayes, C.M., 2019. Synthesis and characterization of nanometer-sized liposomes for encapsulation and microRNA transfer to breast cancer cells. *International journal of nanomedicine*, 14, p.5159.
131. Ai, X., Zhong, L., Niu, H. and He, Z., 2014. Thin-film hydration preparation method and stability test of DOX-loaded disulfide-linked polyethylene glycol 5000-lysine-di-tocopherol succinate nanomicelles. *asian journal of pharmaceutical sciences*, 9(5), pp.244-250.

132. Raj, S., Mali, S.C. and Trivedi, R., 2018. Green synthesis and characterization of silver nanoparticles using *Enicostemma axillare* (Lam.) leaf extract. *Biochemical and biophysical research communications*, 503(4), pp.2814-2819.
133. Coté, GG., 2009. Diversity and distribution of idioblasts producing calcium oxalate crystals in *Dieffenbachia seguine* (Araceae). *American Journal of Botany*, 96(7), pp. 1245-1254.
134. Arditti, J. Rodriguez, E., 1982. *Diffenbachia*: uses, abuse and toxic constituent: a review. *Journal of Ethnopharmacology*, 5(3), pp.293-302.
135. Burrows, G.E and Tyrl, R.J., 2013. *Toxic plants of north America*. John Wiley and Sons.
136. Marandure, T., 2013. Concept and key issues of ethnoveterinary medicine in Africa: A review of its application in Zimbabwe. *African Journal of Agricultural Research*, 11(20), pp. 1836-1841.
137. Akhtar, M.S., Hossain, M.A. and Said, S.A., 2017. Isolation and characterization of antimicrobial compound from the stem bark of traditionally used medicinal plant *Adenium obesum*. *Journal of Traditional and Complementary Medicine*, 7(3), pp 296-300.
138. Hossain, M.A., Al-Musalami, A.H.S., Akhtar, M.S and Said, S., 20014. A comparison of the antimicrobial effectiveness of different polarities crude extracts from the leaves of *Adenium obesum* used in Omani traditional medicine for the treatment of microbial infections. *Asian Pacific Journal of Tropical Disease*, 4, pp. S934-S937.

139. Paul, D., Biswas, k. and Sinha, S.N., 2015. Biological activities of *Adenium obesum* (Forssk.) Roem. And Schult.: a concise review. *Malaya Journal of Biosciences*, 2(4), pp.214-221.
140. Ndongo, D., 2017. Antibacterial, antioxidant and phytochemical investigation of *Acacia arenaria*, *Aloe esculenta* and *Pechuel-loeschea leubnitziae* (Doctoral dissertation, University of Namibia).

SUPPLEMENTARY PICTURES



Figure 1: Tetradecane

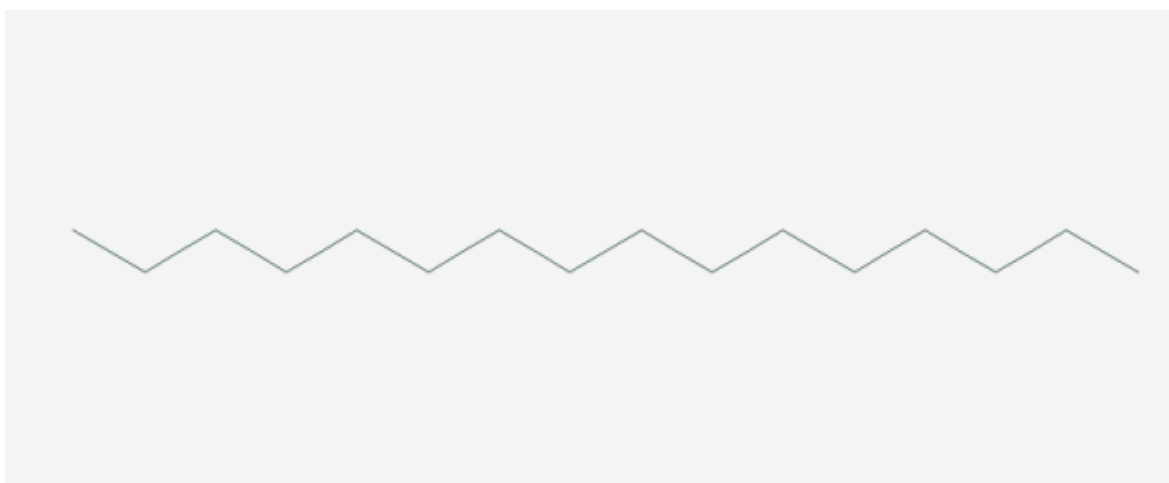


Figure 2: Hexadecane

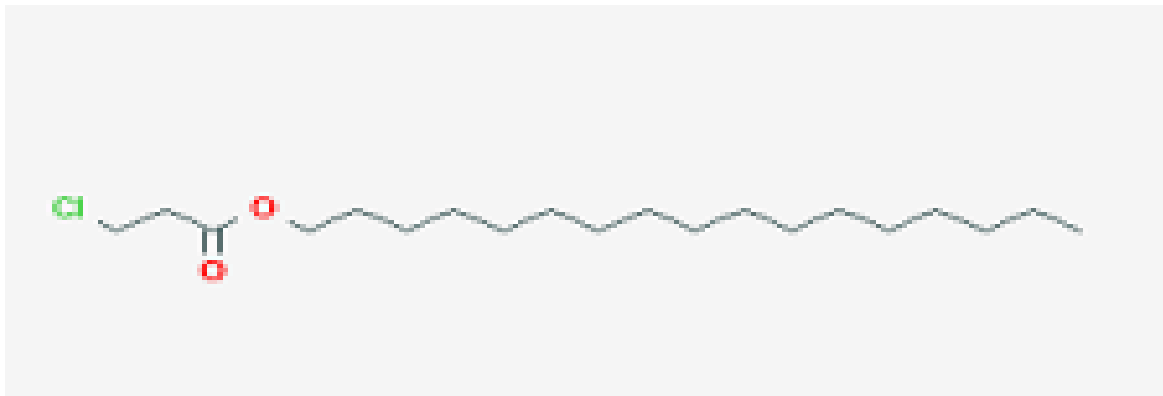


Figure 3: 3-chloropropionic acid, heptadecyl ester



Figure 4: n hexadecanoic acid

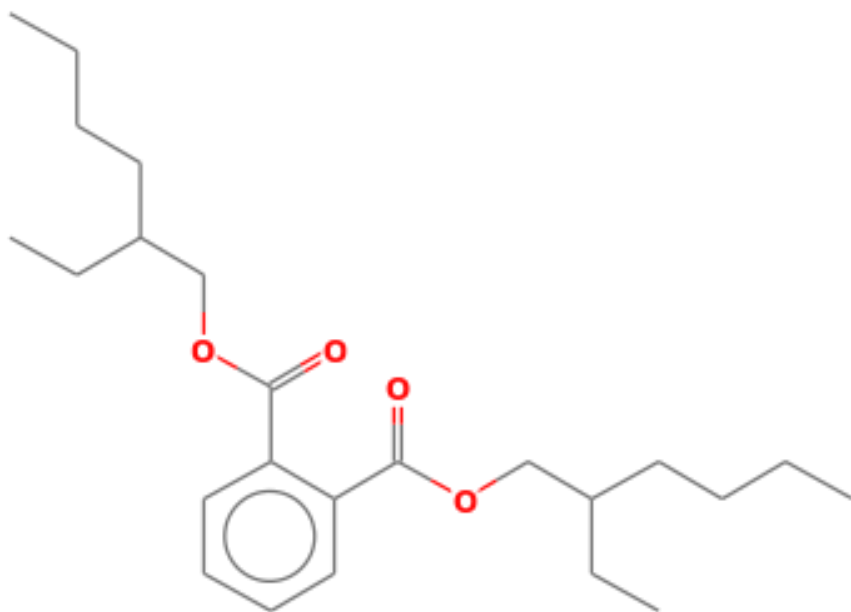


Figure 5: Bis (2-ethylhexyl) phthalate

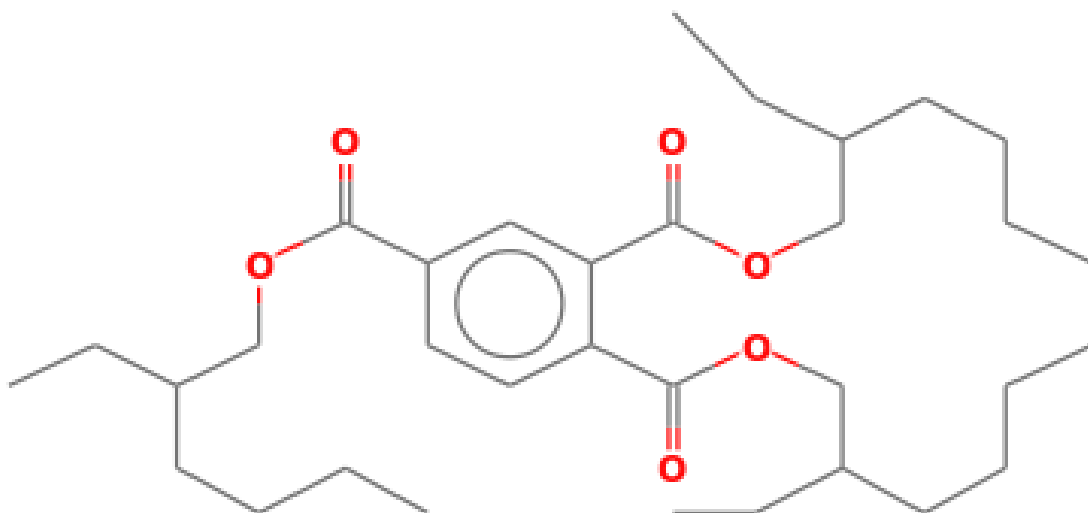


Figure 6: tri(2-ethylhexyl) trimellitate

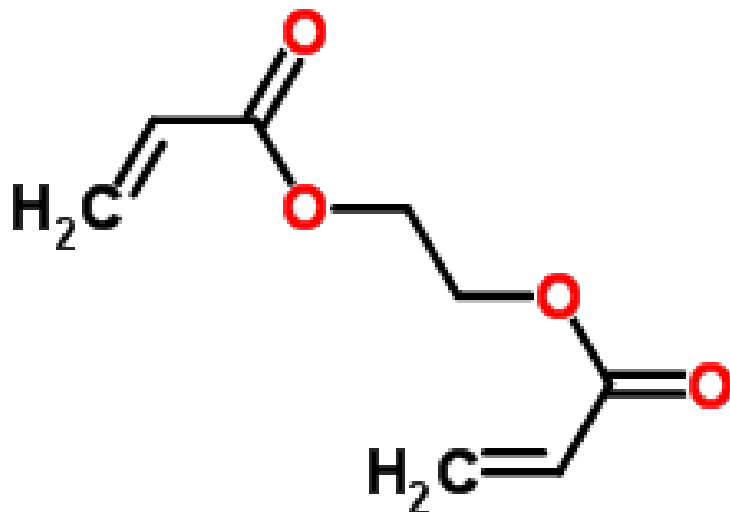


Figure 7: Ethylene diacrylate



Figure 8: Hexadecanoic acid, methyl ester

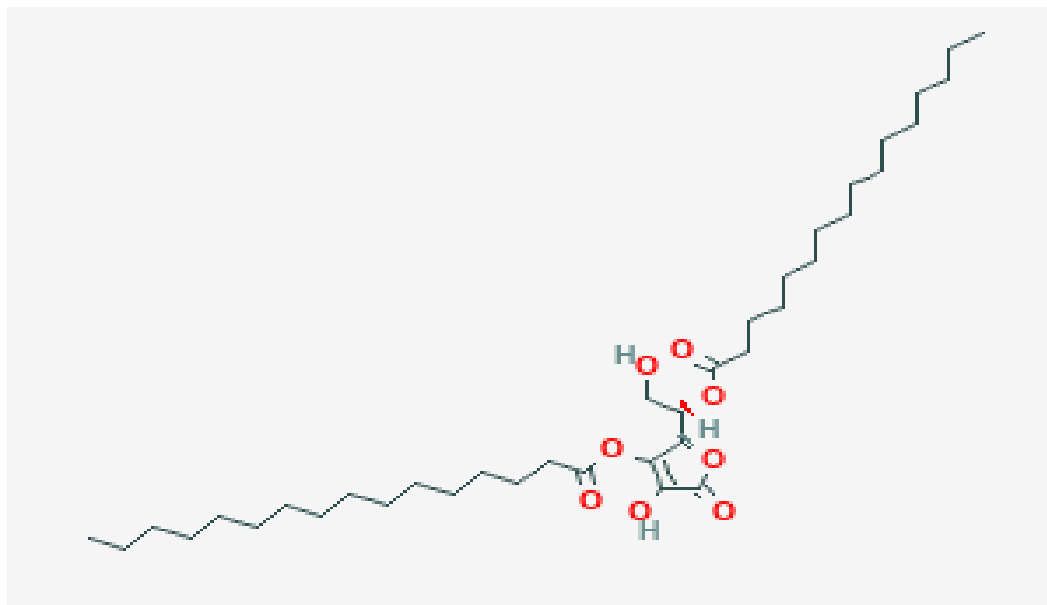


Figure 9: 1-(+)-Ascorbic acid 2,6-dihexadecanoate

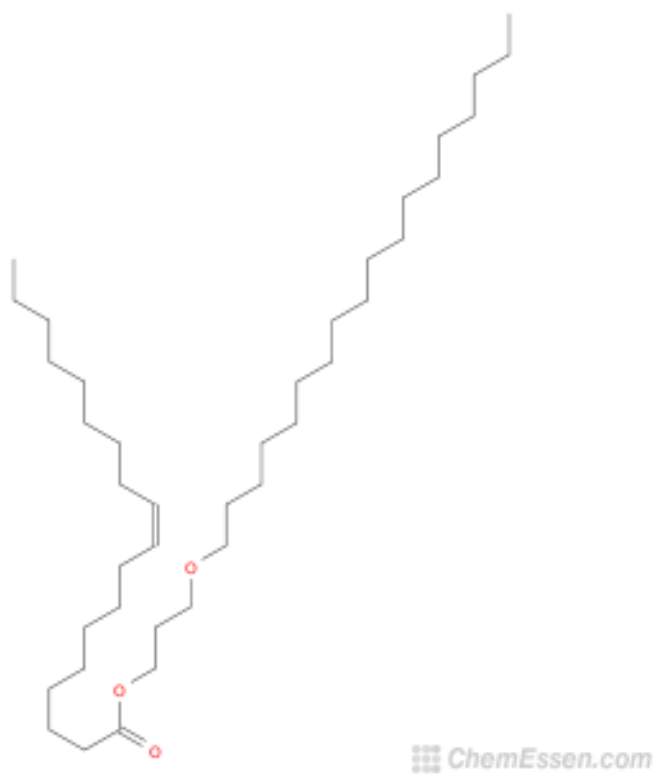


Figure 10: oleic acid 3-(octadecyloxy)propyl ester

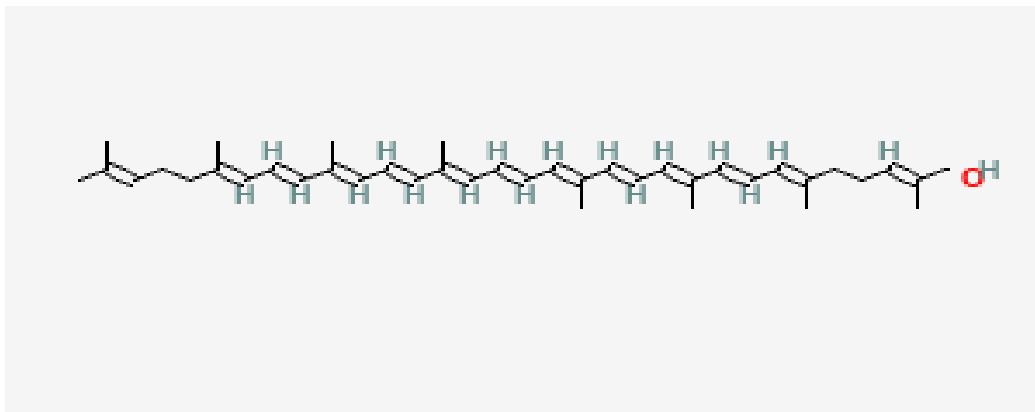


Figure 11: Lycoxanthin